Translational dose optimisation of tigecycline using *in vitro* and *in silico* approaches

Dissertation

to obtain the academic degree
Doctor rerum naturalium (Dr. rer. nat.)

submitted to the Department of Chemistry,
Clinical Pharmacy,
Institute of Pharmacy,
Faculty of Mathematics, Informatics and Natural Sciences
University of Hamburg

by

Lisa Franziska Amann

born in Hamburg

Hamburg 2024

The results presented in this dissertation were obtained from April 2019 until July 2022 supervised by Prof. Dr. Sebastian G. Wicha at the Department of Clinical Pharmacy, Institute of Pharmacy, University of Hamburg.

First Reviewer: Prof. Dr. Sebastian G. Wicha

Second Reviewer: Prof. Dr. Christoph Ritter

Thesis defence committee: Prof. Dr. Sebastian G. Wicha

                                                          Prof. Dr. Wolfgang Maison

                                                          Prof. Dr. Peter Heisig

Date of thesis defence and approval: 12.04.2024

Success is not final, failure is not fatal: It is the courage to continue that counts.

Winston Churchill (1874 − 1965)

I. List of publications

Original articles included in the cumulative dissertation

L. F. Amann, E. Ruda Vicente M. Rathke; A. Broeker; S. G. Wicha, Stability studies with tigecycline in bacterial growth medium and impact of stabilizing agents. European Journal of Clinical Microbiology & Infectious Diseases (2021)

L. F. Amann, A. Broeker, M. Riedner; H. Rohde, P. Nordmann, J.-W. Decousser, S. G. Wicha, Pharmacokinetic/pharmacodynamic evaluation of tigecycline dosing in a hollow fiber infection model against clinical *bla*-KPC producing *Klebsiella pneumoniae* isolates. Diagnostic Microbiology & Infectious Disease (2023)

L. F. Amann, R. Alraish, A. Broeker, M. Kaffarnik, S. G. Wicha, Tigecycline Dosing Strategies in Critically Ill Liver-Impaired Patients. Antibiotics (2022).

L. F. Amann, S. G. Wicha, Operational characteristics of full random effects modelling ('frem') compared to stepwise covariate modelling ('scm')." Journal of Pharmacokinetics and Pharmacodynamics (2023)

Original articles

N. Kroemer, **L. F. Amann**, A. Farooq, C. Pfaffendorf, M. Martens, J-W. Decousser, N. Grégoirec, P. Nordmann, S. G. Wicha, Pharmacokinetic/pharmacodynamic analysis of ceftazidime/avibactam fosfomycin combinations in an in vitro hollow fiber infection model against multidrug-resistant Escherichia coli, Microbiology Spectrum (2023).

B. Wulkersdorfer, F. Bergmann**, L. F. Amann**, A. Fochtmann-Frana, V. al Jalali, E. Kurdina, E. Lackner, S. G. Wicha, C. Dorn, B. Schäfer, G. Ihra, T. Rath, C. Radtke, M. Zeitlinger. Effect of albumin substitution on pharmacokinetics of piperacillin/tazobactam in patients with severe burn injury admitted to the intensive care unit., Journal of Antimicrobial Chemotherapy (2023).

K. Iqbal; H. Rohde, J. Huang, T. Tikiso, **L. F Amann**; M. Zeitlinger, S. G Wicha. A PKPD model-based analysis of tedizolid against Enterococci using the hollow-fibre infection model, Journal of Antimicrobial Chemotherapy (2022).

Conference contributions

Oral presentation

L. F. Amann, S. G Wicha; Pharmacokinetic/pharmacodynamic evaluation of tigecycline against Klebsiella pneumoniae – higher doses or lower breakpoints needed? European Congress of Clinical Microbiology & Infectious Diseases (ECCMID 2022, oral presentation)

L. F Amann, A. Broeker, S. G. Wicha; Continuous infusion of tigecycline as an improved treatment option? Insights from a hollow fiber study. International Society of Antimicrobial Pharmacology (ISAP Annual Meeting, 2020, oral presentation)

Poster presentation

L. F. Amann, S. G Wicha; Extrapolation of static time kill curve data to predict pharmacodynamic hollow fiber experiment data using in PK/PD modelling. European Congress of Clinical Microbiology & Infectious Diseases (ECCMID 2022, poster presentation)

L. F. Amann, R. Alraish, A. Broeker, M. Kaffarnik, S. G. Wicha; Stepwise Covariate Modelling (SCM) versus Full Random Effects Modelling (FREM) for covariate modelling of correlated covariates exemplified with tigecycline and liver function markers. Population Approach Group in Europe (PAGE, 2021, virtual poster presentation)

L. F. Amann, A. Broeker, S. G. Wicha; Continuous infusion of tigecycline as an improved treatment option? Insights from a hollow-fiber study. European Congress of Clinical Microbiology & Infectious Diseases (ECCMID 2021, virtual poster presentation)

B. Wulkersdorfer, **L. F. Amann,** A. Fochtmann-Frana, K. Elizaveta, E. Lackner, S. G Wicha, C. Dorn, B. Schäfer, G. Ihra, T. Rath, C. Radtke, M. Zeitlinger; Effect of Albumin on Protein Binding and Pharmacokinetics of Piperacillin/Tazobactam in Patients with Severe Burn Injury. European Congress of Clinical Microbiology & Infectious Diseases (ECCMID 2021, virtual poster presentation)

L. F. Amann, E. Ruda Vicente, M. Rathke, A. Broeker, S. G. Wicha; Stability studies with tigecycline in bacterial growth medium and impact of stabilizing agents. European Congress of Clinical Microbiology & Infectious Diseases (ECCMID 2020, cancelled due to COVID-19 pandemic)

II. Contents

III.   List of abbreviations

ADME	Absorption, Distribution, Metabolism, Elimination
AUC	Area under the concentration time curve
bla	Beta-lactamase
Ca-MHB	cation-adjusted Mueller-Hinton broth
CFU	Colony forming units
cIAI	Complicated intra-abdominal infections
CL	Clearance
CLSI	Clinical and Laboratory Standards Institute
C_{max}	Maximum concentration
C_{min}	Minimum or through concentration
CRE	Carbapenem resistant *Enterobacterales*
cSSI	Complicated skin and skin structure infections
df	Degrees of freedom
dOFV	Drop of Objective Function Value
ECOFF	Epidemiological Cut-Off value
EMA	European Medical Agency
ESBL	Extended Spectrum Beta-Lactamase
EUCAST	European Committee for Antimicrobial Testing
frem	Full random effects modelling
FDA	Food and Drug Administration (USA)
HFIM	Hollow Fiber Infection Model
I	Susceptible, increased exposure
ICU	Intensive care unit
IIV	Inter-individual variability

IOV	Inter-occasion variability
KPC	*Klebsiella pneumoniae* carbapenemase
LD	Loading dose
LiMAx	Liver Maximum capacity test
MELD	Model for end stage liver disease score
MHK	Minimale Hemmkonzentration
MIC	Minimal inhibitory concentration
MD	Maintenance dose
MDRO	Multi-drug resistant organism
N	Number of individuals in da dataset
NLME	Nonlinear mixed effects modelling
OFV	Objective function value
OXA-48	Oxacilinase-48
PK	Pharmacokinetics
PD	Pharmacodynamics
PopPK	Population Pharmacokinetics
Q	Intercompartmental clearance
R	Resistant
RNA	Ribonucleic acid
S	Susceptible, standard dosing regimen
scm	Stepwise covariate modelling
SSE	Stochastic simulation and estimation
TDM	Therapeutic drug monitoring
$T_{> MIC}$	Time or percent time above the MIC
V_c	Central volume of distribution

IV.   Zusammenfassung

Infektionskrankheiten, insbesondere solche, die durch gramnegative Erreger verursacht werden, belasten zunehmend das Gesundheitssystem und stellen medizinisches Personal vor große Herausforderungen. Die verfügbaren Antibiotika verlieren aufgrund der vermehrt auftretenden Resistenzentwicklung ihre Wirksamkeit, und gleichzeitig geht die Zahl der neu zugelassenen innovativen antibiotischen Arzneimittel besorgniserregend zurück. Tigecyclin ist ein Reserveantibiotikum und wird bei komplizierten Infektionen eingesetzt. Die zugelassene Dosis (100 mg Initialdosis gefolgt von 50 mg Erhaltungsdosis) hat sich als zunehmend unzureichend erwiesen, sodass hochdosiertes Tigecyclin (100 mg, 100 mg q12h) für Infektionen empfohlen wurde, welche durch multiresistente Krankheitserreger ausgelöst wurden (bis zu einer minimalen Hemmkonzentration (MHK) von 1 mg/L). Die klinische Datenlage, auf die sich diese Empfehlung stützt, ist jedoch begrenzt.

Ziel dieser Arbeit war es, das Potenzial von Tigecyclin durch Dosisoptimierungsstudien zu evaluieren. Hierfür wurden *in vitro*- und pharmakometrische Ansätze genutzt.

Tigecyclin ist ein instabiler Arzneistoff, was das Experimentdesign und die Handhabung im Labor einschränkt. Daher hat **Veröffentlichung I** den Einfluss von antioxidativen Zusätzen (Ascorbinsäure und Pyruvat) auf die Arzneistoffstabilität in der kationenstabilisierten Mueller-Hinton Bouillon untersucht. Es stellte sich heraus, dass Tigecyclin durch den Zusatz von 2 % Pyruvat mit Beibehaltung der antibiotischen Aktivität stabilisiert werden konnte. Diese Stabilisierung ermöglichte die in **Veröffentlichung II** durchgeführten Langzeit Tigecyclin *in vitro* Versuche gegen klinische *Klebsiella pneumoniae* Isolate im Hollow Fiber Infektionsmodell.

Die Experimente in **Veröffentlichung II** zielten darauf ab, die *in vitro* Wirksamkeit von Tigecyclin gegen klinische *Klebsiella pneumoniae* Isolate mittels erhöhter Tagesdosis, oder durch neue Dosierungsschemata zu verbessern. Zudem wurde die Resistenzentwicklung erfasst und genomisch analysiert. Nur ein Vielfaches der zugelassenen Dosis (Initialdosis 200 mg, Erhaltungsdosis 100 mg q8h vs. zugelassene Initialdosis 100 mg, zugelassene Erhaltungsdosis: 50 mg q12 h) verhinderte ein Wiederanwachsen von Subpopulationen mit einer MHK von 0,125 mg/L. Infolgedessen wurde auf ein limitiertes Dosisoptimierungspotenzial geschlossen. Diese

MHK liegt jedoch deutlich unter dem aktuellen klinischen Epidemiologischen Cut-Off Wert (ECOFF) von *Klebsiella pneumoniae* (2 mg/L). Darüber hinaus zeigte sich ein durch die Tigecyclinexposition induziertes Wiederanwachsen von resistenten Subpopulationen, für die eine bis zu 32-fach erhöhte MHK gemessen werden konnte. Tigecyclin-induzierte Mutationen konnten identifiziert werden und entsprachen zuvor beschriebenen klinischen Beobachtungen. Darüber hinaus stützen die Beobachtungen in **Veröffentlichung II** die Hypothese, dass klinisches Versagen mit dem Fortschreiten der Infektion zusammenhängen könnte. Daraus wurde geschlussfolgert, dass der derzeit empfohlene klinische Grenzwert von MIC 1 mg/L für die Tigecycline Hochdosistherapie (100 mg, 100 mg q12 h) bei Infektionen, die durch multiresistente Bakterien verursacht sind, nicht ausreichend ist.

Veröffentlichung III quantifizierte die Pharmakokinetik von Tigecyclin in kritisch kranken, lebergeschädigten Intensivpatienten, einer unterrepräsentieren Patientenpopulation. Mittels einer pharmakometrischen Kovariatenanalyse wurde eine Dosisanpassung unter Verwendung klinischer Parameter, insbesondere Leberparameter, ausgewertet und mit der aktuell empfohlenen Child-Pugh-Score basierenden Dosisreduktion verglichen. Diese klinischen Daten zeigten, eine deutlich abweichende Pharmakokinetik (e.g. Clearance (CL) von 8.6 L/h zu denjenigen, die nicht kritisch krank sind (e.g. CL: 16.8 L/h[1], 18.6 L/h[2]). Darüber hinaus hat sich gezeigt, dass eine Reduktion der Erhaltungsdosis von 50 mg auf 25 mg in dieser Population in der gleichen Arzneimittelexposition resultiert, wie 100 mg bei nicht kritisch kranken Patienten. Es wurde jedoch keine Korrelation zwischen der Arzneimittelexposition und der klinischen Heilung festgestellt. Gesamtbilirubin (≥ 10 mg/dL) und der MELD-Score (≥ 30) haben sich als prädiktive Messgrößen für die Arzneimittelexposition herausgestellt, allerdings waren sie dem Child-Pugh-Score als Orientierung für Dosisanpassungen nicht überlegen.

Insgesamt gibt es mehrere Möglichkeiten zur Durchführung einer pharmakometrischen Kovariatenanalyse, wobei einige Methoden heutzutage nur selten angewendet werden oder wenig in der Literatur vertreten sind. Daher wurde in der **Veröffentlichung IV** eine umfassende Evaluierung von der am häufigsten verwendete 'Stepwise covariate modelling' Methode ('scm') mit der neuartigen 'Full random effects modelling' ('frem') Methode vorgenommen. Hierfür wurde unter verschiedenen Annahmen über Datensatzgröße, des Kovariateneffekts und der Kovariaten-

Kollinearität eine Simulationsstudie durchgeführt. Zudem hat diese Studie, den 'frem$_{posthoc}$' eingeführt, um dessen Eignung für eine Kovariatenselektion ausgehend von einem 'frem' Model zu untersuchen. Die Ergebnisse zeigten, dass die statistische Teststärke (Power) die wahre Kovariate in kleinen Datensätzen zu finden für beide Methoden gering war, was sowohl für 'scm' als auch 'frem$_{posthoc}$' zur Überschätzung und Ungenauigkeit der Kovariatenkoeffizienten in führte. Allerdings war die statistische Teststärke von 'frem$_{posthoc}$' in kleinen Datensätzen im Vergleich zu 'scm' bis zu dreimal höher. Zusätzlich zeigte diese Methode bei großen Datensätzen (N > 100) eine vergleichbare Zuverlässigkeit wie der 'scm'. Ohne den Selektionsschritt lieferten 'frem' Modelle in kleinen Datensätzen unverzerrte Schätzungen mit besserer Genauigkeit als 'scm'. Insgesamt erwies sich frem$_{posthoc}$' als eine geeignete neue Anwendung von 'frem', um die Selektion von Kovariaten zu leiten, während die statistische Teststärke (Power), Präzision und Genauigkeit, in kleinen Datensätzen von 'frem$_{posthoc}$' dem 'scm' Modellen überlegen war.

Zusammenfassend lässt sich sagen, dass die vorgestellten Ergebnisse eine langfristige *in vitro* Untersuchung von Tigecyclin ermöglichten, jedoch zeigten, dass das Potenzial zur Dosisoptimierung für *Klebsiella pneumoniae* auf eine MHK von 0.125 mg/L begrenzt war. Darüber hinaus trug diese Arbeit zu einem tieferen und quantitativen Verständnis von Tigecyclin in schwerkranken Patienten bei und kommt zu dem Schluss, dass die Verwendung als Monotherapie in Frage gestellt und gegebenenfalls neu bewertet werden muss.

V. Abstract

Infectious diseases, especially those caused by gram-negative pathogens, are increasingly burdening the global healthcare system and pose major challenges for medical staff. Available anti-infective drugs are losing their efficacy, due to increasing resistance development. At the same time the number of newly approved, innovative antibiotics is declining at an alarming rate. Tigecycline is a last resort antibiotic that is used for complicated infections. The approved dose (100 mg loading dose (LD), followed by 50 mg maintenance dose (MD) q12h) has shown increasingly insufficient clinical effectivity, resulting in high-dose tigecycline (100 mg, 100 mg q12h) recommendations for infections caused by multidrug-resistant pathogens up to a minimal inhibitory concentration (MIC) of 1 mg/L. However, this is based on limited clinical data.

The aim of this work was to evaluate the dose optimization potential of tigecycline. Therefore, in vitro and pharmacometric approaches were applied.

Tigecycline is an instable drug, which limits experimental design and laboratory handling. Therefore, **Publication I** elaborated on the influence of antioxidant additives (ascorbic acid and pyruvate) on tigecycline stability in cation-adjusted Mueller Hinton broth. It was found that tigecycline could be stabilized by adding 2% pyruvate while its antibiotic activity was maintained. Subsequently, these results enabled the long-term *in vitro* hollow fiber studies of tigecycline against clinical *Klebsiella pneumoniae* isolates, which are described in **Publication II**.

Publication II aimed to improve tigecycline's *in vitro* efficacy against *Klebsiella pneumoniae* isolates using increased daily doses, or new dosing regimens. In addition, resistance development was recorded and genomically analyzed. As a result, only an intensified dose and regimen (200 mg LD, 100 mg q8h MD vs. approved 100 mg LD, 50 mg q12h MD) prevented regrowth of *Klebsiella pneumoniae* subpopulations with a MIC of 0.125 mg/L. Consequently, a limited *in vitro* dose optimization potential was concluded. However, the investigated MIC is far lower than the current clinical epidemiological cut-off value (ECOFF) of *Klebsiella pneumoniae* (2 mg/L). Furthermore, a drug-induced regrowth of resistant subpopulations was observed, in which an up to 32-fold increased MIC could be measured. Tigecycline-induced mutations were identified and corresponded to previously described clinical observations. Moreover, the observations made in **Publication II** support the hypothesis that clinical failure may be related to progression of infection. Therefore, it

was inferred that the currently recommended breakpoint of MIC 1 mg/L for infections caused by MDR-strains and for tigecycline high-dose therapy (100 mg, 100 mg q12h) might be insufficient.

Publication III described tigecycline monotherapy pharmacokinetics in an underrepresented special patient population: the critically ill, liver impaired patients. A pharmacometric covariate analysis was used to investigate a covariate-based dose reduction guided by clinical liver parameters. Additionally, their ability to guide a dose adaptation was compared to the currently used Child-Pugh score. As a result, this population had significantly different pharmacokinetics (e.g., clearance (CL) of: 8.6 L/h), compared to those obtained from non-critically ill (e.g. CL: 16.8 L/h[1], 18.6 L/h[2]). Furthermore, it was observed that a maintenance dose reduction from 50 mg to 25 mg in critically ill, severely liver impaired patients exhibited the same drug exposure as 100 mg in non-critically ill patients. However, no correlation between drug exposure and clinical cure was observed. Moreover, total bilirubin (≥ 10 mg/dL) and MELD-score (≥ 30) have been identified as predictive measures for drug exposure, whereas they were not superior to the Child Pugh score to guide a dose reduction. Overall, there are several ways to perform pharmacometric covariate analysis, with some methods rarely used or at least poorly represented in the literature. Therefore, **Publication IV** provided an in-depth evaluation of the most often used stepwise covariate modelling technique ('scm'), compared to the novel full random effects modelling ('frem'). Therefore, various assumptions of dataset size, covariate effect magnitude and -collinearity were evaluated in a simulation study. Moreover, this study introduced 'frem$_{posthoc}$' to guide, a covariate backward elimination from a 'frem' model. Both 'scm' and 'frem$_{posthoc}$' showed overestimated and unprecise covariate coefficients in small N datasets with a low power to identify the true covariate. The power of 'frem$_{posthoc}$' was up to three times higher compared to 'scm', which also resulted in better accuracy and precision of the estimates. Both methods were highly reliable in large datasets (N > 100). Without the selection step 'frem' models provided unbiased estimates with superior precision compared to 'scm' in small N datasets. Overall, 'frem$_{posthoc}$' turned out as a suitable new application of the 'frem' to guide covariate selection without forfeiting power, precision, and accuracy in large datasets, while showing superiority to 'scm' in small N datasets.

In summary, the presented results enabled a long-term *in vitro* investigation of tigecycline, but found that its dose optimization potential was limited for *Klebsiella pneumoniae* to an MIC of 0.125 mg/L. Moreover, this work contributed to a deeper and quantitative understanding of tigecycline in critically ill patients and concluded that its use in monotherapy must be questioned and possibly reevaluated.

1   Introduction

1.1   Infectious diseases and antibiotic therapy

Anne Miller became the first person in the world to be saved by an antibiotic back in 1942[3]. Since then, penicillin revolutionized the treatment of infectious diseases and many new antibiotics have greatly reduced the mortality and saved thousands of lives across all age groups. The commercialisation of antibiotics was a major milestone in history of medicine and were once considered as 'medical miracle'[4], but their use, but also overuse and misuse of them, have led to development of antibiotic resistance. Thus, infectious diseases reoccur as a major cause of death[3]. The golden age of antibiotics refers to a period between 1940 and 1960 when several important antibiotics were discovered and brought into clinical use. Since then the discovery and development has slowed down and only a few new drug classes have been introduced: oxazolidinones, lipopeptides, mutilins[5]. This is due to multiple factors, including increasing difficulties to find new targets, high cost and lengthy development processes and the rise of antibiotic resistance. The lack of new antibiotics has become a major concern, as existing antibiotics are becoming less effective, and the development of new antibiotics still is a slow process. This conclusively created difficulties for health care systems worldwide[6].

Infections caused by antibiotic resistance bacteria can affect any person, but multimorbid special patient populations, e.g. critically ill patients, are threatened by a higher risk of mortality[7]. Despite the efforts made by introducing guidelines or antibiotic stewardships in clinical practice, 700.000 deaths were assigned to infections caused by drug resistant pathogens globally[6]. As an example, in 2017 (United States of America) 9100 deaths out of 194.400 infections occurred with extended spectrum beta lactamase (ESBL) producing *Enterobacteriaceae* and 1100 deaths out of 13100 infections were related to carbapenem-resistance *Enterobacteriaceae*[3]. Most prominent representative of this multi resistant gram-negative family are *Escherichia coli* and *Klebsiella pneumoniae* with an increasing incidence over the past years. The following section introduces multiseriate gram-negative bacteria with a focus on *Klebsiella Pneumoniae*.

1.1.1   Gram-negative and multidrug resistant bacteria

Gram-negative bacteria have a peptidoglycan cell wall, which is between a cytoplasmic cell membrane and the outer membrane, distinguishing them from gram-positives. As a result, antibiotic drug pharmacokinetics are innately different with respect to penetration and retention. They rapidly acquire resistance against antibiotics through new, inactivating proteins, target alterations, restricted cell entries or efflux pumps[8,9].

The term multi-drug resistant organism (MDRO) literally means 'resistant to more than one available antibiotic' [10,11], which makes them difficult to treat in the clinics.

1.1.1.1   *Klebsiella pneumoniae*

Klebsiella pneumoniae is a major representative of the family *Enterobacterales*. This bacterium is an essential pathogen causing life threatening nosocomial infections such as pneumonia, surgical wound infections, meningitis, and bloodstream infections[12].

ESBL is a type of enzyme produced by different bacteria, including *Klebsiella pneumoniae*. This enzyme can inactivate a wide range of beta lactam antibiotics, and for infections caused by bacteria carrying this enzyme, carbapenems remain a last treatment option. Nevertheless, carbapenem hydrolyzing enzymes in *Klebsiella pneumoniae*, for instance *Klebsiella pneumoniae* carbapenemase (KPC), oxacilinase-48 (OXA-48), New Delhi Metallo-beta-lactamase (NDM) or Verona integron-encoded metallo-beta lactamase, have been increasingly reported which further challenge its treatment.

Tigecycline is no first line treatment option for MDR bacterial infection, but it has *in vitro* activity against ESBLS, NDM, carbapenem resistant *Enterobacterales* (CRE), CRE-KPC, CRE-OXA-48[13,12]. Thus, tigecycline remains a last resort antibiotic therapy in cases where no other treatment options are available.

1.1.2   Tigecycline

Tigecycline is a last resort antibiotic, approved by the Food and Drug Administration (FDA) in 2005 as a first in class glycylcycline. It evolved by addressing resistance mechanisms against tetracyclines derived from minocycline as a backbone[14]. Tigecycline has a broad spectrum of activity against

gram-positive and gram-negative bacteria, whereas *Pseudomonas aeruginosa* is not susceptible.[15,16] The mechanism of action is a steric hindrance of the 30S ribosomal subunit with blocking the entry of amino-acetyl transfer ribonucleic acid (RNA) into the A side[17,18].

Tigecycline is approved to treat complicated skin and skin structure infections (cSSI)[19], complicated intra-abdominal infections (cIAI)[20], as well as community acquired pneumoniae[21]. The recommended standard dosing composes of 100 mg loading dose (LD) followed by 50 mg q12 h. Severely liver impaired patients (guided by Child Pugh score C) have a 50.6 % reduced drug clearance, thus the maintenance dose (MD) should be reduced to 25 mg[22]. Clinical studies showed a high variability between healthy volunteers, intensive care patients (ICU) and non-ICU patients with reported values for clearance (CL) of $7.5 - 23.1$ L and central volume of distribution (V_c) of $212.2 - 1088$ L[23,22,24,25]. Moreover, tigecycline shows a rarely occurring atypical nonlinear protein binding at therapeutic concentrations[26], meaning that the fraction unbound is higher at lower concentrations (66.3 %) and lower at higher concentrations (41.3 %)[27].

Over the past years, several clinical trials were published, using tigecycline in approved indications, as well as in off-label use. A meta-analysis revealed an increased all-cause mortality when using tigecycline at standard dose (100 mg LD, 50 mg q12h) versus the comparators. The adjusted risk difference for death was 0.6 % ($0.1 - 1.2$ %)[28], leading to an FDA black box warning letter. Overall, the deaths were related to progression of infection during treatment, complications of infections, or other underlying medical conditions (FDA Drug Safety Communication, 09/01/2010, 9/21/2013).

To address this, clinical trials used an increased MD of 100 mg q12h and observed increased microbial eradication and clinical cure, while maintaining a comparable side effect profile as the standard dose regimen[24,29,30,31,32]. In December 2018, this lead to the EUCAST recommendation of high dose tigecycline (100 mg q12h) for the treatment of infections caused by muti-resistant pathogens up to an MIC of 1 mg/L[33]. This was confirmed and re-evaluated in July 2022[34]. As uncertainty about efficacious doses remains, further improvements are required[24,35,36].

1.1.3   Special patient populations

A special patient population describes a population, which does not reflect most of the humankind (e.g., paediatrics, elderly, obese, pregnant women, or patients suffering from severe diseases). They

are more vulnerable compared to healthy humans, necessitating specific considerations for safe and efficacious dosing regimens.

The paradigm 'one size fits all' ignores the heterogeneity of a patient population and many labels of already marketed drugs used to ignore this fact during their clinical trials. Thus, these patients remain unstudied which results in uncertainty about efficacy and safety of a dosing regimen. The FDA affirms the importance of drug dosing information in special patient populations by emphasizing the diversity of clinical trial populations[37]. Progress is made in this field on the clinical development side, whereas missing knowledge for already approved drugs is caught up in so called 'small N' clinical trials with up to 20-50 individuals in a rather academical framework. In these trials however, uncertainty about accuracy and precision of the results, as well as uncertainty about the choice of covariate analysis methods arise since population pharmacokinetics analysis were originally developed to study larger cohorts.

1.1.3.1   *Critically ill patients*

In case of life-threatening multimorbidity, a patient is called critically ill. Physiological changes of the cardiovascular or pulmonary system and/or renal, hepatic function are commonly present and increase the risk of mortality. Those mentioned factors influence the pharmacokinetics (PK), but also the pharmacodynamic (PD) of drugs. High patient heterogeneity and rare data availability impede PK predictions.

Infectious diseases are frequently present at intensive care units and more likely related to MDRO[38,39]. The risk of sub- or super therapeutic doses inducing therapeutic failure, which may cause resistance development or drug intoxication is higher in ICU compared to non-ICU patients. Hence, antibiotic treatment is challenging in this population[40].

Suboptimal care leads to progression of infections up to sepsis or septic shocks and are a major challenge for ICU clinicians. Sepsis or septic shocks are associated with a high mortality and are a leading cause of deaths[41]. Critically illness comes along with organ dysfunction or even failure, worsening in case of sepsis.

The kidney and liver represent important drug elimination organs. In cases of organ impairment, drugs might accumulate in the human body, driving dose reductions. Mainly the creatinine clearance serves as a surrogate parameter for kidney function and as a guide for dose adjustments,

whereas no individual biomarker informing about drug liver clearance has been identified yet. Drugs that are highly cleared via the liver are typically dose-adjusted employing the Child Pugh score[42,43]. This bears some limitations, as a static assignment to scores does not cover disease progression. Moreover, only little information about covariate-based dosing options is available for liver-impaired patients. To address this, researchers develop population PK (popPK) models describing the relationship between drug concentrations and patients' individual covariates to explain variabilities in exposure. By using covariates for dose adjustment, novel dosing strategies can be derived.

The following section introduces liver specific parameters as possible covariates in popPK models.

1.1.4   Individual patient parameters for liver function assessment

The liver is a multifunctional organ of the human body and has its major function in biotransformation, transport- and excretion of xenobiotics. Derived from the livers' critical functions, organ impairment can have a severe impact on multiple mechanisms, including the PK of a drug. To assess liver function in critically ill patients, a variety of parameters and liver function tests are routinely included in diagnostics. There are directly measurable parameters such as aspartate aminotransferase, alanine aminotransferase, γ-glutamyl-transferase, alkaline phosphatase, bilirubin, albumin levels, and coagulation factors. In case of damaged or inflamed liver tissues, enzymes are released into the bloodstream. This can cause the elevation of laboratory measured parameters which are used in diagnoses of liver diseases. Liver function parameters are not solely related to liver disease, as they can also be elevated temporarily in case of infections or alcohol consumption. Liver enzymes can indirectly inform about liver cell damage, but they do not provide specific information about the metabolization processes or biliary excretion of a drug.

Hence, those routinely measured serum liver function parameters are known to be less predictive to inform about drug exposure, as they are not suitable to predict liver failure by its own[44].

Therefore, physicians developed scores carrying bundled liver information e.g., Child Pugh or MELD score. Alternatively, dynamic tests are applied based on intravenous administration of hepatically cleared substances. These tests measure either plasma disappearance, metabolite concentrations in urine or in exhaled air[45,46].

The Child Pugh Score, assess the severity of liver disease, particularly cirrhosis and was originally developed to predict mortality during surgery in 1964 and further developed in 1973[47]. Nowadays, it is used to inform about liver transplantation necessity and treatment decisions. The Child Pugh score is graded from A to C with increasing severity of dysfunction (mild, moderate, severe) and calculated by bilirubin, albumin, prothrombin time, ascites, and encephalopathy grades. Consequently, it displays a multiorgan assessment.

To develop dose recommendations for cirrhotic patients, the FDA 'Guidance for Industry' recommends hepatic impairment trials with patients of all three Child Pugh score categories[48]. Dose adjustment via the Child Pugh score has been added to several drug lables[49]. But still the static classification schemes lack sensitivity to inform about drug elimination since none of the considered biomarkers correlates with hepatic drug clearance as creatinine clearance does with renal drug clearance. The prescribing information of tigecycline recommends Child Pugh Score based dose adjustment for patients with severe liver impairment, because in these patients the drug clearance is severely reduced. Moreover, tigecycline clearance has also shown correlation with total bilirubin[50] and MELD[51] score, opening up important dose adjustment opportunities for this last resort antibiotic.

Another composite score is the model for end-stage liver disease (MELD score) which includes bilirubin, serum creatinine and the international normalized ratio of prothrombin time[52]. It was developed to assess the severity of liver disease and predict the likelihood of three month survival in patients with chronic liver disease or those awaiting liver transplantation[53]. Until now MELD score was barely academically investigated as a parameter for dose adjustment in cirrhotic patients[51,54]. Since data is rare and authorities refrain from recommending an investigation yet, MELD score needs further evaluation.

The Liver Maximum capacity test (LiMAx®) is a novel breath test to determine the current liver function or to monitor disease progression via metabolization of 13C-methacetin[55]. A published pharmacokinetic study described a strong association of LiMAx test to hepatic linezolid clearance in liver impaired patients[56]. This publication reports a pilot study investigating the potential use of LiMAx for dose adjustments with the advantage of capturing the metabolic capacity of the organ of interest. Further investigations of its ability to guide dosing decisions for hepatically metabolized drugs is promising.

1.2   *In vitro* experiments

Interesting approaches for dose improvements are *in vitro* experiments. Such experiments can guide dose optimization, as they inform about an exposure response relationship of a drug to a pathogen of interest. Dynamic *in vitro* experiments help to simulate the human-like pharmacokinetics of dosing regimens of interest allowing for insights into exposure and time dependent pharmacological effects, without ethical concerns regarding animal testing or a clinical trial. However, *in vitro* testing with tigecycline is challenging: The drug is sensitive to oxygen, light, temperature, and pH. Therefore, freshly prepared (< 12 h) cation-adjusted Mueller Hinton broth (ca-MHB) should be used to prevent degradation, as no cost efficacious stabilizing agent was identified yet[57,58,59].

1.2.1.1   *MIC determination*

The lowest antibiotic concentration that prevents visible bacterial growth is called minimum inhibitory concentration (MIC). Its determination is standardized according to the Clinical and Laboratory Standards Institute (CLSI) guideline[60].

The MIC is an important clinical drug and dosing decision guide and bacteria are categorized to either susceptible (S), increased exposure (I) and resistant (R) by the European Committee On Antimicrobial Susceptibility Testing (EUCAST)[61]. These categories are defines as following:

- (S) defines the standard dose regimen to be likely to for therapeutic success.
- (I) characterizes the bacteria as susceptible, whereas an increased exposure is necessary to achieve therapeutic success.
- (R) defines resistance corresponding to a high likelihood of therapeutic failure.

The MIC breakpoint for tigecycline against *Staphylococcus aureus* is currently defined as ≤ 0.5 mg/L for susceptible (S) and >0.5 mg/L for resistant (R) bacteria[62]. *Enterobacterales* (e.g., *Klebsiella pneumoniae)* are deemed to respond to tigecycline high dose regimen up to an MIC of 1 mg/L[62,33].

1.2.1.2   *Time kill curves*

Time kill curves are an experimental tool used to evaluate the bactericidal or bacteriostatic activity of antimicrobial agents against bacterial pathogens. They involve monitoring the growth or survival of a bacterial population over time in the presence of an antimicrobial agent.

In a typical time kill curve experiment, a standardized inoculum of the bacteria is exposed to a range of concentrations of the antimicrobial agent in vitro. At predefined time points, samples are taken from the culture flask and plated on nutrient agar to determine the number of viable bacteria present at that time point. The number of bacteria is mostly expressed as $\log_{10}$ colony forming units (CFU)/mL. The resulting data is used to plot a time kill curve, which shows the change in bacterial viability over time in response to the antimicrobial agent.

1.2.1.3   *Hollow fiber infection model*

The hollow fiber infection model (HFIM) is a dynamic *in vitro* tool used in preclinical studies to evaluate the effect of antimicrobial agents against bacterial pathogens over time. Programmable pumps are used to replicate clinical dosing regimens and their corresponding human-like PK profiles. The drug is added to the central reservoir, containing the bacterial growth medium. The elimination kinetics are controlled by the addition of drug free media to the central reservoir, whereas the volume is kept constant over the experiment duration. Concentration time profiles are thereby mimicked precisely. The test organisms are retained in a dialysis-like cartridge and thereby physically separated from the central reservoir by a semi-permeable membrane. Liquids are continuously recirculating to assure nutrient supply, as well as the distribution infused drug. An exemplary setup is shown in Figure 1.

In the scope of PK/PD investigations, the hollow fiber system has firstly been described by Blaser et. al[63] and found its broad application in *in vitro* exposure response analysis for antibiotics against *Mycobacterium tuberculosis*[64]. *Mycobacterium tuberculosis* is a very slowly growing bacteria, and the continuous nutrient supply of the HFIM supports a user individual adaptation of experiment duration up to months. Moreover, the European Medical Agency (EMA) published an option letter[65]. Within this letter, they underlined their support for preclinical tests using this method to investigate resistance development over time, as well as to investigate combination therapy.

This work used the HFIM to investigate tigecycline concentrations against clinical isolates.
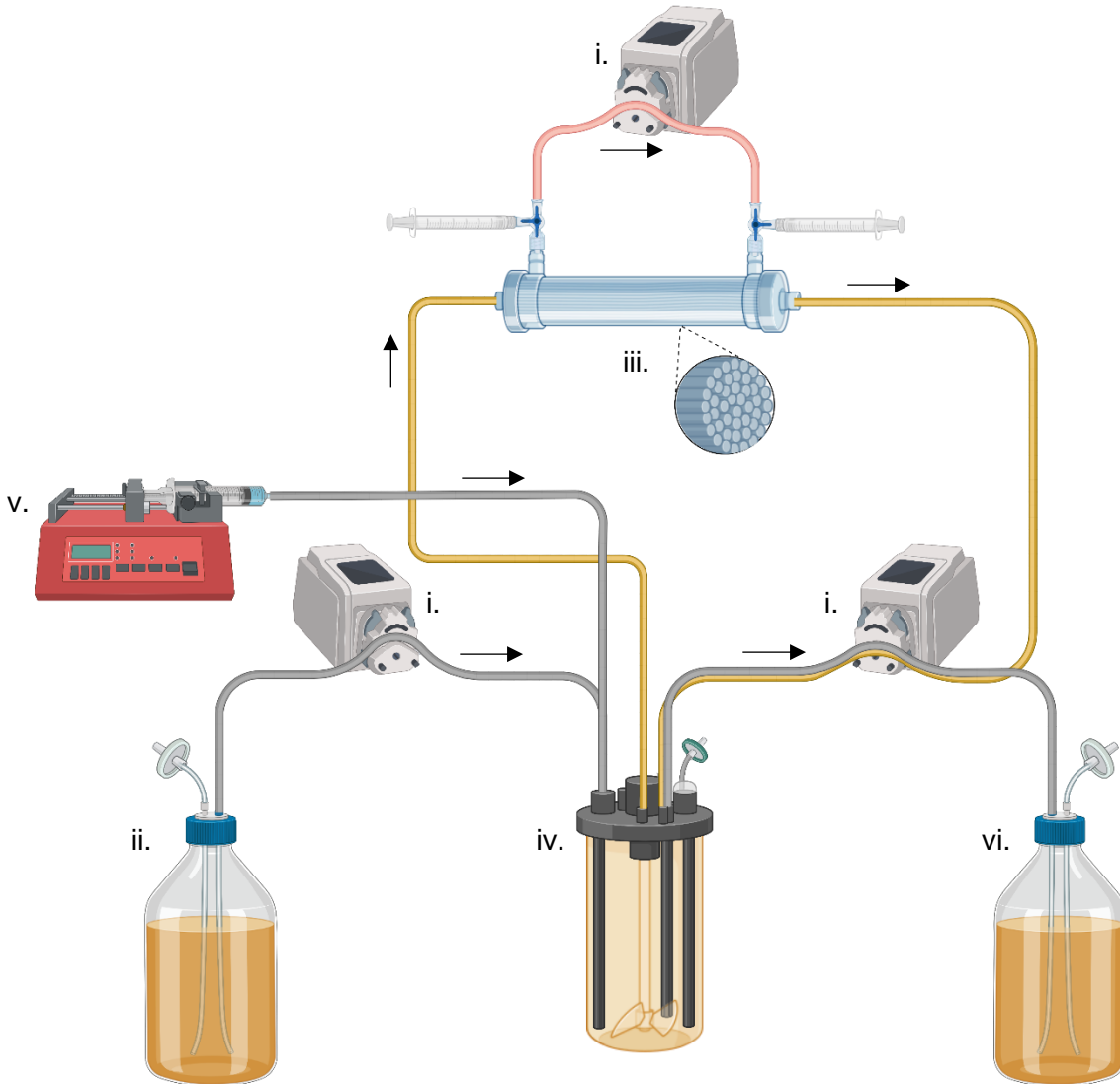
Figure 1 Schematic set up of the hollow fiber infection model. All liquid flows are guided via peristaltic pumps (i.). Continuous nutrient supply is guaranteed via drug-free bacterial growth medium (ii.). Bacteria are kept in the dialysis cartridge (iii.) and are circulating against the direction circulation of the central compartment to assure equal distribution of nutrients, drug and to prevent biofilm formation. The drug is infused into the central compartment (iv.) by a programmable syringe pump (v.) and eliminated drug and bacterial waste products are collected in a waste bin (vi.). The graphic was created with BioRender.com

1.3   Pharmacometric modelling and simulations

1.3.1   Pharmacometrics

Pharmacometrics is an emerging science at the intersection between pharmaceutical sciences, mathematics, statistics, and data science. A pharmacometric model can mathematically describe the complexity of the human body, e.g. the adsorption, distribution, metabolism, and elimination processes. The aim is to quantify and characterize drug behavior and to assist in e.g., understanding variability within a population, dose optimisation, dose selection, or simulating new scenarios. Nowadays those models are also of regulatory interest and requested for drug applications[66].

1.3.2   Pharmacokinetics

In a generic sense, PK describes 'what the body does to the drug' and can be structured in adsorption, distribution, metabolism, and elimination; short 'ADME' principles. Through the interaction of these processes, drug specific concentration-time profiles can be derived providing information about drug exposure. To quantitatively measure the drug behaviour within the body, common PK parameters include flow parameters such as CL or intercompartmental clearance (Q), as well as disposition parameters such as central (V_c) or peripheral volume of distribution (V_p). The CL is a rate, that expresses the ability of the body to eliminate the drug, usually reported with a unit of [L/h]. If a clinical trial collected PK measurements in urine, CL can also be quantified for renal and non-renal elimination processes. The V_c, commonly reported in [L] is an apparent volume reflecting the distribution of a drug in the central compartment and can be influenced by e.g., protein binding. The central compartment is usually defined as the blood or plasma and highly perfused tissues. The V_p represent the apparent volume in which the drug is distributed in the deep tissues outside of the central compartment. These include less perfused organs, such as fat or skin and is influenced by the lipophilicity of a drug or tissue binding.

The drug exposure in plasma or target site can be expressed as maximum concentration (C_{max}), minimum concentration (C_{min}) or the area under the concentration time curve (AUC).

Individual patient characteristics can alter ADME processes resulting in individual drug exposure in dependence of the patients' specific dispositions (e.g., body, disease, or genetic).

Those patient variables are called covariates and are often related to CL or V_c, the major representatives of PK parameters shaping concentration time profiles. CL can be separated into renal and non-renal clearance; the latter often being associated with hepatic clearance. In general, CL is the PK parameter of authority's interest to guide the dose in special patient populations as it determines the maintenance dose of a drug.

1.3.3   Pharmacodynamics

Pharmacodynamics (PD) can be described as 'what does the drug to the body' and with that, it is a key component to understand the dose-exposure-response relationship of a drug. In general, the desired pharmacological effect can be any process of the human body that gets stimulated, depressed, or blocked by a drug. Parameters to describe the PD usually include potency, efficacy, and toxicity: Potency refers to the concentration of a drug required to produce a specific effect, while efficacy describes the maximum effect that a drug can produce. Toxicity refers to the harmful effects of a drug on the body and can be separated into on-target and off-target toxicity.

In the case of antimicrobial drugs, the pharmacodynamics are related to bacteriostatic or bactericidal effects on the pathogens.

1.3.4   PK/PD

By combining the PK and PD information, a dose-exposure-response relationship can be established, which is used to guide the optimal dosage. Optimally, the identified dose and dose regimen achieve a therapeutic effect while side effects are minimized.

In the field of antimicrobial therapy, PK is usually described as plasma or target site concentrations and PD as clinical treatment outcome, e.g., clinical cure or microbial eradication. For *in vitro* experiments PD refers to antibacterial effect with e.g., reduction in bacterial load over time.

A PK/PD index is a way to express the combined information of PK and PD. For infectious diseases three different exposure response relationships haven been identified to link bacterial susceptibility to treatment success: On the one hand a concentration dependent case, expressed as AUC divided by the MIC (AUC/MIC), or C_{max} divided by MIC (C_{max}/MIC). On the other hand, if the drug effect on the bacteria is time dependent, it is expressed as time or percent time above the MIC ($T_{> MIC}$)[67]. In

case an index refers to unbound drug concentrations the abbreviation is complemented by an '*f*'. The magnitude of the desired treatment success with the suitable dose for each index (PK/PD target), is induvial for the bacteria, the antibiotic, and the location of infection. These targets are developed in either *in vitro* experiments, animal models or clinical trials[68]. A reevaluation of doses to achieve these targets is potentially necessary, as the drug PK may be altered in special patient populations (e.g., critically ill patients).

For tigecycline an AUC/MIC exposure-relationship was identified in mice and confirmed in clinical trials with a magnitude of 6.96 and 17.9 to treat cSSI and cIAI, respectively[69].

1.3.5   Nonlinear Mixed Effects Modelling

Mathematical models are applied to describe PK/PD characteristics within a patient population. Nonlinear mixed effects modelling (NLME) is the most used methodology in the scope of the population approach, first introduced by Sheiner et. al [70], and has replaced the naive pooling or standard two stage approach. This work used NLME in all performed modelling work, which will be explained in more detail in the following section.

The term 'nonlinear' in NLME refers to nonlinear regression giving the best vector of model parameters using approximation algorithms. These algorithms are either based on maximum likelihood estimation, or Monte Carlo sampling methods[71,72].

Moreover, 'mixed effects' in NLME stands for the ability to estimate fixed (structural model parameters) and random effects parameters (variability components) simultaneously for a population[73]. As a result, parameters describing the population and each individual are obtained. The NLME population approach can answer questions like 'why do individuals differ' or 'how do they differ quantitatively' and this by using very sparse, unbalanced, up to rich datasets. A population pharmacometric model composes of a structural model, a statistical model, and a covariate submodel[74]. The following section introduces these sub models.

1.3.5.1   *Structural base model*

The structural base model in sense of NLME modelling describes the central tendency of population parameters to fit the observed data. This set of model parameters refers to fixed effects, such as typical clearance, or volume of distribution of the respective study population.

1.3.5.2   *Statistical model*

The statistical model expresses variability of the population model. One the one hand, differences in PK between individuals within a population are described via the inter-individual variability (IIV) or also known as between subject variability term. On the other hand, the statistical model may also include the inter-occasion variability (IOV). This relates the PK variability within one individual across multiple time points. Those occasions could be defined as e.g., dosing timepoints or clinical visits. Furthermore, residual variability or unexplained variability refers to the remaining discrepancies that remain unaccounted for in the individual prediction after considering all the known factors or sources of variability in the pharmacometric model. These terms of variabilities refer to the random effects of a developed model.

1.3.5.3   *Covariate analysis*

The covariate model includes intrinsic and extrinsic patient individual variables, such as demographics (e.g., age, sex, race), organ/disease specific information (e.g., creatinine clearance, Child Pugh score, type of infection), or study design information (e.g., formulation types, food intake) into the pharmacometric model. The aim of including covariates is to better explain the observed IIV among patients within a population, which also increases the model predictability. Furthermore, they help to understand the PK-PD relationships, so that a covariate model can also provide a valuable base for dose optimizations. Typically, the dataset includes several covariates, although not all of them are necessarily useful and informative for the resulting model. This can be due to lacking statistical significance or clinical relevance. Covariates can either be continuous (bilirubin, MELD score) or categorical (Child Pugh score) which is addressed in the model code differently: The relationship of a continuous covariates on the structural model parameter of interest can be a linear, power, or exponential function. Categorical covariates are usually included as fractional change of the parameter of interest. To analyze covariates in a dataset, statistical methods based on the log likelihood ratio test or full model approaches are available.

The commonly used statistical method is the so-called stepwise covariate modelling technique ('scm')[75], which was also applied to this work. This method fully relies on statistical criteria and captures the covariate effects in fixed-effect coefficients. The basic scm algorithm proceeds in a forward inclusion step and a backward elimination phase usually related to p-values of <0.05, <0.01

respectively. In the forward inclusion each pre-defined parameter-covariate combination is tested univariately. The objective function value (OFV) provides a quantitative measure of how well the model represents the observed data and is calculated as minus twice the log-likelihood function in NONMEM. A p-value of 0.05 is related to a drop of objective function value (dOFV) of -3.84 (degrees of freedom (df) =1, χ^2 distribution). The combination that yields the largest dOFV is retained in the model. The remaining parameter-covariate relationships are then tested again in the updated model and the one with the largest dOFV is again retained in the model. This stepwise inclusion proceeds until no more significant relationships can be identified. Conditional on the model identified during the forward inclusion, the backward elimination procedure removes the significant covariates in a stepwise manner at a stricter significance level (e.g., OFV: 6.63, df = 1, p-value: 0.01). Once all parameter-covariate relationships are significant, the final covariate model has been built.

On the other hand, full model approaches are available. In this thesis, the full random effects modelling technique ('frem') is used as a full model approach[76]. 'Frem' is a novel technique and barely represented in literature so far[77,78,79]. This method treats covariates as observations, meaning that covariates are handled as random effects in this method[80]. In detail, the 'frem' routine estimates a full IIV random effect covariance matrix in the omega block. This includes parameter IIV, covariate IIV and the covariance between these two. To perform this estimation, the standard deviation, but also the typical covariate value is calculated. By utilizing this estimation technique, correlated covariates can be included in the model while single covariate effects are identifiable and missing covariates can be derived from covariances[81]. Furthermore, the common covariate relationships (linear, exponential, power) that are tested in fixed effect covariate models can also be explored in a 'frem' model. For this either an IIV or covariate data transformation is needed. The full fixed effects model, representing another full model approach, is mathematically equivalent to a 'frem' model. Thereby a 'frem' model can be translated into a full fixed effects model by calculating the covariate coefficient from the ratio of the covariance between the parameter and covariate variability to the covariate variance.

1.3.6 Application of PK/PD models

'Learning and confirming' is essential in drug development[82]. Over the past decades the integration of available data and knowledge enhanced drug development efficiency, decision making and reduced costs[83]. Pre-clinical or early-stage data can be used to generate hypotheses that are being investigated and ideally confirmed in large clinical trials. What is the optimal dose? What drug exposure can we expect if the patient has a kidney or liver impairment? How often should we administer the drug? How many study participants do we need in our trial? There are almost unlimited sets of 'what if' scenarios to generate hypotheses where simulations can extrapolate to the unknown[84]. With an adequate model as a basis, Monte Carlo simulations[85] are used in the field of infectious diseases to generate data for e.g., PK/PD target evaluations and effective dose regimes, that have not been studied yet. Additionally, there are more advanced simulations like stochastic simulation and estimation (SSE). In the drug development setting, SSEs are used for clinical trials simulations, which aim to optimize sampling timepoints as well as number of study participants to overall create a framework that provides accurate and precise model parameters. In this work SSEs were applied to evaluate the performance of 'scm' and 'frem' in different clinical settings. With that power, accuracy, and precision of parameters across unlimited scenarios of interest can be evaluated and applied to drug development.

2   Objectives

Critically ill patients are at considerable risk of antibiotic treatment failure and resistant bacteria are on the rise. As new therapy options are scarce, dose improvement of available drugs is a way to tackle the current situation. Tigecycline remains a last option for clinicians. The aim of this thesis was to evaluate the dose optimization potential of tigecycline using *in vitro* and clinical data, both supported by pharmacometric approaches. For the *in vitro* part, a stability study aimed to prevent tigecycline degradation as a prerequisite to conduct long duration hollow fiber experiments. These experiments served as a tool to investigate dose escalations and changes in dose regimens against clinical *Klebsiella pneumoniae* strains with the aim to enhance tigecycline's *in vitro* efficacy. In the clinical environment we have an unmet need for dose improvements in special patient populations. The Child Pugh score guides a covariate-based dosing strategy for tigecycline in liver impaired patients. As this is a static parameter, the aim was to compare its ability to predict drug exposure in comparison to non-static liver function parameters, based on a clinical dataset. For this a pharmacometric covariate model served as a tool, while several methods are available and uncertainty about method selection small N datasets is present. To enlighten method characteristics a simulation study compared the characteristics of the most often used 'scm' and novel 'frem' method .

This work is based on four publications covering investigations for the translational dose optimization of tigecycline using *in vitro* and in silico approaches. The individual scopes of publication I-IV were as follows:

Publication I: Stability studies with tigecycline in bacterial growth medium

- Creating conditions to use tigecycline in long-duration *in vitro* experiments
- Investigation of low-cost supplements (pyruvate and ascorbic acid) for their ability to protect the sensitive, unstable tigecycline from degradation
- Quantifying tigecycline stability in cation-adjusted Mueller Hinton broth
- Comparing tigecycline's antibiotic activity in supplemented and non-supplemented cation adjusted Mueller Hinton broth using time kill curves over 24h

Publication II: Pharmacokinetic/pharmacodynamic evaluation of tigecycline dosing in a hollow fiber infection model against clinical *bla*-KPC producing *Klebsiella pneumoniae* isolates.

- Mimicking human tigecycline pharmacokinetics using the hollow fiber infection model
- Exploring dose optimization opportunities of escalated daily doses, and variations of the dose regimen up to continuous infusions to enhance the *in vitro* efficacy
- Investigation of resistance development before and after tigecycline exposure via MIC determination and manifestation of genetic changes using whole genome sequencing of resistant strains
- Establishing a PK/PD model to describe the dose-exposure-response relationship of tigecycline against *Klebsiella pneumoniae* and translation to clinical patients using Monte Carlo simulations

Publication III: Tigecycline in liver impaired critically ill patients

- Development of a population pharmacokinetic model to describe tigecycline pharmacokinetics in critically ill liver impaired patients
- Assessment of covariate relationships to predict tigecycline drug exposure in this underrepresented study population
- Dose adjustment simulations using the developed covariate model to challenge the Child Pugh score

Publication IV:A covariate analysis method comparison: Full random effects modelling ('frem') vs. stepwise covariate modelling ('scm')

- Enhancing the understanding of covariate modelling techniques through a simulation study that compares the most often used stepwise covariate modelling technique to the novel full random effects approach
- Comparative interpretation of results from a practical use perspective and a statistical similar framework using simulated clinical datasets, which include various assumptions of dataset size, covariate effect magnitude and -collinearity

3   Cumulative part

The cumulative part of this thesis presents the key results of four, shorty summarized, peer-reviewed publications. This work focused on various aspects to optimize tigecycline's dose through an *in vitro* and clinical perspective, supported by pharmacometric approaches.

The articles are published in *European Journal of Clinical Microbiology & Infectious Diseases*[86], *Diagnostic Microbiology & Infectious Disease*[87], *Antibiotics*[88] and *Journal of Pharmacokinetics and Pharmacodynamics*[89].

3.1   Publication I

Stability studies with tigecycline in bacterial growth medium and impact of stabilizing agents

Lisa F. Amann[1], Emilia Ruda Vicente[1], Mareike Rathke[1], Astrid Broeker[1], Maria Riedner[2], Sebastian G. Wicha[1]

[1]Department of Clinical Pharmacy, Institute of Pharmacy, University of Hamburg, Hamburg, Germany

Synopsis

Tigecycline is known to be sensitive to temperature, light, and oxygen, thus the planning and execution of *in vitro* experiments are challenging. However, the *in vitro* stability is key to obtain reliable information on bacterial susceptibility, which is also used to guide therapeutic decisions in clinical practice. This study investigated antioxidative stabilizing agents as additives to the cation-adjusted Mueller Hinton bacterial growth medium and tigecycline's degradation was quantitatively analysed by a chromatography assay. The stabilizing chemicals pyruvate, ascorbic acid, and the combination of both were directly investigated in their suitability for *in vitro* testing. Time-kill curves using the strain *Staphylococcus aureus* (ATCC29213) were performed in freshly prepared vs. aged growth medium with and without stabilizing agents.

A supplementation with ascorbic acid led to rapid degradation and thus to a loss of the antibacterial activity of tigecycline. This study revealed that tigecycline could be stabilized by 2% pyruvate in aged medium and its antibacterial activity was equivalent to that of freshly prepared broth without supplementation. With the identification of pyruvate as a stabilizer, this study enabled the use of tigecycline in long-term *in vitro* testing, e.g. in hollow fiber experiments..

BRIEF REPORT

Stability studies with tigecycline in bacterial growth medium and impact of stabilizing agents

Lisa F. Amann[1] · Emilia Ruda Vicente[1] · Mareike Rathke[1] · Astrid Broeker[1] · Maria Riedner[2] · Sebastian G. Wicha[1]

Abstract

Purpose This study aimed to examine the degradation of tigecycline in Mueller Hinton broth (ca-MHB), as knowledge about bacterial susceptibility is key for therapeutic decisions.

Methods Antioxidative stabilizers were evaluated on tigecycline stability in a quantitative chromatography assay and tigecycline induced kill against *Staphylococcus aureus* (ATCC29213) was determined in time kill studies.

Results Ascorbic acid caused rapid degradation of tigecycline and resulted in loss of antibacterial activity. Tigecycline was stabilized in aged broth by 2% pyruvate and bacterial growth, and tigecycline killing was similar to fresh broth without supplementation, but independent of age.

Conclusion Our results underline the importance of using freshly prepared ca-MHB or the need for stabilizers for tigecycline susceptibility testing while using aged ca-MHB.

Keywords Tigecycline · Stability · Degradation · Mueller Hinton broth · Time-kill studies

Introduction

Tigecycline is a broad-spectrum antibiotic and indicated for complicated skin and intra-abdominal infections, as well as community-acquired pneumonia [1]. Tigecycline is known to be light and oxygen sensitive [2, 3]. A growth medium age–related effect on tigecycline stability was described, probably mediated by the amount of dissolved oxygen, which can lead to inconsistencies in MIC values [4]. A novel formulation stabilized tigecycline up to 7 days by adding 0.3% ascorbic acid and 6% pyruvate as oxygen-reducing agents [2]. Nevertheless, these additives were only tested in saline and antibacterial activity was determined with *Escherichia coli* in Oxyrase-treated Mueller Hinton broth to remove the dissolved oxygen. Hence, the degradation kinetics

of tigecycline and potential impact of bacterial killing in aged vs. fresh cation-adjusted Mueller Hinton broth (ca-MHB) and the impact of stabilizing agents remain unknown.

The objective of this study was (i) to quantify the degradation process in fresh and aged ca-MHB using different stabilizing agents and (ii) to evaluate their impact on bacterial growth and tigecycline-induced kill, to derive recommendations for consistent in vitro susceptibility testing of tigecycline.

Material and methods

Materials

Lyophilized powder of tigecycline was obtained from Pfizer (New York, United States of America, LOT: J49085). *Staphylococcus aureus* (ATCC29213) was obtained from the American Type Culture Collection (Manassas, Virginia, USA). All other chemicals were purchased from Sigma-Aldrich.

Stability assay

Preparation of tigecycline samples A stock solution of tigecycline (1.0 mg/mL) was prepared in 0.9% saline solution and diluted to 10 μg/mL with fresh (< 12 h) or aged (up to 7 days

✉ Sebastian G. Wicha
sebastian.wicha@uni-hamburg.de

[1] Department of Clinical Pharmacy, Institute of Pharmacy, University of Hamburg, Bundesstraße 45, DE-20146 Hamburg, Germany

[2] Department of Chemistry, University of Hamburg, Martin-Luther-King-Platz 6, 20146 Hamburg, Germany

at 4 °C or room temperature) ca-MHB, with and without stabilizing agents, incubated at 37 °C for 24 h, protected from light stored in a Eppendorf vial rack. Stock solutions of stabilizing agents were adjusted to pH 7.0 and spiked to ca-MHB after storing. Aged ca-MHB, stored at 4 °C, spiked with 2% pyruvate (ca-MHB$_{7days\_p2\%}$), as well as the combination of 6% pyruvate and 0.3% ascorbic acid were tested (ca-MHB$_{7days\_p6\%+aa0.3\%}$). Ca-MHB spiked with 0.3% ascorbic acid was tested in freshly prepared ca-MHB (ca-MHB$_{aa0.3\%}$). Furthermore, we investigated tigecycline stability in non-supplemented ca-MHB stored 7 days at room temperature (ca-MHB$_{7days\_RT}$) versus supplementation with 2% or 6% pyruvate. The pH of ca-MHB was measured and equivalent to the manufacturer given value (pH 7.3).

HPLC analysis Calibration curve, quality control, and samples were measured by UHPLC (Ultimate 3000 SD Dionex, Softron GmbH, Germering, Germany) equipped with a Nucleoshell RP 18 (MachereyNagel, Dueren, Germany) using UV detection at 350 nm. Samples containing 0.3% ascorbic acid reached the lower limit of quantification. Therefore, a QTRAP 5500 mass spectrometer (SCIEX, Framingham, Massachusetts, USA) coupled with a 1290 Infinity HPLC II (Agilent Technologies, California, USA) was used to quantify tigecycline in these samples. A detailed description of the analytical method is described in Supplement Text 1.

Preparation of standards and quality control For each measurement, a calibration from 0.1 to 10 mg/L using seven calibrators and double determination was prepared. Two independently prepared quality controls were analyzed in each run with a high and a low concentration of tigecycline. The inaccuracy and imprecision of the assay across all analytical runs was < 12% and < 4%, respectively.

Time-kill studies

The effect of stabilizing agents on bacterial growth was tested with *Staphylococcus aureus* (ATCC29213), as recommended by CLSI [5] in three settings: (i) fresh and aged ca-MHB without adjuvants, (ii) ca-MHB$_{aa0.3\%}$, or (iii) ca-MHB$_{7days\_p2\%}$. Stock solutions of ascorbic acid (25%) were adjusted to pH 7 and spiked to aged ca-MHB to obtain a final concentration of 0.3%. The pH of the spiked ca-MHB was not altered in the presence of the stabilizing agents and identical to the value given by the manufacturer (pH 7.3). The "reference" MIC was tested in freshly prepared broth according to the CLSI guideline before the experiment [5].

Time kill curves were determined in $n = 2$ at an initial inoculum of 10^6 CFU/mL and incubated for 120 min at 37 °C to logarithmic growth phase before the antibiotic was added. Tigecycline concentrations of 0.5× MIC (0.063 μg/mL), 1× MIC (0.125 μg/mL), 2× MIC (0.25 μg/mL), 4× MIC (0.5 μg/mL), and 8× MIC (1 μg/mL), as well as growth controls were studied over 24 h. The resulting MIC was determined visually, at 24 h, in presence of stabilizing agents or in aged ca-MHB, evaluating turbidity of testing solution alongside the time kill studies.

Results

Stability studies

The stability of tigecycline in fresh and aged ca-MHB with and without adding stabilizing agents was investigated (Table 1). In 7-day-old, non-stabilized ca-MHB, a recovery of 80.1% was found within 24 h. Conversely, in fresh, non-stabilized ca-MHB, 99.6% tigecycline was measured. Moreover, tigecycline degraded already to a remaining

Table 1 Tigecycline concentrations expressed as a relative percentage of the initially measured tigecycline concentrations (= 100%) in cation-adjusted Mueller Hinton broth (ca-MHB) with or without supplementation, incubated in the dark at 37 °C over 24 h stored in Eppendorf vial racks. Ca-MHB age of 0 days was defined as ca-MHB preparation less than 12 h before the experiment started. Ca-MHB was stored up to 7 days at 4 °C or at room temperature. Storage conditions and age refer to Ca-MHB without supplements in absence of tigecycline before the 24 h incubation period with tigecycline with and without supplements at 37 °C was initiated

Matrix	Age (days)	Storage cond.	Recovery at 24 h (%)	Range (%)	p value
Ca-MHB	0		99.6	94.5–103.5	0.412
	1	4 °C	89.7	87.4–94.8	$0.400 \cdot 10^{-2}$
	7	4 °C	80.1	82.8–75.6	$2.44 \cdot 10^{-6}$
	7	Room temperature	27.9	25.9–30.0	$2.2 \cdot 10^{-16}$
Ca-MHB + 0.3% ascorbic acid	0		4.7	3.5–5.1	$2.47 \cdot 10^{-6}$
Ca-MHB + 2% pyruvate	0		98.8	97.0–100.3	$9.20 \cdot 10^{-2}$
	7	4 °C	97.1	96.4–99.6	$8.40 \cdot 10^{-2}$
	7	Room temperature	87.8	86.6–88.8	$1.69 \cdot 10^{-11}$
Ca-MHB + 0.3% ascorbic acid + 6% pyruvate	0		97.2	93.4–100.2	0.079
	7	4 °C	95.1	91.3–97.3	$6.40 \cdot 10^{-2}$
Ca-MHB + 6% pyruvate	7	Room temperature	97.1	95.6–98.5	$1.1 \cdot 10^{-2}$

concentration of 89.7% using the same ca-MHB solution 1 day after preparation. The stabilizing agents had various effects: In ca-MHB$_{aa0.3\%}$, tigecycline degraded rapidly and only 4.7% remained in a freshly prepared solution within 24 h. In ca-MHB$_{7days\_p2\%}$, we observed a stabilizing effect and 97.1% were recovered. Moreover, the combination of 6% pyruvate and 0.3% ascorbic acid, as recommended by *Jitkova* et al. [2], was inferior to 2% pyruvate alone, and a remaining concentration of 97.2%, if freshly prepared, and 95.1% in ca-MHB$_{7days\_p6\%+aa0.3\%}$ was measured. Furthermore, the stability of tigecycline was investigated in ca-MHB$_{7days\_RT}$ and the age dependency of tigecycline stability was even more observable. In MHB$_{7days\_RT}$ with 2% pyruvate, a remaining concentration of 87.8% was measured (Table 1), whereas in non-stabilized ca-MHB$_{7days\_RT}$, only 27.9% tigecycline were recovered. As described above, the combination of 0.3% ascorbic acid and 6% pyruvate was not superior to pyruvate alone so that pyruvate was increased to 6% to enhance tigecycline stability in MHB$_{7days\_RT}$ and 97.1% could be recovered after 24 h.

Time kill studies

Time kill curves were conducted to investigate the impact of tigecycline degradation on observed pharmacodynamic effects (Fig. 1). The results show that neither ascorbic acid ($p = 0.410$) nor pyruvate ($p = 0.161$) affected the natural growth in absence of tigecycline, compared to non-supplemented ca-MHB. Using fresh ca-MHB, > 1.5-log killing at > 2× MIC and moderate killing at 1× MIC were observed after 24 h. In contrast to that, at 1× MIC in 1-week-aged ca-MHB, no killing but a growth to > 1-log higher CFU/mL was observed compared to fresh broth. The growth/killing pattern in ca-MHB$_{7days\_p2\%}$ was not different from freshly prepared ca-MHB.

The strong degradation process related to 0.3% ascorbic acid translated to substantially reduced killing: Antibacterial activity at 1× MIC ceased 1 h after addition of tigecycline, and regrowth was observed even at 8× MIC.

In fresh or stabilized ca-MHB$_{7days\_p2\%}$, an MIC of 0.125 mg/L was determined. The use of aged broth led to determination of a MIC of 0.25 mg/L, in ca-MHB$_{aa0.3\%}$ > 1 mg/L, respectively, concluded by visible turbidity.
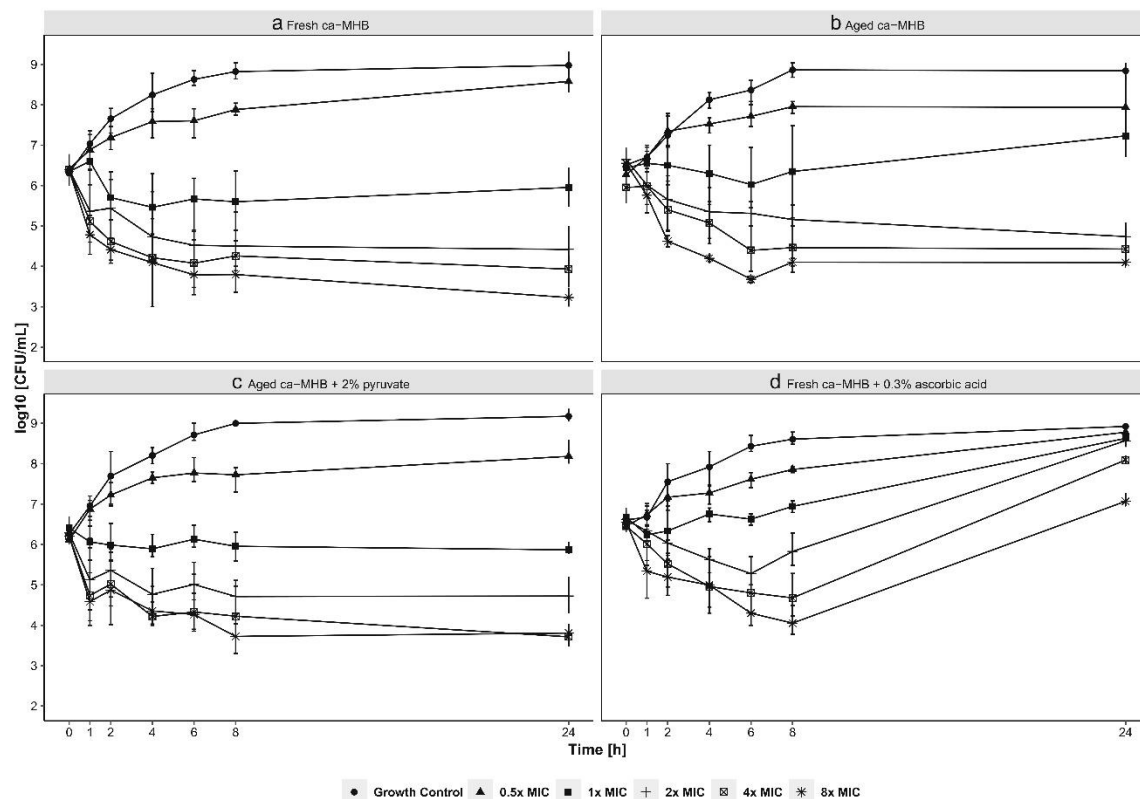
Fig. 1 Time kill curves: colony-forming units (CFU) per mL over time by MIC (minimal inhibitory concentration) of tigecycline. The reference MIC was determined according the CLSI guideline using freshly prepared ca-MHB and was 0.125 mg/L. Error bars denote range of minimum to maximum value. All experiments were carried out in duplicates. **A** Freshly prepared ca-MHB. **B** Aged ca-MHB (7 days at 4 °C). **C** Aged ca-MHB (7 days at 4 °C) supplemented with 2% pyruvate. **D** Fresh ca-MHB containing 0.3% of ascorbic acid

Discussion

The present study elucidates the stability of tigecycline in the most important bacterial growth medium ca-MHB thereby using state-of-the-art bioanalytical assays as a prerequisite to obtain quantitative stability data in combination with pharmacodynamic studies [6]. Moreover, pyruvate and ascorbic acid as potential stabilizing agents for tigecycline in ca-MHB were comprehensively assessed.

The results of the present study in freshly prepared vs. aged ca-MHB are in line with a previous study [4]. However, our study adds quantitative information as previously, solely the pharmacodynamic age-dependence of ca-MHB was studied [4]. The use of freshly prepared broth might not be possible in routine labs, or is also impractical in long-term in vitro studies such as hollow-fiber experiments. The addition of Oxyrase has been proposed to stabilize tigecycline in broth to reduce the amount of dissolved oxygen to stabilize tigecycline [3]. Yet, Oxyrase represents a costly agent and the herein proposed antioxidative pyruvate is much more economic. Pyruvate might prevent tigecycline's oxidation at its phenolic group [7] in order to stabilize ca-MHB regardless of the ca-MHB age.

Another important aspect is that stability data generated in saline does not allow inferring about ca-MHB: *Jitkova* et al [2] found that 6% pyruvate in saline resulted in an insufficient stabilization, with a remaining tigecycline concentration of approx. 70% after 24 h. In contrast to that, we found a recovery of 97.1% in ca-MHB$_{7days\_p2\%}$ after 24 h. The differences for ascorbic acid are even more striking: By solely adding ascorbic acid, we quantified rapid degradation, even though pH control was applied, suggesting that ascorbic acid induces a destabilizing reaction in ca-MHB. A mass spectroscopic full scan could not detect any known degradation product. *Jitkova* et al. found that ascorbic acid alone was also insufficient to fully stabilize tigecycline in saline but did not observe a destabilization as quantified by us. In saline solution, 67.6% of freshly prepared tigecycline were recovered after 3 days [2]. Furthermore, a strong degradation of tigecycline occurs in non-stabilized ca-MHB$_{7days\_RT}$ and 2% pyruvate is not sufficient to prevent tigecycline from degradation; hence, 6% pyruvate is needed for stabilization. The broth aging process occurs faster at room temperature, so that 2% pyruvate cannot conserve tigecycline. Even though ca-MHB$_{7days\_RT}$ with 6% pyruvate shows comparable results as ca-MHB$_{7days\_p2\%}$ stored at 4 °C, we recommend storing the broth at 4 °C and supplement with 2% pyruvate before use, or the use of fresh ca-MHB, to save costs.

The measured kinetic data were consistent the pharmacodynamic effects in our study, i.e., faster and more intense regrowth was observed when tigecycline degraded faster. If ca-MHB age is not controlled, a twofold higher MIC value might be found due to tigecycline degradation, which can be avoided by addition of 2% pyruvate. The use of ascorbic acid, although stabilizing tigecycline in saline, cannot be recommended in ca-MHB.

Compliance with ethical standards

References

1. Pfizer. Tygacil® Full Prescribing Information. 2005
2. Jitkova Y, Gronda M, Hurren R et al (2014) A novel formulation of tigecycline has enhanced stability and sustained antibacterial and antileukemic activity Sbarba P Dello, ed. PLoS One 9:e95281. https://doi.org/10.1371/journal.pone.0095281
3. Bradford PA, Petersen PJ, Young M, Jones CH, Tischler M, O'Connell J (2005) Tigecycline MIC testing by broth dilution requires use of fresh medium or addition of the biocatalytic oxygen-reducing reagent Oxyrase to standardize the test method. Antimicrob Agents Chemother 49:3903–3909 Available at: http://aac.asm.org/cgi/doi/10.1128/AAC.49.9.3903-3909.2005
4. Hope R, Warner M, Mushtaq S, Ward ME, Parsons T, Livermore DM (2005) Effect of medium type, age and aeration on the MICs of tigecycline and classical tetracyclines. J Antimicrob Chemother 56:1042–1046 Available at: http://academic.oup.com/jac/article/56/6/1042/753027/Effect-of-medium-type-age-and-aeration-on-the-MICs
5. CLSI (2015) M07-A10: Methods for dilution antimicrobial susceptibility tests for bacteria that grow aerobically; Approved Standard. Available at: http://shop.clsi.org/site/Sample_pdf/M07A10_sample.pdf
6. Wicha SG, Kloft C (2016) Simultaneous determination and stability studies of linezolid, meropenem and vancomycin in bacterial growth medium by high-performance liquid chromatography. J Chromatogr B 1028:242–248
7. Fawzi M, Zhu T, Shah S. Tigecycline compositions and methods of preparation. WO Pat 2,006,099,258 2006; 2. Available at: http://patentscope.wipo.int/search/en/WO2006099258

3.2 Publication II

Pharmacokinetic/pharmacodynamic evaluation of tigecycline dosing in a hollow fiber infection model against clinical bla-KPC producing Klebsiella Pneumoniae isolates.

Lisa F. Amann[1], Astrid Broeker[1], Maria Riedner[2], Holger Rohde[3], Jiabin Huang[3] Patrice Nordmann[4], Jean-Winoc Decousser[5], Sebastian G. Wicha[1]

[1]Dept. of Clinical Pharmacy, Institute of Pharmacy, Universität Hamburg, Germany

[2]Technology Platform Mass Spectrometry, Universität Hamburg, Germany

[3]Institut für Medizinische Mikrobiologie, Virologie und Hygiene, Universitätsklinikum Hamburg-Eppendorf, Hamburg, Germany

[4]Medical and Molecular Microbiology, University of Fribourg, Switzerland

[5]Dynamic Team – EA 7380, Faculté de santé, Université Paris-Est-Créteil Val-De-Marne, France

Synopsis

Tigecycline is not often used in clinics, but if used patients suffer from severe, possibly life-threatening infections. Its use is restricted to cases where no other treatment is suitable, e.g. case in of infections caused by gram-negative bacteria. Clinical studies have shown suboptimal response to tigecycline, likely due to progression of infection during the treatment. Moreover, conflicting study results about higher doses have been reported. This study investigated the dose optimization potential of tigecycline using the dynamic hollow fiber infection model against clinical *Klebsiella pneumoniae* strains with MIC values ranging from 0.125 mg/L to 0.5 mg/L. Escalated daily doses, and variations of the dose regimen were compared to the approved dose regimen.

No antibiotic activity was maintained at clinically used doses and a dose escalation to 200 mg, 100 mg q8h was only effective against the strain with the lowest MIC of 0.125 mg/L. But this is a MIC at the lower end of the ECOFF distribution. Moreover, a fast tigecycline induced regrowth of resistant subpopulations, carrying clinically known mutations, was observed.

We thereby conclude that the currently used breakpoint of 1 mg/L might be too optimistic to treat *Klebsiella pneumoniae* infections, especially with respect to prevention of blood-stream infections.

Pharmacokinetic/pharmacodynamic evaluation of tigecycline dosing in a hollow fiber infection model against clinical *bla*-KPC producing *Klebsiella Pneumoniae* isolates

Lisa F. Amann [a], Astrid Broeker [a], Maria Riedner [b], Holger Rohde [c], Jiabin Huang [c], Patrice Nordmann [d], Jean-Winoc Decousser [e], Sebastian G. Wicha [a],[*]

[a] *Deptartement of Clinical Pharmacy, Institute of Pharmacy, Universität Hamburg, Hamburg, Germany*
[b] *Technology Platform Mass Spectrometry, Universität Hamburg, Hamburg, Germany*
[c] *Institut für Medizinische Mikrobiologie, Virologie und Hygiene, Universitätsklinikum Hamburg-Eppendorf, Hamburg, Germany*
[d] *Medical and Molecular Microbiology, University of Fribourg, Fribourg, Switzerland*
[e] *Dynamic Team–EA 7380, Faculté de santé, Université Paris-Est-Créteil Val-De-Marne, France*

ARTICLE INFO

ABSTRACT

The FDA announced a boxed warning for tigecycline due to progression of infections caused by Gram-negative bacteria and increased risk of mortality during treatment. Plasma exposure of tigecycline might not prevent bacteraemia in these cases from the focuses. Hence, we evaluated intensified dosing regimens and breakpoints that might suppress bloodstream infections, caused by progression of infection by e.g., Gram-negatives. A pharmacometric model was built from tigecycline concentrations (100–600 mg daily doses) against clinical Klebsiella pneumoniae isolates (MIC 0.125–0.5 mg/L). Regrowth occurred at clinically used doses and stasis was only achieved with 100 mg q8h for the strain with the lowest studied MIC of 0.125 mg/L. Stasis at 24 h was related to fAUC/MIC of 38.5. Our study indicates that even intensified dosing regimens might prevent bloodstream infections only for MIC values $\leq$0.125 mg/L for tigecycline. This indicates an overly optimistic breakpoint of 1 mg/L for Enterobacterales, which are deemed to respond to the tigecycline high dose regimen (EUCAST Guidance Document on Tigecycline Dosing 2022).

1. Introduction

The rapid worldwide emergence of antimicrobial resistance, especially in Gram-negative strains, is a leading cause of death and has become a major health crisis [1]. Severe nosocomial infections, caused by carbapenemase producing *Klebsiella pneumoniae* are associated with a high mortality rate and are difficult to treat [2]. Tigecycline represents a last-resort antibiotic in case other treatment options are not available. Tigecycline is a glycylcycline antibiotic, inhibiting the 30S subunit of the ribosome. It is indicated for complicated intra-abdominal infections (cIAI), complicated skin and skin structure infections (cSSI), as well as community acquired pneumonia and one of the last opportunities to treat carbapenemase producing *Klebsiella pneumoniae* (cp-KP). Several clinical data analysis have shown a reduced efficacy for the standard dose (100 mg loading dose (LD), followed by 50 mg q12 h) [3–6]. Furthermore, the US Food and Drug Administration (FDA) announced to

a black box warning letter due to a higher risk of mortality during treatment compared to other antibiotics [7]. Since early clinical use of tigecycline, resistance development has been reported [8,9] and a considerable amount of clinical studies showed a resistance development during tigecycline treatment [10–12] In 2018, the European committee on antimicrobial susceptibility testing (EUCAST) revised tigecycline's breakpoint for *Enterobacterales* [13] and published an updated guidance document on tigecycline dosing in 2022 [14]. Seriously ill patients with infections caused by multi-resistant pathogens should not receive standard dosing (50 mg q12h with a loading dose (LD) of 100 mg), but high dose tigecycline (100 mg q12h with or without a loading dose of 200 mg). Clinical data on the use of high dose tigecycline is limited but was recommended by Cunha et al. [15] and infections caused by pathogens (*Enterobacterales*, other than *E. coli*) with an MIC up to 1 mg/L could be treated with that regimen [13,16,17]. The FDA breakpoint for susceptible Enterobacterales is < 2 mg/L and with

that higher, compared to the EUCAST breakpoint. However, no details about dose regimen specific breakpoints are provided (https://www.fda.gov/drugs/development-resources/tigecycline-injection-products, last accessed 03 November 2023).

Yet, in case of severe infections, the infection can progress and ultimately lead to systemic bloodstream infections. Indeed, plasma exposure of tigecycline might not prevent bacteraemia in case of progression of the infection from the focus. The present study using the dynamic hollow fiber infection model (HFIM) evaluated optimisation of tigecycline doses and dosing regimens by mimicking human-like concentration time profiles in conjunction with pharmacokinetic/pharmacodynamic (PK/PD) modelling to investigate if higher doses or lower breakpoints are needed to enhance tigecycline's antibacterial effect to suppress progression of the infection to the blood stream.

2. Materials and methods

2.1. Bacterial isolates and susceptibility testing

Three clinical *Klebsiella pneumoniae* isolates were used for this study: The isolates *Klebsiella pneumoniae* 2977 (KPC-2, OXA-9, TEM-1; referred to as KP 2977) and *Klebsiella pneumoniae* R307 (KPC-2, OXA-2, OXA-9, TEM-1, CTX-M-2; referred to as KP 307) were collected in France in 2012 by rectal swabs and *Klebsiella pneumoniae* -N864 (KPC-3, OXA-9, TEM-1, referred to as referred to as KP N864) was isolated from a wound in Switzerland in 2019. Information on susceptibility to beta lactam class antibiotics are provided in Supplement Table S1.

Freshly thawed isolates were subcultured on Columbia agar (Carl Roth GmbH + Co. KG, Karlsruhe, Germany) for 24 h at 37°C before each experiment.

The MIC was determined before and after the experiments using the broth dilution method according to the CLSI guidelines and EUCAST [18,19] with freshly prepared [20] cation-adjusted Mueller-Hinton broth (ca-MHB) (Sigma-Aldrich, St. Louis, MO, USA). Tigecycline was purchased from the United States Pharmacopeial Convention, Rockville, MD 20852-1790, USA.

2.2. Genetic analysis of resistant subpopulations

Wild type *K. pneumonia* KP 307 and tigecycline-resistant derivates (KP 307-148, KP 307-149) were subjected to whole genome sequencing according to recently published procedures [21]. Total numbers of 1,882,055, 1,305,753 and 1,473,150 2×151 paired-end reads were generated from the Illumina sequencer, respectively. Bases less than Q30, as well as adapter sequences of the reads were trimmed, and any reads shorter than 36 nt removed using Trimmomatic v0.36 [22]. The retained high-quality reads in the sample KP 307 were fed into the SPAdes assembler (version 3.7.1) [23] for de novo genome assembly, resulting in a putative genome of 5,795,692 bp, with a mean depth of 87.1x. The Prokaryotic Genome Annotation Pipeline (PGAP) [24] identified 5822 putative open reading frames (ORFs) from the genome. The trimmed reads of the samples KP 307-148 and KP 307-149 were then mapped to the newly assembled and annotated genome (CP114785) with the aligner BWA [25]. The variants were called with the tool "GATK4 HaplotypeCaller" [26] from the alignments and annotated using SnpEff [27]. The accession numbers for the sequencing raw reads in the NCBI Sequence Read Archive (SRA) are SRR22681172, SRR22681384, and SRR22681383.

2.3. Hollow fiber infection model

The dynamic *in vitro* experiments were performed as previously described [28] at 37°C over 72 h with n=1 per scenario. Tigecycline's *in vitro* antibiotic effect induced by human-like concentration-time profiles were evaluated against the three clinical *Klebsiella pneumoniae* isolates outlined above. Tigecycline is known to be an instable drug in *in vitro*

experiments, as it degrades in the presence of oxygen. To prevent this, 2 % of sterile filtrated pyruvate was added as an antioxidative supplement to the bacterial growth medium (ca-MHB) [29]. Furthermore, the experiment was conducted in a dark incubator and the light exposure was limited to short sampling windows. The HFIM set up is further outlined in Supplement Text 1 and graphically displayed in Supplement Fig. S1. The inoculum was 10^6 CFU/mL and the experiment was started after 2 h of preincubation. A growth control experiment was performed without tigecycline solely containing the bacteria. The following dosing scenarios were covered in this study using the PK model described below (in PK simulations):

I.) Current clinical recommendations: Standard dose (100 mg LD, 50 mg q12h, 30 min short infusion) and high dose (100 mg q12 h, 30 min short infusion).

II.) Continuous infusion of high dose (100 mg LD as 30 min short infusion, 200 mg q24h)

III.) Shortening the dose interval with high dose (200 mg LD, 100 mg q8h as 30 min short infusion).

IV.) Supratherapeutic dose with 200 mg LD, 600 mg q24 h as continuous infusion.

2.4. Pharmacokinetic simulations

Human unbound concentration time profiles [30] for the above mentioned doses and dose regimens were simulated in R (version 3.6.1) using mrgsolve (version 0.10.7) using the published population PK parameters of the study of van Wart et al. [31]. The program R served for data analysis and pump rate calculation to mimic the 95th percentile concentrations of the population PK.

2.5. Determination of pharmacokinetics and pharmacodynamics

Pharmacokinetic samples were collected from the central compartment and stored at -80°C. The quantification of tigecycline was performed via LC-MS/MS, as previously described [29].

The bacterial count during the experiment was determined via a droplet plate assay (Columbia agar plates (Carl Roth, Germany)) at selected time points between 0 to 72 h

2.6. Pharmacokinetic-Pharmacodynamic modelling

PK/PD modelling was performed with NONMEM(R) 7.5 (ICON Development solutions, Ellicott City, USA) using first order conditional estimation with interaction (FOCE+I, ADVAN13 subroutine). The measured tigecycline concentrations in the HFIM were used to develop a PK model to provide most accurate PK profiles for PK-PD modelling. For that, we investigated a one, two and three compartment model. For residual unexplained variability, a proportional, additive, or combined error model was evaluated. Moreover, inter-experiment variability (lognormally distributed), as well as inter-occasion variability was tested on clearance (CL), central volume of distribution (Vc), inter-compartmental clearance (Q), and peripheral volume of distribution (Vp).

A sequential PK-PD approach with fixed individual parameters linked to the PD model describing the bacterial counts over the experiment duration was pursued. To describe tigecycline mediated killing, we evaluated a slope and power model, a sigmoidal maximum effect model (Emax model) and a sigmoidal maximum inhibition model (Imax model) on the bacterial growth rate. The growth inhibition model linked the tigecycline concentration (C) to the antibiotic effect on the susceptible (S), as well as the resistant (R) subpopulation. The maximum growth inhibition (IMAX) was assumed to be 1 assuming full inhibition of bacterial growth as indicated by the raw data. The IC_{50} described the tigecycline concentration inhibiting the maximum growth rate by 50% (Eq. 1 and Eq. 2). The killing of the bacteria observed after full growth inhibition for each subpopulation was parameterised by the killing rate
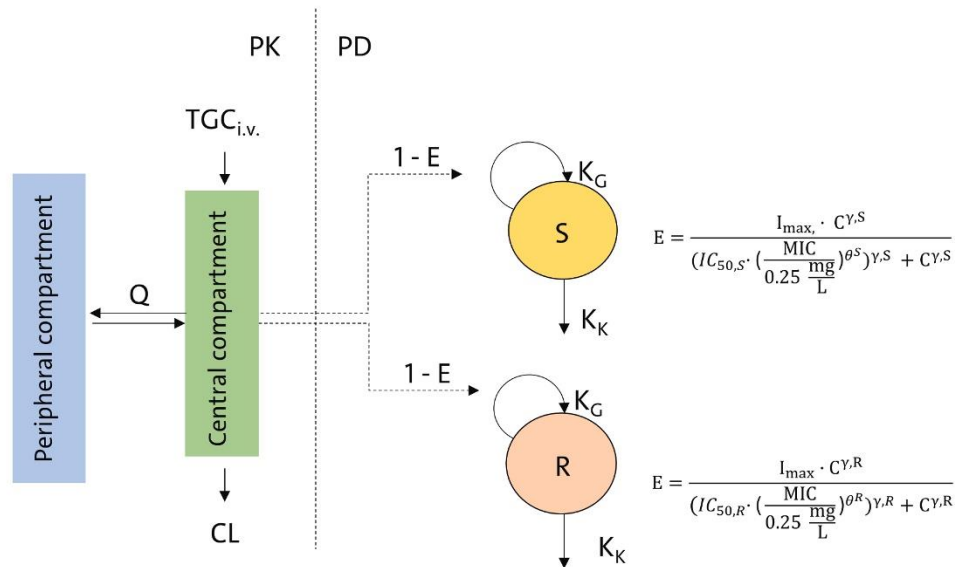
Fig. 1. Pharmacokinetic pharmacodynamic model structure. CFU were expressed by the sum of S and R. Parameters of the model are explained in the text and in Table 2.
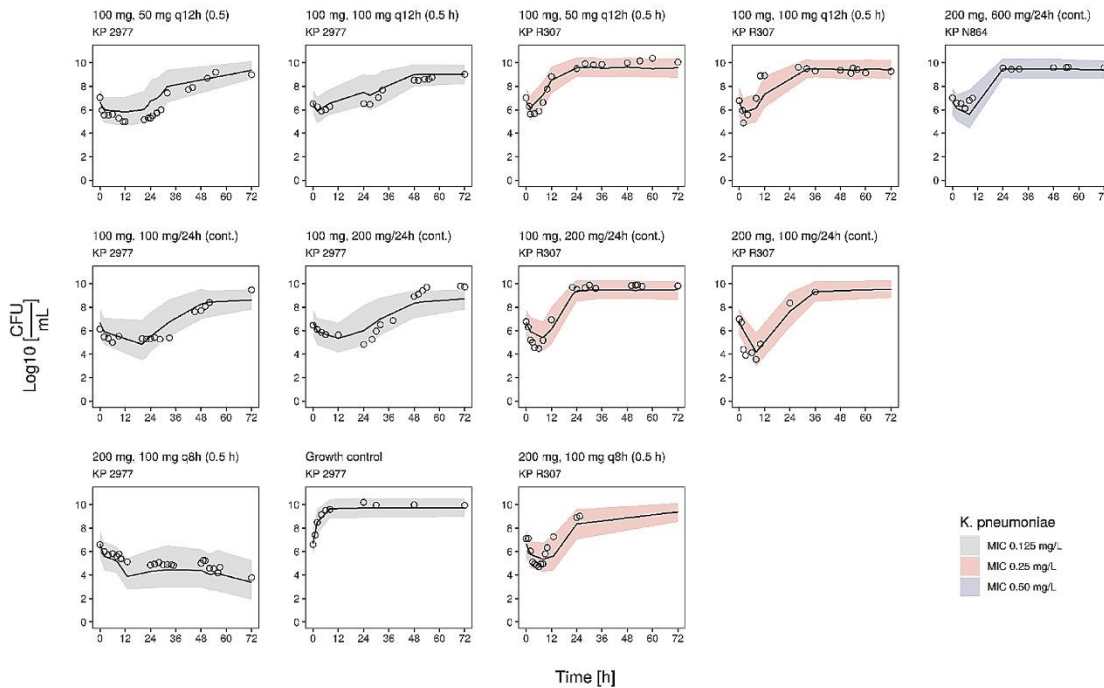
Fig. 2. Colony forming units (CFU/mL) over time (points) together with predictions from the developed PK/PD model (lines) and their 95 % prediction intervals (shaded areas) for different dosing regimens (facets) against three clinical *bla*-KPC producing *Klebsiella pneumoniae* isolates (colours).

KK. B_{max} describes the maximal possible bacterial load within the HFIM. To account for the different susceptibility of the three bacterial strains in this study, the MIC was introduced as a scaling factor of the IC_{50} and normalised to the median MIC of 0.25 mg/L. Candidate models were evaluated by goodness-of-fit plots, and visual predictive checks. The sampling importance resampling [32] technique was used to determine parameter uncertainty. The model structure is displayed in Fig. 1.

Table 1

Change of tigecycline MIC values against three clinical bla-KPC producing Klebsiella pneumoniae isolates after tigecycline exposure to different dosing regimens.

Klebsiella Pneumoniae	Tigecycline dose regimen	MIC before experiment [mg/L]	MIC after experiment [mg/L]	Factor
KP 2977	100 mg LD, 50 mg q12h (sti)	0.125	2.0	16 x MIC
KP 2977	100 mg LD, 100 mg q12h (sti)	0.125	0.5	4 x MIC
KP 2977	100 mg LD, 100 mg q24h (cont)	0.125	0.5	4 x MIC
KP 2977	100 mg LD, 200 mg q24h (cont)	0.125	0.5	4 x MIC
KP 2977	200 mg LD, 100 mg q8h (sti)	0.125	0.25	2 x MIC
KP 2977	Growth control	0.125	0.125	1x MIC
KP 307	100 mg LD, 50 mg q12h (sti)	0.25	2.0	8 x MIC
KP 307	100 mg LD, 100 mg q12h (sti)	0.25	2.0	8 x MIC
KP 307	100 mg LD, 200 mg q24h (cont)	0.25	4.0	16 x MIC
KP 307	200 mg LD, 100 mg q24h (cont)	0.25	4.0	16 x MIC
KP 307	200 mg LD, 100 mg q8h (sti)	0.25	8.0	32 x MIC
KP N864	200 mg LD, 600 mg q24h (cont)	0.5	4.0	8 x MIC

Abbreviations: short term infusion (sti), continuous infusion (cont.), *Klebsiella pneumoniae* (KP), Minimum inhibitory concentration (MIC), area under the concentration time curve (AUC)

$$dS/dt = S \cdot KG \cdot \left(1 - \frac{(S+R)}{B_{MAX}}\right) \cdot \left(1 - \left(\frac{I_{max} \cdot C^{\gamma,S}}{\left(IC_{50,S} \cdot \left(\frac{MIC}{0.25 \frac{mg}{L}}\right)^{\theta,S}\right)^{\gamma,S} + C^{\gamma,S}}\right)\right) - KK_S \cdot S \tag{1}$$

$$dR/dt = R \cdot KG \cdot \left(1 - \frac{(S+R)}{B_{MAX}}\right) \cdot \left(1 - \left(\frac{I_{max} \cdot C^{\gamma,R}}{\left(IC_{50,R} \cdot \left(\frac{MIC}{0.25 \frac{mg}{L}}\right)^{\theta,R}\right)^{\gamma,R} + C^{\gamma,R}}\right)\right) - KK_R \cdot R \tag{2}$$

The *f*AUC/MIC was evaluated by nonlinear regression at 12 h and 24 h to determine a breakpoint for bacteriostasis.

2.7. Clinical trial simulations

Monte Carlo simulations (n=500, performed in R using mrgsolve version 0.10.7) were used to simulate concentration-time profiles of standard and high dose tigecycline using the population PK model including covariates from van Wart et al. [31]. Furthermore, intensified dosing regimens with an increased loading dose (200 mg) and an extrapolation of the standard dose given every 8 h were simulated [31]. The model of van Wart et al. included the following values: CL: 15.7 L/h, Vc: 115 L, Vp: 644 L, Q: 70.9 L/h, IIV$_{CL}$: 35.1 %CV, IIV$_{Vc}$: 43.2 %CV, IIV$_Q$: 49.3 %CV [31] and their covariances between η_{CL} and η_{Vc} (r^2 = 0.385), η_{CL} and η_Q (r^2 = 0.095) and η_Q and η_{Vc} (r^2 = 0.666). The 500 simulations included 250 male and 250 female patients. Serum creatinine was sampled, such that the sex adjusted calculated creatinine clearance reflected the published mean and standard deviation [31,33]. The unbound concentrations [30] were linked to the PD model, developed from HFIM experiment data. The simulations were analysed at 24 h and 72 h.

3. Results

3.1. Bacterial isolates and susceptibility testing

The tigecycline MIC values was 0.125 mg/L for *Klebsiella pneumoniae* strain KP 2977, 0.25 mg/L for KP 307 and 0.5 mg/L for KP N864.

3.2. Hollow fibre experiments

3.2.1. Pharmacokinetics
The measured tigecycline PK adequately matched the originally planned PK profiles for the respective experiments. Individual model predictions well described the observed concentrations (Supplement, Fig. S2). Furthermore, concentrations within the bacterial compartment showed minor deviations from the central compartment, see Supplement Table S2.

3.2.2. Pharmacodynamics
For each performed HFIM experiment, the time course of determined colony forming units per mL (CFU/mL) is displayed in Fig. 2.
For the KP 2977 (MIC of 0.125 mg/L), neither the standard dose (100 mg LD, 50 mg q12h, 30 min short infusion), nor high dose (100 mg q12h) tigecycline prevented regrowth to maximum bacterial counts. The high dose regimen given as continuous infusion (100 mg LD, 200 mg q24h) revealed a prolongation, but no suppression of the regrowth. A dosing regimen with 200 mg LD, 100 mg q8h daily dose, revealed a
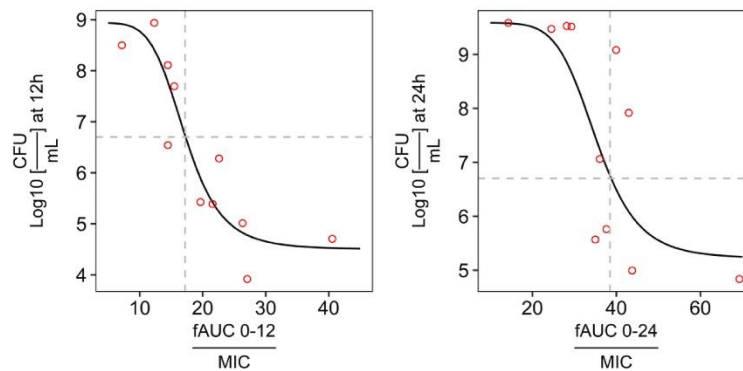
Fig. 3. Observed log10cfu/mL vs. *f*AUC/MIC at 12 h and 24 h, together with a fitted sigmoidal maximum effect model using extended least squares (solid line). Gray dashed y-intercept displays the estimated start inoculum (6.7 $\log_{10}$CFU/mL) of the pharmacometric PD model with corresponding x-intercept (left: *f*AUC$_{0-12h}$/MIC of 17.2, right: *f*AUC$_{0-24h}$/MIC of 38.5) which is related to an exposure to achieve stasis).

sustainable antibiotic effect against KP 2977 with a reduction from 10^7 to 10^4 CFU/ml within 72 h.

High dose tigecycline against KP 307 (MIC 0.25 mg/mL) showed an initial one $\log_{10}$ CFU/mL decline, but a fast growth to 10^9 CFU/mL followed, which was also observed for the continuous high dose tigecycline infusion scenario. The dose regimen of 200 mg LD followed by 100 mg q8h initially reduced the bacteria from 10^7 to 10^5 CFU/mL but did not show stasis or a reduction of CFU/mL until the end of experiment.

For the strain KP N864 with the highest MIC (0.5 mg/L), we tested a very intense dosing scenario of 200 mg LD, 600 mg q24h given continuously to maintain the concentration at least 100 % above the MIC, but stasis was only achieved for 10 h.

The MIC was quantified before and at the end of the experiment. In all scenarios with regrowth, the MIC increased to 16x MIC at 100 mg loading dose followed by 50 mg q12h, and up to 32 x MIC for KP 307 with 200 mg LD, 100 mg q8h. This dose against KP 2977 achieved a sustainable antibiotic effect and was also able to supress the resistance development. In this scenario the MIC increased only by a factor of one (Table 1).

Fig. 3 shows the PK/PD index evaluation using the *f*AUC/MIC target. The observed data revealed that a *f*AUC$_{0-12h}$/MIC of 17.2, *f*AUC$_{0-24h}$/MIC of 38.5 was required to achieve stasis.

3.2.3. Genetic analysis of resistant subpopulation

To identify evidence for the genetic basis of changes in tigecycline

Table 2

Parameter estimates of the developed pharmacokinetic/pharmacodynamic model. Parameter uncertainty was evaluated by sampling importance resampling. For interexperiment/ interindividual variability, the coefficient of variation (%CV) was obtained by $\sqrt{(e^{\omega^2}) - 1}$ with ω^2 representing the estimated variance in NONMEM.

| Model parameter	Explanation	Estimate	95 % confidence interval
CL	Tigecycline clearance (L/h)	20.2	15.4–25.1
Vc	Central volume of distribution (L)	109	85.2–144
Q	Intercompartmental clearance (L/h)	56.3	45.9–69.7
Vp	Peripheral volume of distribution (L)	706	447–1138
RES$_{PK}$	Proportional residual error (pharmacokinetics) (%)	20.5	18.4–23.2
IIV$_{CL}$	Interexperimental variability on CL (%CV)	15.8	1.70–33.9
IIV$_{Vc}$	Interexperimental variability on Vc (%CV)	44.4	26.4–69.7
IIV$_Q$	Interexperimental variability on Q (%CV)	35.1	16.2–53.5
IIV$_{Vp}$	Interexperimental variability on Vp (%CV)	80.4	51.7–122
IOV$_{CL}$	Inter-occasion variability on CL	40.6	21.6–57.9
IOV$_{V1}$	Inter-occasion variability on V1	20.7	4.30–41.8
S$_0$	Bacterial inoculum of susceptible bacteria at t$_0$ ($\log_{10}$CFU/mL)	6.66	6.40–6.90
IIV$_{S0}$	Variability of inoculum of susceptible subpopulation (%)	7.29	5.10–9.40
R$_0$	Bacterial inoculum of resistant bacteria at t$_0$ ($\log_{10}$CFU/mL)	2.0	1.95–3.18
IIV$_{R0}$	Variability of inoculum of resistant subpopulation (%)	34.0	24.6–41.2
B$_{MAX}$	Maximum bacterial count (log10CFU/mL)	9.8	9.75–10.0
I$_{MAX}$	Maximum inhibition of growth of R and S	1	Fixed
IC$_{50,S}$	Tigecycline concentration at the half maximal growth inhibition for the susceptible bacterial subpopulation (mg/L) for MIC of 0.25 mg/L	0.12	0.07–0.20
IC$_{50, R}$	Tigecycline concentration at the half maximal growth inhibition for the resistant bacterial subpopulation (mg/L) for MIC of 0.25 mg/L	0.19	0.09–0.33
γ^R	Hill factor for the resistant subpopulation	0.47	0.40–0.56
γ^S	Hill factor for the susceptible subpopulation	1	Fixed
K$_G$	Growth rate of bacterial subpopulations (h^{-1})	3.68	3.20–4.14
K$_K$	Killing of susceptible and resistant subpopulation (h^{-1})	1.56	1.21–1.94
θ_S	Covariate MIC on IC$_{50,S}$	0.29	0.01–0.55
θ_R	Covariate MIC on IC$_{50,R}$	1.73	1.53–1.94
RES$_{PD}$	Additive residual error (pharmacodynamics) ($\log_{10}$CFU/mL)	1.02	0.74–1.23
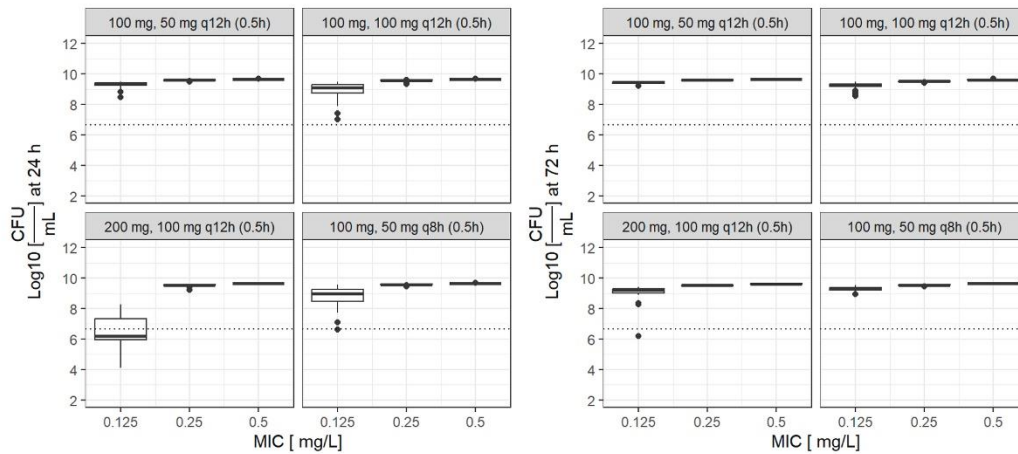
Fig. 4. Clinical trial simulations of standard dose (100 mg loading dose (LD), 50 mg q12 h), high dose (100 mg q12 h), intensified standard dose (100 mg LD, 50 mg q8 h), as well as variation of the loading dose (200 mg LD, 100 q 12h). Colony forming units (CFU/mL) at 24 h and 72 h are displayed for each simulated dosing scenario. Gray dashed y-intercept displays the estimated start inoculum (6.7 $\log_{10}$CFU/mL) of the pharmacometric PD model.

susceptibility, genomes of two tigecycline-resistant *K. pneumonia* isolates obtained after exposure to a) the clinically recommended high dose tigecycline (100mg, 100 mg q12) (KP 307-149) and b) from the scenario observing the highest increase of MIC at the end of experiment (200 mg, 100 mg q8) (KP 307-148) were sequenced. Comparative genome analysis of KP307-148 with wild-type KP 307 identified a total of 21 nonsynonymous single nucleotide polymorphisms (SNPs) and 15 insertion/deletion polymorphisms (INDELs) in coding regions. Of those three have previously been associated with tigecycline resistance in *Enterobacterales* (*ramR, lon, msbA*; Supplement Table S3, marked yellow). In KP 307-149, only one nonsynonymous SNP was identified in a coding region (Supplemental Table S3, marked cyan). Moreover, only one INDEL was found, intriguingly being identical to an insertion within *mrkD* (encoding for a fimbria adhesion) also identified in KP307-148 (Supplement Table S3, marked blue).

3.2.4. PK-PD modelling

The developed PK-PD model (Fig. 1) described all mimicked scenarios in the HFIM well (Fig. 2, Supplement Fig. S2). Parameter estimates of the developed model are reported in Table 2. Tigecycline PK in the HFIM was best described by a two-compartment model (dAIC: -235 to a one compartment model, dAIC: -0.54 to a three-compartment model). Inter-experiment variability on clearance (15.8 %CV), central volume of distribution (44.1 %), inter-compartmental clearance (35.1 % CV), and peripheral volume of distribution (80.4 %CV) strongly improved the model fit. For the residual unexplained variability, a proportional error model was appropriate (dOFV to combined error model: -0.18, dOFV to additive error model: +779). Moreover, inter-occasion variability was supported on clearance (40.6 %CV) and central volume of distribution (20.7 %CV).

A two-compartment bacterial population model was chosen to model the colony forming units (CFU/mL) over time, as a one compartment PD model was not able to describe the biphasic killing pattern in the data. Additionally, a sigmoidal variant of the IMAX model was supported for the resistant subpopulation (γR), see Fig. 1. A sigmoidal slope model for S and R was inferior with respect so model fit (dAIC: +133), so as the sigmoidal Emax model on R (dAIC: +358) or on both subpopulations (dAIC: +747).

3.2.5. Simulations

The Monte Carlo simulations revealed a regrowth to maximum bacterial counts for KP 307, KP 864 within the first 24 h using the

standard dose regimen (Fig. 4). Neither the high dose scenario with or without loading dose, nor the scenario using the standard dose given q8h prevented regrowth. On the other hand, the scenario of high dose tigecycline with a loading dose (200 mg, 100 mg q12h) achieved a reduction from (t_{0h}: $10^{6.7}$ to $10^{6.5}$ CFU/mL against KP 2977 (MIC of 0.125 mg/L at 24 h), see Fig. 4. In contrast to that, analysing the data at 72 h showed lower effect sizes. The initially observed antibiotic effect of high dose tigecycline with loading dose of 200 mg against KP 2977 was not permanent, and we observed a regrowth to 10^9 CFU/mL. With that, tigecycline reduced the KP 2977 count only by -$10^{0.5}$ CFU/mL, compared to KP 307 and KP N864 at 72 h. In the van Wart's et al. study population, male patients exhibited a 20.6% higher clearance compared to female patients. The simulations demonstrated a significant difference of CFU/ml between male and female patients within the first 24 h (200 mg, 100 mg q12h, MIC of 0.125 mg/L: $10^{5.9}$ vs. $10^{6.8}$ CFU/mL, p-value: $5.2 \cdot 10^{-5}$ using a t-test), however the antibiotic effect was not sustained over time, see Supplement Fig. S3.

4. Discussion

The study explored different dosing regimens against three *Klebsiella pneumoniae* isolates to establish a PK/PD relationship. Despite the isolates initially being considered susceptible to tigecycline, regrowth was observed at standard doses. The study found that altering the dosing regimen sustained effectiveness against one isolate (MIC 0.125 mg/L). Yet regrowth in other scenarios indicated possible resistance to tigecycline, as shown by an increase in minimum inhibitory concentration (MIC) after treatment.

According to EUCAST guidelines indicating susceptibility to high dose tigecycline [14] among the tested clinical isolates, this study revealed limited in vitro efficacy at standard doses. It corresponded with observed suboptimal clinical effectiveness [3,6,7,17].

Moreover, high dose regimens failed to delay regrowth, as the regrowth started prior to the second dose. Falagas et al.'s systematic review concluded that evidence supporting the use of high dose tigecycline is limited [17]. While no significantly improved microbial eradication was observed, there was a possibility of enhanced clinical outcomes. The published studies overall exhibit a high risk of bias and uncertainty, attributed to small study sizes and a range of severe infections in critically ill patients [6,17,34]. Additionally, there have been no randomized controlled trials conducted to verify the efficacy of high dose tigecycline.

In our study, increased dosing (200 mg LD, 100 mg q8h) successfully suppressed regrowth prior to 12 hours, specifically against Klebsiella pneumoniae 2977, the strain with the lowest MIC of 0.125 mg/L. Stasis was not observed within the first 24 hours with standard clinical doses. Hence, tigecycline efficacy in the HFIM was seemingly dependant on the MIC prior to drug exposure and presence of resistance genes. Emergence of tigecycline resistance has been repeatedly reported to occur during treatment *in vivo*. In fact, using KP 307 as an example, comparative WGS identified frameshift mutations in *ramR* and *lon*, being reported to negatively control expression of *ramA* [35,36]. Therefore, it appears plausible to assume that in KP 307-148, up-regulation of *ramA* and subsequent overexpression of *acrAB* is likely contributing to tigecycline resistance in the isolate [35]. This mechanism has also been shown to be relevant *in vivo*, supporting the clinical validity of the model employed.

According to EUCAST, the studied strains are deemed susceptible, but the present data indicates that the breakpoint might be set too optimistic, at least if the exposure shall also safely prevent progression of the infection into the bloodstream. Similarly, this conclusion applies to the FDA breakpoint, where isolates with MIC $\leq$ 2 mg/L are deemed susceptible. Ambrose et al. revealed that clinical response and PK-PD target attainment (AUC/MIC $\geq$ 6.96) is only poorly correlated at MIC values >0.25 mg/L for Enterobacteriaceae, which is in line with our analysis. However, the ECOFF of *Klebsiella pneumoniae* is 2 mg/L [13]. This means that the investigated MICs of strains are rather an optimistic selection from the overall bacterial population. This underlines the need to further evaluate the use of tigecycline against *Klebsiella pneumoniae* and further review of clinical breakpoints.

Tigecycline showed atypical nonlinear protein binding *in vitro* and we assumed a static fraction unbound of 66.3 %, as most of our mimicked concentrations were below 0.3 mg/L [30]. Stein et al. suggested higher exposure at the target site, but these values were derived from homogenized biopsy samples, that represent a mixture of both free and bound concentrations from different compartments (cells, interstitial fluid, capillaries) [37].

Therefore, these values need to be interpreted with caution. Microdialysis is a more accurate method to evaluate unbound tissue concentrations, showing similarity between unbound tissue and plasma concentration [38]. Moreover, in a recent microdialysis study conducted by Dorn et al., the concentrations in the interstitial fluid of subcutaneous tissue were not observed to be higher than in plasma [39]. A common assumption is that only unbound drug can exhibit PD activities, which also applies to target sites. Therefore, we assume that the here mimicked unbound plasma concentrations can provide insight into tissue target site concentrations of tigecycline and its capability to prevent bacteraemia. Comparing tigecycline concentrations in the sampling and bacterial compartments showed minor differences. We assumed negligible losses from adsorption to the hollow fiber membrane. This is supported by Broeker et al.'s findings of no tigecycline adsorption to a polysulfone membrane in critically ill patients undergoing renal replacement therapy [40].

Tigecycline effectiveness relies on both the immune system presence and the bacterial load [41], leading to higher cure rates in patients with lower bacterial burdens at the target site. However, the inoculum of 10^7 used in this study might not accurately depict this. The HFIM lacks the host immune response and cannot mimic surgical interventions or drainage. It represents optimal growth conditions, unlike infection sites with lower nutrient supply and reduced pH, thus reflecting worst-case scenarios for immunosuppressed patients.

5. Conclusion

In conclusion, the clinically used tigecycline doses did not have an in vitro antibiotic activity against carbapenemase producing Klebsiella pneumoniae whereas drug exposure induced a strong MIC increase. Dose escalation to q8h high dose tigecycline might be a treatment option for infections caused by Klebsiella pneumoniae with an MIC $\leq$ 0.125 mg/L to prevent progression of infection and transition to bloodstream infection. Combination treatments with tigecycline should be further explored to prevent resistance development.

CRediT authorship contribution statement

Lisa F. Amann: Data curation, Formal analysis, Investigation, Methodology, Conceptualization, Visualization, Software, Writing – original draft. **Astrid Broeker:** Data curation, Formal analysis, Investigation, Methodology. **Maria Riedner:** Data curation, Formal analysis, Investigation, Methodology. **Holger Rohde:** Data curation, Formal analysis, Investigation, Methodology. **Jiabin Huang:** Data curation, Formal analysis, Investigation, Methodology. **Patrice Nordmann:** Data curation, Formal analysis, Investigation, Methodology. **Jean-Winoc Decousser:** Data curation, Formal analysis, Investigation, Methodology. **Sebastian G. Wicha:** Conceptualization, Project administration, Resources, Supervision, Writing – review & editing.

Declaration of Competing Interest

All authors, nothing to declare.

Supplementary materials

Supplementary material associated with this article can be found, in the online version, at doi:10.1016/j.diagmicrobio.2023.116153.

References

[1] Antibiotic resistance threats in the United States. Atlanta, Georgia: CDC; 2019. https://doi.org/10.15620/cdc:82532.

[2] Gasink LB, Edelstein PH, Lautenbach E, Synnestvedt M, Fishman NO. Risk factors and clinical impact of klebsiella pneumoniae carbapenemase-producing K. pneumoniae. Infect Control Hosp Epidemiol 2009;30:1180–5. https://doi.org/10.1086/648451.

[3] De Pascale G, Montini L, Pennisi M, Bernini V, Maviglia R, Bello G, et al. High dose tigecycline in critically ill patients with severe infections due to multidrug-resistant bacteria. Crit Care 2014;18:R90. https://doi.org/10.1186/cc13858.

[4] Ramirez J, Dartois N, Gandjini H, Yan JL, Korth-Bradley J, McGovern PC. Randomized phase 2 trial to evaluate the clinical efficacy of two high-dosage tigecycline regimens versus imipenem-cilastatin for treatment of hospital-acquired pneumonia. Antimicrob Agents Chemother 2013;57:1756–62. https://doi.org/10.1128/AAC.01232-12.

[5] Leng B, Yan G, Wang C, Shen C, Zhang W, Wang W. Dose optimization based on pharmacokinetic/pharmacodynamic target of tigecycline. J Glob Antimicrob Resist 2021. https://doi.org/10.1016/j.jgar.2021.04.006.

[6] Zha L, Pan L, Guo J, French N, Villanueva EV, Tefsen B. Effectiveness and safety of high dose tigecycline for the treatment of severe infections: a systematic review and meta-analysis. Adv Ther 2020;37:1049–64. https://doi.org/10.1007/s12325-020-01235-y.

[7] McGovern PC, Wible M, El-Tahtawy A, Biswas P, Meyer RD. All-cause mortality imbalance in the tigecycline phase 3 and 4 clinical trials. Int J Antimicrob Agents 2013;41:463–7. https://doi.org/10.1016/j.ijantimicag.2013.01.020.

[8] Babinchak T, Ellis-Grosse E, Dartois N, Rose GM, Loh E. The efficacy and safety of tigecycline for the treatment of complicated intra-abdominal infections: analysis of pooled clinical trial data. Clin Infect Dis 2005;41:S354–67. https://doi.org/10.1086/431676.

[9] Hentschke M, Wolters M, Sobottka I, Rohde H, Aepfelbacher M. ramR mutations in clinical isolates of klebsiella pneumoniae with reduced susceptibility to tigecycline. Antimicrob Agents Chemother 2010;54:2720–3. https://doi.org/10.1128/AAC.00085-10.

[10] Neonakis I, Stylianou K, Daphnis E, Maraki S. First case of resistance to tigecycline by Klebsiella pneumoniae in a European University Hospital. Indian J Med Microbiol 2011;29:78–9. https://doi.org/10.4103/0255-0857.76535.

[11] Sun Y, Cai Y, Liu X, Bai N, Liang B, Wang R. The emergence of clinical resistance to tigecycline. Int J Antimicrob Agents 2013;41:110–6. https://doi.org/10.1016/j.ijantimicag.2012.09.005.

[12] Du X, He F, Shi Q, Zhao F, Xu J, Fu Y, et al. The rapid emergence of tigecycline resistance in blaKPC–2 harboring klebsiella pneumoniae, as mediated in vivo by mutation in tetA during tigecycline treatment. Front Microbiol 2018;9:1–7. https://doi.org/10.3389/fmicb.2018.00648.

[13] European Committee for Antimicrobial Susceptibility Testing (EUCAST) Guidance Document on Tigecycline Dosing, 2018. https://www.eucast.org/fileadmin/src/media/PDFs/EUCAST_files/General_documents/Tigecycline_Guidance_document_20181223.pdf.

[14] European Committee for Antimicrobial Susceptibility Testing (EUCAST), Guidance Document on Tigecycline Dosing, 2022. https://www.eucast.org/fileadmin/src/media/PDFs/EUCAST_files/Guidance_documents/Tigecycline_Guidance_document_v2_20220720.pdf.

[15] Cunha BA, Baron J, Cunha CB. Once daily high dose tigecycline - pharmacokinetic/pharmacodynamic based dosing for optimal clinical effectiveness: dosing matters, revisited. Expert Rev Anti Infect Ther 2017;15:257–67. https://doi.org/10.1080/14787210.2017.1268529.

[16] Xie J, Roberts JA, Alobaid AS, Roger C, Wang Y, Yang Q, et al. Population pharmacokinetics of tigecycline in critically ill patients with severe infections. Antimicrob Agents Chemother 2017;61:1–10. https://doi.org/10.1128/AAC.00345-17.

[17] Falagas ME, Vardakas KZ, Tsiveriotis KP, Triarides NA, Tansarli GS. Effectiveness and safety of high-dose tigecycline-containing regimens for the treatment of severe bacterial infections. Int J Antimicrob Agents 2014;44:1–7. https://doi.org/10.1016/j.ijantimicag.2014.01.006.

[18] European Committee for Antimicrobial Susceptibility Testing (EUCAST) of the European Society of Clinical Microbiology and Infectious Diseases (ESCMID), Determination of minimum inhibitory concentrations (MICs) of antibacterial agents by broth dilution. doi:10.1046/j.1469-0691.2003.00790.x.

[19] CLSI. M07-A10: Methods for Dilution Antimicrobial Susceptibility Tests for Bacteria That Grow Aerobically; Approved Standard. vol. 35. 2015.

[20] Bradford PA, Petersen PJ, Young M, Jones CH, Tischler M, O'Connell J. Tigecycline MIC testing by broth dilution requires use of fresh medium or addition of the biocatalytic oxygen-reducing reagent oxyrase to standardize the test method. Antimicrob Agents Chemother 2005;49:3903–9. https://doi.org/10.1128/AAC.49.9.3903-3909.2005.

[21] Both A, Büttner H, Huang J, Perbandt M, Belmar Campos C, Christner M, et al. Emergence of ceftazidime/avibactam non-susceptibility in an MDR Klebsiella pneumoniae isolate. J Antimicrob Chemother 2017;72:2483–8. https://doi.org/10.1093/jac/dkx179.

[22] Bolger AM, Lohse M, Usadel B. Trimmomatic: a flexible trimmer for Illumina sequence data. Bioinformatics 2014;30:2114–20. https://doi.org/10.1093/bioinformatics/btu170.

[23] Bankevich A, Nurk S, Antipov D, Gurevich AA, Dvorkin M, Kulikov AS, et al. SPAdes: A new genome assembly algorithm and its applications to single-cell sequencing. J Comput Biol 2012;19:455–77. https://doi.org/10.1089/cmb.2012.0021.

[24] Tatusova T, DiCuccio M, Badretdin A, Chetvernin V, Nawrocki EP, Zaslavsky L, et al. NCBI prokaryotic genome annotation pipeline. Nucleic Acids Res 2016;44:6614–24. https://doi.org/10.1093/nar/gkw569.

[25] Li H, Durbin R. Fast and accurate short read alignment with Burrows–Wheeler transform. Bioinformatics 2009;25:1754–60. https://doi.org/10.1093/bioinformatics/btp324.

[26] McKenna A, Hanna M, Banks E, Sivachenko A, Cibulskis K, Kernytsky A, et al. The genome analysis toolkit: a MapReduce framework for analyzing next-generation DNA sequencing data. Genome Res 2010;20:1297–303. https://doi.org/10.1101/gr.107524.110.

[27] Cingolani P, Platts A, Wang LL, Coon M, Nguyen T, Wang L, et al. A program for annotating and predicting the effects of single nucleotide polymorphisms, SnpEff: SNPs in the genome of Drosophila melanogaster strain w1118; iso-2; iso-3. Fly (Austin) 2012;6:80–92. https://doi.org/10.4161/fly.19695.

[28] Sevillano D, Aguilar L, Alou L, Giménez MJ, González N, Torrico M, et al. Exposure–response analysis of tigecycline in pharmacodynamic simulations using different size inocula of target bacteria. Int J Antimicrob Agents 2010;36:137–44. https://doi.org/10.1016/j.ijantimicag.2010.03.021.

[29] Amann LF, Vicente ER, Rathke M, Broeker A, Riedner M, Wicha SG. Stability studies with tigecycline in bacterial growth medium and impact of stabilizing agents. Eur J Clin Microbiol Infect Dis 2021;40:215–8. https://doi.org/10.1007/s10096-020-03970-0.

[30] Dorn C, Kratzer A, Liebchen U, Schleibinger M, Murschhauser A, Schlossmann J, et al. Impact of experimental variables on the protein binding of tigecycline in human plasma as determined by ultrafiltration. J Pharm Sci 2018;107:739–44. https://doi.org/10.1016/j.xphs.2017.09.006.

[31] Van Wart SA, Owen JS, Ludwig EA, Meagher AK, Korth-Bradley JM, Cirincione BB. Population pharmacokinetics of tigecycline in patients with complicated intra-abdominal or skin and skin structure infections. Antimicrob Agents Chemother 2006;50:3701–7. https://doi.org/10.1128/AAC.01636-05.

[32] Dosne A-G, Bergstrand M, Harling K, Karlsson MO. Improving the estimation of parameter uncertainty distributions in nonlinear mixed effects models using sampling importance resampling. J Pharmacokinet Pharmacodyn 2016;43:583–96. https://doi.org/10.1007/s10928-016-9487-8.

[33] Dash A, Galsky MD, Vickers AJ, Serio AM, Koppie TM, Dalbagni G, et al. Impact of renal impairment on eligibility for adjuvant cisplatin-based chemotherapy in patients with urothelial carcinoma of the bladder. Cancer 2006;107:506–13. https://doi.org/10.1002/cncr.22031.

[34] Paul M, Carrara E, Retamar P, Tängdén T, Bitterman R, Bonomo RA, et al. European Society of Clinical Microbiology and Infectious Diseases (ESCMID) guidelines for the treatment of infections caused by multidrug-resistant Gram-negative bacilli (endorsed by European society of intensive care medicine). Clin Microbiol Infect 2022;28:521–47. https://doi.org/10.1016/j.cmi.2021.11.025.

[35] Campos CB, Aepfelbacher M, Hentschke M. Molecular analysis of the ramRA locus in clinical Klebsiella pneumoniae isolates with reduced susceptibility to tigecycline. New Microbiol 2017;40:135–8.

[36] Fang L, Chen Q, Shi K, Li X, Shi Q, He F, et al. Step-Wise Increase in Tigecycline Resistance in Klebsiella pneumoniae Associated with Mutations in ramR, lon and rpsJ. PLoS One 2016;11:e0165019. https://doi.org/10.1371/journal.pone.0165019.

[37] Stein GE, Smith CL, Missavage A, Saunders JP, Nicolau DP, Battjes SM, et al. Tigecycline penetration into skin and soft tissue. Surg Infect (Larchmt) 2011;12:465–7. https://doi.org/10.1089/sur.2011.022.

[38] Bulik CC, Wiskirchen DE, Shepard A, Sutherland CA, Kuti JL, Nicolau DP. Tissue penetration and pharmacokinetics of tigecycline in diabetic patients with chronic wound infections described by using in vivo microdialysis. Antimicrob Agents Chemother 2010;54:5209–13. https://doi.org/10.1128/AAC.01051-10.

[39] Dorn C, Petroff D, Kratzer A, Kees F, Kloft C, Zeitlinger M, et al. Tigecycline soft tissue penetration in obese and non-obese surgical patients determined by using in vivo Microdialysis. Eur J Drug Metab Pharmacokinet 2022;47:749–55. https://doi.org/10.1007/s13318-022-00789-2.

[40] Broeker A, Wicha SG, Dorn C, Kratzer A, Schleibinger M, Kees F, et al. Tigecycline in critically ill patients on continuous renal replacement therapy: a population pharmacokinetic study. Crit Care 2018;22:341. https://doi.org/10.1186/s13054-018-2278-4.

[41] Tsala M, Vourli S, Daikos GL, Tsakris A, Zerva L, Mouton JW, et al. Impact of bacterial load on pharmacodynamics and susceptibility breakpoints for tigecycline and Klebsiella pneumoniae. J Antimicrob Chemother 2017;72:172–80. https://doi.org/10.1093/jac/dkw354.

3.3 Publication III

Tigecycline Dosing Strategies in Critically Ill Liver-Impaired Patients

Lisa F. Amann[1], Rawan Alraish[2], Astrid Broeker[1], Magnus Kaffarnik[2], Sebastian G. Wicha[1]

[1]Department of Clinical Pharmacy, Institute of Pharmacy, University of Hamburg, Germany

[2]Department of Surgery, Charité-Universitätsmedizin Berlin, Germany

Synopsis

Tigecycline is a last treatment option for patients with severe infections, but pharmacokinetic data in vulnerable liver-impaired patient population are lacking. Thus, dose adjustments to support rational and effective treatments are necessary. The present study investigated the pharmacokinetics of tigecycline in 39 patients with acute and chronic liver impairment, displaying the largest study in this patient collective so far. With a population pharmacokinetic model, covariate-based dosing strategies for that special patient population were evaluated and Monte Carlo simulation applied. Possible covariates were obtained from liver and kidney related physiological parameters. This study revealed, that tigecycline clearance was strongly reduced, leading to remarkably high drug exposure, compared to non-critically ill populations. Moreover, high tigecycline exposure was best predicted with the Child Pugh score and no other (liver-related) covariates were superior. Furthermore, patients reached high dose tigecycline (100 mg q12h) exposure of non-critically ill patients with a dose reduction (25 mg as a maintenance dose). Therapy failure was related to chronic liver disease and renal failure, but survival was not related to drug exposure. Due to the high variability of tigecycline pharmacokinetics across different study groups further investigations to enhance clinical outcome are warranted.

antibiotics

MDPI

Article

Tigecycline Dosing Strategies in Critically Ill Liver-Impaired Patients

Lisa F. Amann [1], Rawan Alraish [2], Astrid Broeker [1], Magnus Kaffarnik [2] and Sebastian G. Wicha [1,*]

[1] Department of Clinical Pharmacy, Institute of Pharmacy, University of Hamburg, 20146 Hamburg, Germany; lisa.amann@uni-hamburg.de (L.F.A.); broeker.astrid@gmail.com (A.B.)
[2] Department of Surgery, Charité-Universitätsmedizin Berlin, 13353 Berlin, Germany; rawan.alraish@charite.de (R.A.); mkaffarnik@posteo.de (M.K.)
* Correspondence: sebastian.wicha@uni-hamburg.de; Tel.: +49-40-42838-3487

Abstract: This study investigated tigecycline exposure in critically ill patients from a population pharmacokinetic perspective to support rational dosing in intensive care unit (ICU) patients with acute and chronic liver impairment. A clinical dataset of 39 patients served as the basis for the development of a population pharmacokinetic model. The typical tigecycline clearance was strongly reduced (8.6 L/h) as compared to other populations. Different models were developed based on liver and kidney function-related covariates. Monte Carlo simulations were used to guide dose adjustments with the most predictive covariates: Child–Pugh score, total bilirubin, and MELD score. The best performing covariate, guiding a dose reduction to 25 mg q12h, was Child–Pugh score C, whereas patients with Child–Pugh score A/B received the standard dose of 50 mg q12h. Of note, the obtained 24 h steady-state area under the concentration vs. time curve (AUC_{ss}) range using this dosing strategy was predicted to be equivalent to high-dose tigecycline exposure (100 mg q12h) in non-ICU patients. In addition, 26/39 study participants died, and therapy failure was most correlated with chronic liver disease and renal failure, but no correlation between drug exposure and survival was observed. However, tigecycline in special patient populations needs further investigations to enhance clinical outcome.

Keywords: population pharmacokinetics; Child–Pugh score; dose adjustment

1. Introduction

Tigecycline, belonging to the class of glycylcyclines, is a last-resort antibiotic and currently approved for complicated skin and skin structure infections (cSSI), complicated intra-abdominal infections (cIAI), and community-acquired pneumonia. Its broad spectrum includes Gram-negative and Gram-positive strains, as well as multidrug-resistant pathogens [1]. Tigecycline is considered a bacteriostatic drug that inhibits the bacterial protein translation by binding to the 30S ribosomal subunit [2]. The 24 h steady-state area under the drug concentration vs. time curve (AUC_{ss}) to minimum inhibitory concentration (MIC) ratio (AUC/MIC) of >17.9 (cSSI) and >6.96 (cIAI) describes the pharmacokinetic/pharmacodynamic (PK/PD) target of tigecycline [3,4]. The US Food and Drug Administration (FDA) does not recommend tigecycline as a first-line therapy of patients with severe infections. In a pooled analysis comparing tigecycline to other antibiotics in serious infections, there was an increased risk of death (4% (150/3788) vs. 3% (110/3646)), revealing an all-cause mortality of 0.6% (95% CI, 0.1% to 1.2%) probably due to progression of the infection [5]. This increased mortality was seen mostly in patients treated off-label for ventilator-associated pneumonia [5] and led to a black box warning by the US FDA (1 September 2010; 27 September 2013). However, with increasing resistance to first-line antibiotics and/or the lack of other treatment options, tigecycline is often one of a few last opportunities to treat severe infections. In addition to rational evaluation of the indication, the optimal dose is crucial to balance microbial eradication and tolerable side-effects. Several studies have reported increased microbiological eradication with higher tigecycline

doses [6–10]. In addition, previously published studies have reported altered tigecycline pharmacokinetics in ICU patients [6,11]. Therefore, standard dosing may not be suitable for ICU patients, as compared to non-critically ill patients. Dose adjustment for drugs, which are metabolized or eliminated through the liver, is mostly performed by applying Child–Pugh Score (CPS) classification, as no single lab parameter can determine liver function and elimination capacity. The CPS originally assesses prognosis in chronic liver diseases and is generally classified in mild, moderate, and severe hepatic impairment, corresponding to scores of A (CPS$_A$), B (CPS$_B$), and C (CPS$_C$). The tigecycline drug dossier informs about dosage in hepatic insufficiency, guiding no dose adjustment (100 mg initial dose, 50 mg q12h, i.v.) in mild or moderate impaired patients (CPS$_A$, CPS$_B$), but a maintenance dose reduction to 25 mg q12h for severe impaired patients with CPS$_C$. Moreover, cirrhotic patients have a higher risk for infections with Gram-positive bacteria, which can also cause progression of liver failure. In addition to that, the severity of infections in these patients is often increased and correlated with a higher mortality [12]. Nevertheless, dosing decisions are often associated with uncertainty. On the other hand, bilirubin was previously related to tigecycline exposure, but has not been exploited for dose adjustments yet [13,14].

Hence, further data are required to elucidate the pharmacokinetics of tigecycline in liver-impaired critically ill patients. Therefore, we performed a population pharmacokinetic (popPK) analysis of tigecycline in this special patient population while evaluating liver-related clinical laboratory parameters (covariates) using a nonlinear mixed-effects modeling. Based on the developed popPK model, Monte Carlo simulations were used to investigate suitable covariates for dose adjustment and simulations of target attainment.

2. Results

2.1. Study Participants

This study recruited 39 patients, who contributed 283 timed plasma measurements of tigecycline to the pharmacokinetic (PK) model development. Table 1 summarizes patient characteristics, clinical laboratory data, infective pathogens, as well as underlying liver disease. Gram-positive bacteria or multiple pathogens mainly caused the infections. Two patients were undergoing renal replacement therapy (RRT), which was not considered as a relevant co-condition, as a previous study showed no relevant influence of RRT on tigecycline PK [13].

Table 1. Demographic and clinical patient characteristics. Clinical laboratory values are described by median with minimum and maximum values in square brackets.

Patient Characteristics	Total (n = 39)
Male (n)	13 (32.5%)
Female (n)	27 (67.5%)
Age (years)	62 [34, 85]
Weight (kg)	80.0 [44.5, 119]
Clinical laboratory parameters	
ALT (U/L)	33.5 [7.00, 928]
AST (U/L)	55.0 [13.0, 1300]
Total bilirubin (mg/dL)	2.64 [0.190, 18.6]
De-Ritis ratio	1.54 [0.167, 4.00]
γ-Glutamyltransferase (U/L)	120 [23.0, 1670]
INR	1.44 [0.970, 2.69]
LiMAx test [μg/h/kg]	170 [18.0, 596]
MELD score	18 [9.00, 37.0]
Serum creatinine [mg/dL]	1.09 [0.330, 3.31]
eGFR (CKD-EPI)	68.8 [17.2–149.8]
Thrombocytes (g/L)	148 [15.0, 777]
Child–Pugh score A (n)	21
Child–Pugh score B (n)	15
Child–Pugh score C (n)	3

Table 1. *Cont.*

Patient Characteristics	Total (n = 39)
Underlying diseases	
Acute liver impairment	22
Chronic liver disease	17
Klatskin tumor (type I, IIa, IIb, IV)	7
Liver abscess	3
Cholangiocarcinoma	2
Complicated cholecystitis	1
Liver cirrhosis	2
Hypoperfusion of the liver	1
Cholangiogenic sepsis	1
Ascites: none (n)	7
Ascites: Grade 1(n)	16
Ascites: Grade 2 (n)	16
Microbiological isolates	
Enterococcus avium (n)	1
Enterococcus faecalis (n)	4
Enterococcus faecium (n)	10
Escherichia coli (n)	4
Klebsiella pneumoniae (n)	1
MRSA (n)	2
Staphylococcus epidermidis (n)	6
VRE (n)	12

Abbreviations: ALT: Alanine aminotransferase, AST: Aspartate aminotransferase, LiMAx: Maximum liver function capacity, eGFR: estimated glomerular filtration rate, MELD: Model end-stage liver disease, INR: International normalized ratio, MRSA: Methicillin-resistant Staphylococcus aureus, VRE: Vancomycin-resistant Enterococci.

2.2. Pharmacometric Data Analysis

2.2.1. Base Model

To analyze the plasma pharmacokinetics, nonlinear mixed-effects modeling was applied. A two-compartment model with linear disposition and elimination described tigecycline plasma pharmacokinetics and was superior to a one-compartment model to describe plasma pharmacokinetics (difference in Akaike Information Criterion (dAIC): -397). The residual unexplained variability was described by a proportional error model, and neither an additive error (drop of objective function value (dOFV): $+206$) nor a combined additive and proportional error model provided a better model fit (dOFV: -0.013). Interindividual variability (IIV) was supported on clearance (CL) (dOFV: -442), on central volume of distribution (V_c) (dOFV: -48), and on peripheral volume of distribution (V_p) (dOFV: -35). ETA-shrinkage was as low as 0% for CL and 13% for V_c, indicating that most of the individuals contributed to these estimates of IIV. ETA-shrinkage was higher for V_p (43%), indicating that this IIV estimate was not supported by all subjects.

2.2.2. Covariate Analysis

Exploratory graphical analysis and clinical relevance guided covariate selection for a stepwise covariate analysis procedure. For aspartate aminotransferase (AST), alanine aminotransferase (ALT), γ–glutamyltransferase (GGT), platelet count, and international normalized ratio (INR), no trends of individual PK parameters vs. these covariates were observed. Moreover, we did not include serum creatine into the covariate analysis, as estimated glomerular filtration rate (eGFR) carries more information about the kidney function. eGFR, total bilirubin (bilirubin$_{tot}$), the maximum liver function capacity test (LiMAx test), the Model for End-Stage Liver Disease (MELD score), and CPS were tested on CL, and weight, sex, and age on V_c were considered as potential covariates in the population PK model. In the first step of the forward inclusion procedure, eGFR, bilirubin$_{tot}$, CPS, as well as MELD score on CL and weight on V_c were significant covariates and reduced

the IIV significantly (Table 2). From this starting point, three covariate models were built using either composite covariates (Models A and B) or continuous 'raw' covariates (Model C): Model A included CPS as a categorical covariate on CL to represent clinical practice. Model B included the MELD score, and Model C was built following the regular forward inclusion backward elimination procedure using the 'raw' covariates excluding the composite covariates Child–Pugh score and MELD score.

Table 2. Covariate analysis results from base model to first step in the forward inclusion, full models, and backward elimination.

	OFV	Implementation of Covariate Relationship	Model	dOFV	IIV	*p*-Value
Base model	−914.3	Two-compartment model with proportional error model			CL: 48.2% V_c: 85%	
Forward inclusion	−928.6	linear	bilirubin$_{tot}$/CL	−14.3	CL: 40.9%	<0.001
	−947.9	power	bilirubin$_{tot}$/CL	−33.6	CL: 36.5%	<0.001
	−931.7	exponential	bilirubin$_{tot}$/CL	−17.4	CL: 39.2%	<0.001
	−950.4	linear	eGFR/CL	−36.1	CL: 47.3%	<0.001
	−923.4	power	eGFR/CL	−9.0	CL: 43%	0.003
	−942.1	exponential	eGFR/CL	−28.5	CL: 48.4%	<0.001
	−930.8	linear	LiMAx test/CL	−16.5	CL: 59.1%	<0.001
	−926.5	power	LiMAx test/CL	−12.3	CL: 41.7%	<0.001
	−918.1	exponential	LiMAx test/CL	−3.81	CL: 54.6%	0.051
	−926.0	categorical	Child–Pugh/CL	−11.8	CL: 41.6%	<0.001
	−918.2	linear	MELD/CL	−3.94	CL: 39%	0.047
	−919.7	power	MELD/CL	−5.45	CL: 37.9%	0.019
	−918.1	exponential	MELD/CL	−3.83	CL: 38.7%	0.050
	−924.1	linear	WT/V_c	−9.88	V_c: 68.6%	0.002
	−920.9	power	WT/V_c	−6.71	V_c: 73.6%	0.009
	−917.9	exponential	WT/V_c	−3.60	V_c: 77.7%	0.058
	−921.4	linear	age/V_c	−7.08	V_c: 75.5%	0.008
	−916.9	power	age/V_c	−2.60	V_c: 85%	0.107
	−920.8	exponential	age/V_c	−6.51	V_c: 77.7%	0.011
	−918.1	categorical	sex/V_c	−3.9	V_c: 85.9%	0.048
Full model A	−936.0	Child–Pugh/CL (categorical) WT/V_c (linear)		−21.7	CL: 41.6% V_c: 70.0%	
Full model B	−929.5	MELD/CL (power) WT/V_c (linear)		−15.3	CL: 37.9% V_c: 69.1%	
Full model C	−974.4	eGFR (linear), bilirubin$_{tot}$ (power), on CL WT (linear) on V_c		−60.1	CL: 37.5% V_c: 70.9%	
Backward elimination		linear	eGFR/CL	16.9		<0.001
		power	bilirubin$_{tot}$/CL	13.5		<0.001
		linear	WT/V_c	10.1		0.0014

Abbreviations: CL: Clearance, Vc: Central volume of distribution, IIV: Inter-individual variability, bilirubin$_{tot}$: Total bilirubin, eGFR: Estimated glomerular filtration rate (CKD-EPI formula), LiMAx: Liver function capacity test, MELD: Model for end-stage liver disease, WT: Weight.

For Model A, the inclusion of the CPS as a categorical covariate was significant (dOFV: −11.7) and resulted in a descending order of tigecycline CL in relation to CPS. CPS$_C$ patients showed a 50.1% reduced CL compared to patients with a score of CPS$_{A/B}$. In addition, weight on V_c was significant (linear, dOFV: −9.9). IIV$_{CL}$ was reduced from 48.2% to 41.8% and IIV$_{Vc}$ from 85% to 70%. Supplementary Table S1 shows all final parameter estimates of that model.

For Model B, the MELD score, as a composite measure of liver and kidney function parameters, was a significant covariate on clearance (power, dOFV: −5.45). IIV$_{CL}$ was reduced from 48.2% to 37.9%. IIV$_{Vc}$ was reduced from 85% to 69.1% with weight on V_c. Final model parameters are displayed in Supplementary Table S2.

For Model C, the final model included eGFR (linear, dOFV: −16.9) and bilirubin$_{tot}$ (power, dOFV: −13.5) on CL and weight (linear, dOFV: −10.1) on V$_c$. IIV$_{CL}$ was reduced from 48.2% to 38.3% and IIV$_{Vc}$ from 85% to 72.4%. Reduced eGFR and higher bilirubin$_{tot}$ values corresponded to a lower CL to different extents. From the minimum to the maximum eGFR and bilirubin$_{tot}$ value, the CL range totaled 5.62–10.5 L/h and 4.15–11.0 L/h, respectively. Supplementary Table S3 shows the final model parameter estimates of this model. Both the goodness-of-fit plots and prediction-corrected visual predictive checks (pc-vpc) indicated a good overall fit (Supplementary Figures S1 and S2). The median pc-vpc predictions and observations are best overlayed in Model A, and Model B showed a slight increase in confidence intervals at the 95th percentile.

The statistically best fitting model was Model C with an AIC of −952 and residual unexplained variability (RUV) of 12.4%, compared to Model A: −913 and Model B: −909. Nevertheless, the MELD score as a single covariate on clearance (Model B) could best reduce the IIV$_{CL}$ (−10%) and, with that, to the same extent as Model A, which included two covariates on CL.

2.3. Monte Carlo Simulations

Standard- (100 mg loading dose (LD), 50 mg q12h maintenance dose (MD)) and low-dose tigecycline (100 mg LD, 25 mg q12h MD) were simulated (n = 1000). Simulation results were used to explore dose adjustment strategies and probability of target attainment (PTA). In our study population, the simulated AUC$_{ss}$ values after standard dosing using the best fitting covariate model (Model C) were 12.4 mg·h/L in median (2.5th to 97.5th percentile: 4.10–27.1 mg·h/L) and thus in the range of the median 'reference' AUC$_{ss}$ values after high-dose tigecycline (100 mg q12h MD) in non-critically ill patients (10.1 mg·h/L, 5.28–17.1 mg·h/L) (AUC$_{ss-vW}$ in Figure 1), yet more variable, indicating the need for dose adjustments. Indeed, if patients with CPS$_C$ received the standard dose of 50 mg q12h, they displayed a 44.4% increased AUC$_{ss}$ and a 117.5% increased steady-state C$_{min}$ compared to CPS$_{A/B}$. Therefore, only 33% of the patients would lie in the AUC$_{ss}$ reference range due to overexposure (Figure 1).
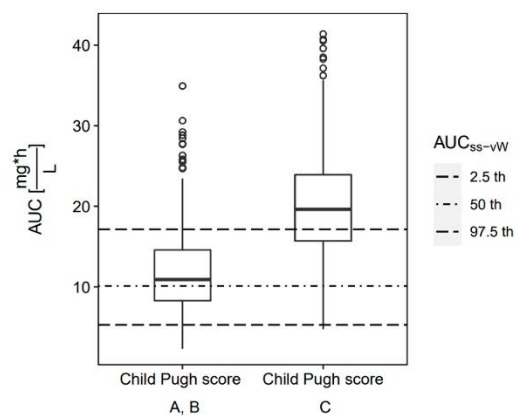
Figure 1. Simulated AUC$_{ss}$ in patients with Child–Pugh A/B and C and standard-dose tigecycline (50 mg q12h MD) compared to the simulated AUC$_{ss-vW}$ 'reference' of high-dose tigecycline (100 mg q12h MD) in non-critically ill patients.

Using CPS$_C$ to guide a dose adjustment to a maintenance dose of 25 mg q12h MD provided the best alignment with the AUC$_{ss}$ 'reference' range, both in terms of the agreement of median AUC$_{ss}$ and the fraction of simulated patients lying within the 2.5th and 97.5th AUC$_{ss}$ interval (Figure 2). For the covariates MELD score, bilirubin, and eGFR, the optimal cut-offs for a dose reduction were found at ≥30, ≥10 mg/dL, or <30 mL/min, respectively.
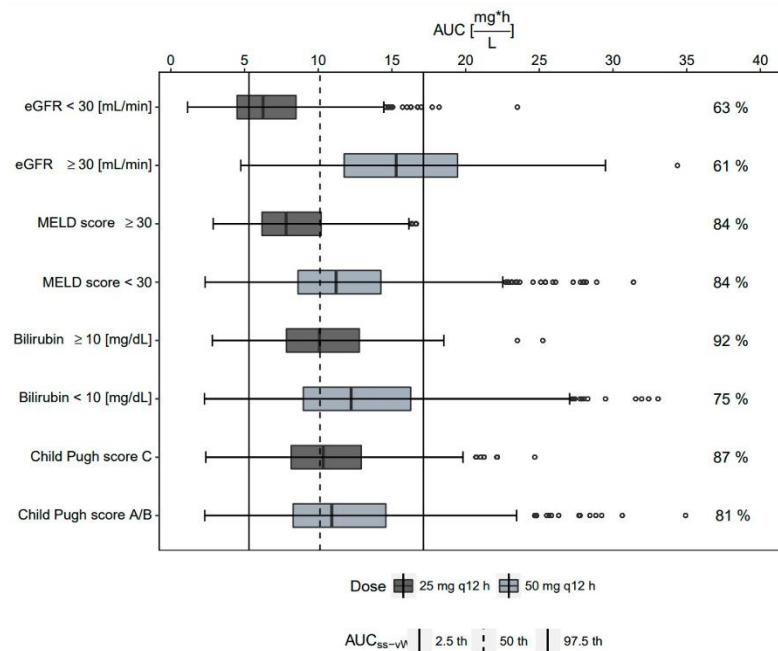
Figure 2. AUC_{ss} from dose-adjusted low-dose tigecycline (25 mg q12h MD) groups vs. non-adjusted groups receiving standard-dose tigecycline (50 mg q12h MD) in our cohort, compared to the 95% interval of 100 mg q12h MD tigecycline from van Wart et al. in non-ICU patients without hepatic impairment (AUC_{ss-vW}, vertical lines). Optimal cutoffs for dose adjustment investigation were CPS_C, total bilirubin $\geq$ 10 mg/dL, MELD score $\geq$ 30, and eGFR $\leq$ 30 mL/min. The quantity [%] of simulated individuals within the 95% interval of AUC_{ss-vW} is displayed.

However, the agreement of both median AUC_{ss} and the fraction of patients lying within the 'reference' range was considerably lower as compared to when using CPS_C to guide dose adjustment, and eGFR was found to perform worst (Figure 2).

2.4. Probability of Target Attainment

The alignment of the probability of PK/PD target attainment vs. MIC curve was highest when using the CPS-guided dosing. Nonetheless, all evaluated dose adjustment strategies provided a high (>90%) probability to attain the target for cIAI ($PTA_{90\%}$, $AUC_{ss}/MIC \geq 6.96$ [4]) for pathogens with a MIC $\leq$ 0.5. For the higher cSSI target ($AUC_{ss}/MIC \geq 17.9$ [3]), $PTA_{90\%}$ was attainted for pathogens with a MIC $\leq$ 0.25 (Figure 3).

2.5. Study Outcome

In this study, 8/39 patients (20%) showed clinical cure, 5/39 (13%) intermediate cure, and failure was observed for 26/39 (67%) patients. To evaluate clinical outcome, this analysis used odds ratios. The strongest correlation between therapy failure was observed for chronic liver disease (OR: 14.2 $CI_{95\%}$: 8.89–24.3), followed by serum creatinine (OR: 4.55, $CI_{95\%}$: 3.34–6.37), where the probability of therapy failure increased with increasing serum creatinine. eGFR, calculated by the CKD–EPI formula, was less significant (OR: 0.98, $CI_{95\%}$: 0.95–0.99), compared to solely serum creatinine. INR with an OR of 0.36 ($CI_{95\%}$: 0.25–0.51), $bilirubin_{tot}$ (OR: 1.30, $CI_{95\%}$: 1.22–1.39) and MELD score (OR: 1.13, $CI_{95\%}$: 1.10–1.16) were significant predictors of death. Neither the CPS_C, AUC_{24h} of tigecycline, nor the pathogen causing the infection or other laboratory data were predictive for therapy failure or death.
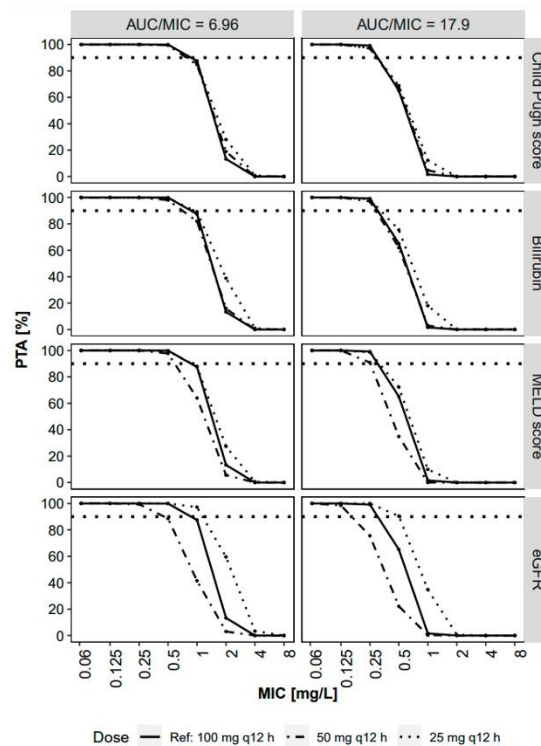
Figure 3. Probability of target attainment (PTA) analysis of AUC_{ss}/MIC ratio ≥ 17.9 and ≥ 6.96 over minimal inhibitory concentration (MIC). Dose adjustment (25 mg q12h MD) was applied for individuals with bilirubin ≥ 10 mg/dL, MELD score ≥ 30, and eGFR ≤ 30 mL/min and compared to non-adjusted (50 mg q12h MD) groups, as well as Child–Pugh score-based dose adjustment. Horizontal dotted line denotes 90% $PTA_{90\%}$.

3. Discussion

The present study aimed to assess the effects of different covariates on tigecycline exposure to evaluate their potential use as predictors for high and potentially suprathera-peutic AUC values and their ability to guide dose adjustments in severe liver impairment. This patient cohort had highly variable AUC values, but the results agreed with previous findings, that CPS_C is able to guide a maintenance dose reduction from 50 mg to 25 mg q12h.

This study recruited a very vulnerable cohort with tigecycline treatment, which has not been represented well in the literature so far. Patients had different stages of acute and chronic liver impairment, exemplified by the strongly reduced typical CL of 7.52 L/h in our cohort compared to healthy volunteers, other ICU patients (e.g., 18.3 L/h [13], 22.1 L/h [15], 13.5 L/h [16]), and non-ICU patients (e.g., CL of 16.8 L/h [17] and 18.6 L/h [18]). Hence, simulated AUC_{ss} values were strongly increased at standard tigecycline dosing. Un-doubtedly, safe and effective treatment is mandatory for these patients. However, dose adjustment for hepatically eliminated drugs is challenging, because the hepatic clearance cannot be solely determined by a single endogenous marker, such as creatinine clearance as a surrogate for renal drug clearance [19]. In our dataset, the CL reduction for patients with severe liver impairment with CPS_C was 50.1% and hence in line with the findings of Korth-Bradley et al. who found a CL reduction of 50.6% [20]. Hence, our results affirm the proposition by Korth-Bradley et al. to use CPS_C to guide dose adjustment. Furthermore, our covariate analysis identified bilirubin$_{tot}$, eGFR, and MELD score as covariates of CL. Tigecycline is not exclusively metabolized, but substantially biliary excreted, explaining

the correlation of bilirubin and MELD score to tigecycline clearance [21]. Moreover, the MELD score was recently suggested for dose adjustment in critically ill, liver decompensated patients, but was not directly compared to the CPS [22]. Furthermore, eGFR was a highly significant covariate in our study population. Kidney function is also affected with progression of liver disease [23], which could explain this strong correlation to tigecycline clearance. Korth-Bradley et al. observed a 20% decreased tigecycline clearance in renally impaired subjects, but no dose changes were recommended, as renal clearance accounts for only 20% of the total body clearance [24]. Our study results are in line with these findings, that strong eGFR reduction is not a signal to adjust the dose. Hence, CPS performed best to equalize tigecycline exposure in dose-adjusted (25 mg q12h MD) vs. non-adjusted patients (50 mg q12h MD), while maintaining an exposure equivalent to 100 mg q12h tigecycline observed in non-critically ill patients [18]. However, the CPS bears some limitations for use in clinical practice, as it is a composition of clinical variables and subjectively determined disease statuses [16,25]. In case CPS is unavailable, bilirubin$_{tot}$ or MELD score might serve as alternatives to guide dose adjustment.

The dose adjustment algorithms evaluated in this study aimed to achieve an exposure profile equivalent to high-dose tigecycline (100 mg q12h MD) in non-ICU patients, as several studies have reported that the standard dose regimen of 50 mg q12h MD is not sufficient to achieve a reliable treatment success [6,10,26–28]. The current EUCAST MIC breakpoints for susceptible *Enterobacterales* and *Staphylococcus* is ≤0.5 mg/L (http://www.eucast.org/clinical_breakpoints/, accessed on 21 March 2022). Our simulations challenge this breakpoint as the PTA$_{90\%}$ results indicate sufficient target attainment at an MIC of 0.5 mg/L only for the cIAI target, but insufficient target attainment for the cSSI target even under high-dose tigecycline conditions. This is in line with the findings of Kispal et al., who concluded with escalating the dose to 150 mg i.v. q12h in patients with higher MICs [29].

The clinical data revealed MELD score and their components (bilirubin and SCR) to be predictive for survival in our collective. Contrarily, higher AUC$_{24h}$ or AUC$_{72h}$ values were not associated with a higher cure rate, indicating that other factors such as the underlying (liver) disease, organ dysfunction, and infection mostly affected the patient outcomes. According to that, previous studies of tigecycline use in critically ill patients associated the Sequential Organ Failure Assessment score (SOFA) with clinical failure [6,30]. Finally, further trials are warranted to enhance safety and efficacy of tigecycline treatment.

This study contributes significantly to the understanding of tigecycline pharmacokinetics in patients with different degrees of liver impairment. As a strength of this study, our study individuals showed a wide spread in covariate values: Well distributed covariate values are needed for derivation of reliable relationships of patient covariates with PK parameters. However, stepwise covariate modeling is known to have problems with selection bias and multiple testing [31], causing uncertainty in the covariate parameter estimates. Even if this study represents the largest in the liver-impaired patient collective with tigecycline monotherapy, a higher patient would be necessary to increase the accuracy of the estimates to further strengthen the conclusions. As another limitation of this study, the study documentation did not include assessment of encephalopathy, and hence, this variable was neglected in the CPS calculation. Several patients were mechanically ventilated, and therefore, assessment of encephalopathy is difficult in ICU patients with the presence of liver-unrelated comorbidity. On the other hand, the investigated dose adjustment with CPS was proven to be a robust covariate even with the related uncertainty.

Another limitation is that tigecycline itself can induce hepatotoxicity. However, the patients included in this study displayed pre-existing liver impairment before treatment with tigecycline was initiated. Moreover, the frequency of tigecycline-induced hepatotoxicity is low as transient elevations of serum aminotransferase levels occurs in only 2–5% of the patients [32], and tigecycline pharmacokinetics was stable over the therapeutic course. Hence, it is very unlikely that the observed high exposure of tigecycline in our collective is a consequence and not a cause of liver impairment.

4. Materials and Methods

4.1. Patients and Study Design

Patients from the surgical ICU of the Charité University Hospital, Berlin, Germany were recruited after ethical approval (EA4/022/13). Parts of the clinical raw data were already previously published [33], but neither were utilized for population PK modeling nor for the development of dose adjustment algorithms. The study cohort included adult patients older than 18 years with acute liver dysfunction secondary to sepsis, as well as patients with chronic liver dysfunction. Moreover, pathogens associated with the infection and clinical outcome were documented. Cure was defined as the resolution or significant improvement of signs and symptoms of the index infection, such that no additional antimicrobials or interventions were required. Clinical failure was defined as death due to infection prior to end of therapy, persisting or recurrent infection requiring additional intervention, or treatment with additional antimicrobials for ongoing symptoms of infection. Moreover, an intermediate cure was defined as trial data, which included death unrelated to the index infection, or extenuating circumstances that precluded classification as cure or failure.

In brief, patients received a loading dose of 100 mg administered as a 30 min infusion, followed by a maintenance dose of 50 mg q12h. Based on the treating physician's assessment, eight patients received high-dose tigecycline with 100 mg q12h. Medical staff sampled at 0.3, 2, 5, 8, and 11.5 h after infusion at least 36 h after the start of therapy. Bioanalytical quantification of tigecycline plasma concentrations was performed, as previously described [34]. In addition to patient characteristics, clinical lab parameters included AST, ALT, GGT, SCR, eGFR according to CKD–EPI formula [35], albumin, bilirubin$_{tot}$, platelet count, and INR. AST and ALT served for De-Ritis ratio calculation. This study also evaluated the MELD score, as well as the LiMAx test, which provides a direct measure of the metabolic capacity of the liver through phenotyping of CYP1A2 metabolism [36]. Furthermore, age, sex, body weight, and ascites status were documented. The CPS was calculated with the given parameters of bilirubin$_{tot}$, albumin, INR, and ascites. Ascites were graded in none, mild (Grade 1), and moderate (Grade 2). The Child–Pugh Score calculations assumed no present encephalopathy, due to missing data. Moreover, no drug interaction of tigecycline was present and fluid balance was not considered. For evaluation of the clinical outcome, this analysis calculated odds-ratios using logistic regression for all laboratory liver parameters, the AUC$_{ss}$ of tigecycline, and pathogens' Gram type.

4.2. Pharmacometrics Analysis

4.2.1. Base Model

This study used the nonlinear mixed-effects modeling program NONMEM® (ICON, Gaithersburg, MD, USA, version 7.5), controlled by PsN 5.0 (Uppsala University, Sweden), for population pharmacokinetic analysis [37]. The population PK models were developed with first-order conditional estimation with interaction (FOCE+I). During model development, different compartments, and residual error models (additional, proportional, and combined) were tested. Inter-individual variability was assumed to be log-normally distributed and tested on all pharmacokinetic parameters, which were tigecycline CL, V_c, inter-compartmental clearance (Q), and peripheral volume of distribution (V_p).

4.2.2. Covariate Analysis

An exploratory graphical analysis in combination with clinical relevance guided covariate selection. A stepwise method, based on the log-likelihood ratio test (forward inclusion: p-value < 0.05, backward elimination: p-value of <0.01), was applied. This study tested continuous covariate relationships such as power, linear, and exponential relationships on the respective pharmacokinetic parameters. In addition to the pure statistical criteria, we defined a strong IIV$_{CL}$ reduction > 10% as a further specification of a covariate to be considered for evaluation of potential dose adjustment.

4.2.3. Final Model Evaluation

We evaluated candidate models by graphical and numerical criteria (goodness-of-fit plots, prediction-corrected visual predictive checks, drop of objective function value, and difference in Akaike Information Criterion between two competing models (lower AIC indicates superior model)). Parameter uncertainty was evaluated using a log-likelihood profiling-based sampling-importance resampling routine (LLP-SIR), a technique for evaluating parameter uncertainty in small datasets [38].

4.2.4. Simulations

Monte Carlo simulations (n = 1000) were utilized to simulate low- (100 mg LD, 25 mg q12h MD) and standard-dose (100 mg LD, 50 mg q12h MD) tigecycline. Covariates were resampled with replacement from the study participants to acknowledge potential correlations of the covariates in our study population. The candidate covariate models were exploited for dose adjustment. The target range for dose adjustment was defined by the AUC_{24h} range (10.12, 5.3–17.4 (50th, 2.5th–95th percentile). This range was achieved by simulating high-dose tigecycline (100 mg LD; 100 mg q12h MD) in non-critically ill patients using published pharmacokinetic information of the clinical study of van Wart et al. [18]. We chose to target the exposure after high-dose tigecycline, as it is associated with a more favorable clinical outcome than standard-dose [6–9].

Moreover, we performed a probability of target attainment analysis ($PTA_{90\%}$) using the target for cIAI ($PTA_{90\%}$, steady-state $AUC_{24h/MIC} \geq 6.96$ [4]) and the higher cSSI target (steady-state $AUC_{24h}/MIC \geq 17.9$ [3]).

5. Conclusions

To summarize, dose reduction in severe liver impairment to a maintenance dose of 25 mg q12h was the best-guided CPS leading to AUC_{ss} values, which are equivalent to those found in non-ICU patients undergoing high-dose tigecycline (100 mg q12h MD), which was previously related to improve outcome. $Bilirubin_{tot}$ and MELD score might serve as alternatives to guide dose adjustment but were inferior to CPS. Hence, a prospective evaluation of the tigecycline dosing strategy in patients with severe liver impairment is warranted.

Informed Consent Statement: Informed consent was obtained from all subjects involved in the study. Written informed consent has been obtained from the patient(s) to publish this paper.

Data Availability Statement: Data are available on reasonable request due to restrictions.

Conflicts of Interest: The authors declare no conflict of interest.

References

1. Boucher, H.W.; Wennersten, C.B.; Eliopoulos, G.M. In Vitro Activities of the Glycylcycline GAR-936 against Gram-Positive Bacteria. *Antimicrob. Agents Chemother.* **2000**, *44*, 2225–2229. [CrossRef] [PubMed]
2. Pfizer Tygacil®Full Prescribing Information. Available online: https://www.pfizermedicalinformation.com/en-us/tygacil/dosage-admin (accessed on 21 March 2022).
3. Meagher, A.K.; Passarell, J.A.; Cirincione, B.B.; Van Wart, S.A.; Liolios, K.; Babinchak, T.; Ellis-Grosse, E.J.; Ambrose, P.G. Exposure-Response Analyses of Tigecycline Efficacy in Patients with Complicated Skin and Skin-Structure Infections. *Antimicrob. Agents Chemother.* **2007**, *51*, 1939–1945. [CrossRef] [PubMed]
4. Passarell, J.A.; Meagher, A.K.; Liolios, K.; Cirincione, B.B.; Van Wart, S.A.; Babinchak, T.; Ellis-Grosse, E.J.; Ambrose, P.G. Exposure-Response Analyses of Tigecycline Efficacy in Patients with Complicated Intra-Abdominal Infections. *Antimicrob. Agents Chemother.* **2008**, *52*, 204–210. [CrossRef] [PubMed]
5. McGovern, P.C.; Wible, M.; El-Tahtawy, A.; Biswas, P.; Meyer, R.D. All-cause mortality imbalance in the tigecycline phase 3 and 4 clinical trials. *Int. J. Antimicrob. Agents* **2013**, *41*, 463–467. [CrossRef] [PubMed]
6. De Pascale, G.; Montini, L.; Pennisi, M.; Bernini, V.; Maviglia, R.; Bello, G.; Spanu, T.; Tumbarello, M.; Antonelli, M. High dose tigecycline in critically ill patients with severe infections due to multidrug-resistant bacteria. *Crit. Care* **2014**, *18*, R90. [CrossRef]
7. De Pascale, G.; Lisi, L.; Ciotti, G.M.P.; Vallecoccia, M.S.; Cutuli, S.L.; Cascarano, L.; Gelormini, C.; Bello, G.; Montini, L.; Carelli, S.; et al. Pharmacokinetics of high-dose tigecycline in critically ill patients with severe infections. *Ann. Intensive Care* **2020**, *10*, 94. [CrossRef] [PubMed]
8. Zha, L.; Pan, L.; Guo, J.; French, N.; Villanueva, E.V.; Tefsen, B. Effectiveness and Safety of High Dose Tigecycline for the Treatment of Severe Infections: A Systematic Review and Meta-Analysis. *Adv. Ther.* **2020**, *37*, 1049–1064. [CrossRef]
9. Xia, G.; Jiang, R. Clinical study on the safety and efficacy of high-dose tigecycline in the elderly patients with multidrug-resistant bacterial infections. *Medicine* **2020**, *99*, e19466. [CrossRef]
10. Ni, W.; Li, G.; Zhao, J.; Cui, J.; Wang, R.; Gao, Z.; Liu, Y. Use of Monte Carlo simulation to evaluate the efficacy of tigecycline and minocycline for the treatment of pneumonia due to carbapenemase-producing Klebsiella pneumoniae. *Infect. Dis.* **2018**, *50*, 507–513. [CrossRef]
11. Li, M.X.; Li, N.; Zhu, L.Q.; Liu, W. Optimization of tigecycline dosage regimen for different infections in the patients with hepatic or renal impairment. *J. Chemother.* **2020**, *32*, 420–428. [CrossRef]
12. Fernández, J.; Gustot, T. Management of bacterial infections in cirrhosis. *J. Hepatol.* **2012**, *56*, S1–S12. [CrossRef]
13. Broeker, A.; Wicha, S.G.; Dorn, C.; Kratzer, A.; Schleibinger, M.; Kees, F.; Heininger, A.; Kees, M.G.; Häberle, H. Tigecycline in critically ill patients on continuous renal replacement therapy: A population pharmacokinetic study. *Crit. Care* **2018**, *22*, 341. [CrossRef] [PubMed]
14. Rubino, C.M.; Bhavnani, S.M.; Forrest, A.; Dukart, G.; Dartois, N.; Cooper, A.; Korth-Bradley, J.; Ambrose, P.G. Pharmacokinetics-Pharmacodynamics of Tigecycline in Patients with Community-Acquired Pneumonia. *Antimicrob. Agents Chemother.* **2012**, *56*, 130–136. [CrossRef] [PubMed]
15. Borsuk-De Moor, A.; Rypulak, E.; Potręć, B.; Piwowarczyk, P.; Borys, M.; Sysiak, J.; Onichimowski, D.; Raszewski, G.; Czuczwar, M.; Wiczling, P. Population Pharmacokinetics of High-Dose Tigecycline in Patients with Sepsis or Septic Shock. *Antimicrob. Agents Chemother.* **2018**, *62*, e02273-17. [CrossRef] [PubMed]
16. Ruiz, J.; Ramirez, P.; Villarreal, E.; Gordon, M.; Sánchez, M.Á.; Martín, M.; Castellanos-Ortega, Á. Effect of pharmacokinetic/pharmacodynamic ratio on tigecycline clinical response and toxicity in critically ill patients with multidrug-resistant Gram-negative infections. *SAGE Open Med.* **2020**, *8*, 2050312120958897. [CrossRef]
17. Van Wart, S.A.; Cirincione, B.B.; Ludwig, E.A.; Meagher, A.K.; Korth-Bradley, J.M.; Owen, J.S. Population Pharmacokinetics of Tigecycline in Healthy Volunteers. *J. Clin. Pharmacol.* **2007**, *47*, 727–737. [CrossRef]
18. Van Wart, S.A.; Owen, J.S.; Ludwig, E.A.; Meagher, A.K.; Korth-Bradley, J.M.; Cirincione, B.B. Population Pharmacokinetics of Tigecycline in Patients with Complicated Intra-Abdominal or Skin and Skin Structure Infections. *Antimicrob. Agents Chemother.* **2006**, *50*, 3701–3707. [CrossRef]
19. Lam, Y.W.F.; Banerji, S.; Hatfield, C.; Talbert, R.L. Principles of Drug Administration in Renal Insufficiency. *Clin. Pharmacokinet.* **1997**, *32*, 30–57. [CrossRef]
20. Korth-Bradley, J.M.; Baird-Bellaire, S.J.; Patat, A.A.; Troy, S.M.; Böhmer, G.M.; Gleiter, C.H.; Buecheler, R.; Morgan, M.Y. Pharmacokinetics and Safety of a Single Intravenous Dose of the Antibiotic Tigecycline in Patients With Cirrhosis. *J. Clin. Pharmacol.* **2011**, *51*, 93–101. [CrossRef]
21. Meagher, A.K.; Ambrose, P.G.; Grasela, T.H.; Ellis-Grosse, E.J. The Pharmacokinetic and Pharmacodynamic Profile of Tigecycline. *Clin. Infect. Dis.* **2005**, *41*, S333–S340. [CrossRef]

22. Bastida, C.; Hernández-Tejero, M.; Aziz, F.; Espinosa, C.; Sanz, M.; Brunet, M.; López, E.; Fernández, J.; Soy, D. Tigecycline population pharmacokinetics in patients with decompensated cirrhosis and severe infections. *J. Antimicrob. Chemother.* **2020**, *75*, 3619–3624. [CrossRef] [PubMed]

23. Durand, F.; Valla, D. Assessment of the prognosis of cirrhosis: Child–Pugh versus MELD. *J. Hepatol.* **2005**, *42*, S100–S107. [CrossRef] [PubMed]

24. Korth-Bradley, J.M.; Troy, S.M.; Matschke, K.; Muralidharan, G.; Fruncillo, R.J.; Speth, J.L.; Raible, D.G. Tigecycline Pharmacokinetics in Subjects With Various Degrees of Renal Function. *J. Clin. Pharmacol.* **2012**, *52*, 1379–1387. [CrossRef] [PubMed]

25. Spray, J.W.; Willett, K.; Chase, D.; Sindelar, R.; Connelly, S. Dosage adjustment for hepatic dysfunction based on Child-Pugh scores. *Am. J. Health Syst. Pharm.* **2007**, *64*, 690, 692–693. [CrossRef]

26. Yang, T.; Mei, H.; Wang, J.; Cai, Y. Therapeutic Drug Monitoring of Tigecycline in 67 Infected Patients and a Population Pharmacokinetics/Microbiological Evaluation of A. baumannii Study. *Front. Microbiol.* **2021**, *12*, 678165. [CrossRef]

27. Ramirez, J.; Dartois, N.; Gandjini, H.; Yan, J.L.; Korth-Bradley, J.; McGovern, P.C. Randomized Phase 2 Trial To Evaluate the Clinical Efficacy of Two High-Dosage Tigecycline Regimens versus Imipenem-Cilastatin for Treatment of Hospital-Acquired Pneumonia. *Antimicrob. Agents Chemother.* **2013**, *57*, 1756–1762. [CrossRef]

28. Xie, J.; Wang, T.; Sun, J.; Chen, S.; Cai, J.; Zhang, W.; Dong, H.; Hu, S.; Zhang, D.; Wang, X.; et al. Optimal tigecycline dosage regimen is urgently needed: Results from a pharmacokinetic/pharmacodynamic analysis of tigecycline by Monte Carlo simulation. *Int. J. Infect. Dis.* **2014**, *18*, 62–67. [CrossRef]

29. Kispal, B.; Walker, S.A.N. Monte Carlo simulation evaluation of tigecycline dosing for bacteria with raised minimum inhibitory concentrations in non-critically ill adults. *Eur. J. Clin. Pharmacol.* **2021**, *77*, 197–205. [CrossRef]

30. Montravers, P.; Dupont, H.; Bedos, J.-P.; Bret, P. Tigecycline use in critically ill patients: A multicentre prospective observational study in the intensive care setting. *Intensive Care Med.* **2014**, *40*, 988–997. [CrossRef]

31. Ribbing, J.; Niclas Jonsson, E. Power, Selection Bias and Predictive Performance of the Population Pharmacokinetic Covariate Model. *J. Pharmacokinet. Pharmacodyn.* **2004**, *31*, 109–134. [CrossRef]

32. Anonymous. *LiverTox: Clinical and Research Information on Drug Induced Liver Injury*; National Institute of Diabetes and Digestive and Kidney Diseases; Tigecycline; Bethesda, MD, USA, 2019. Available online: https://www.ncbi.nlm.nih.gov/books/NBK547888/ (accessed on 21 March 2022).

33. Alraish, R.; Wicha, S.G.; Frey, O.R.; Roehr, A.C.; Pratschke, J.; Stockmann, M.; Wuensch, T.; Kaffarnik, M. Pharmacokinetics of tigecycline in critically ill patients with liver failure defined by maximal liver function capacity test (LiMAx). *Ann. Intensive Care* **2020**, *10*, 106. [CrossRef] [PubMed]

34. Wicha, S.G.; Frey, O.R.; Roehr, A.C.; Pratschke, J.; Stockmann, M.; Alraish, R.; Wuensch, T.; Kaffarnik, M. Linezolid in liver failure: Exploring the value of the maximal liver function capacity (LiMAx) test in a pharmacokinetic pilot study. *Int. J. Antimicrob. Agents* **2017**, *50*, 557–563. [CrossRef] [PubMed]

35. Levey, A.S.; Stevens, L.A.; Schmid, C.H.; Zhang, Y.L.; Castro, A.F.; Feldman, H.I.; Kusek, J.W.; Eggers, P.; Van Lente, F.; Greene, T.; et al. A New Equation to Estimate Glomerular Filtration Rate. *Ann. Intern. Med.* **2009**, *150*, 604–612. [CrossRef] [PubMed]

36. Jara, M.; Bednarsch, J.; Valle, E.; Lock, J.F.; Malinowski, M.; Schulz, A.; Seehofer, D.; Jung, T.; Stockmann, M. Reliable assessment of liver function using LiMAx. *J. Surg. Res.* **2015**, *193*, 184–189. [CrossRef] [PubMed]

37. Lindbom, L.; Pihlgren, P.; Jonsson, N. PsN-Toolkit—A collection of computer intensive statistical methods for non-linear mixed effect modeling using NONMEM. *Comput. Methods Programs Biomed.* **2005**, *79*, 241–257. [CrossRef] [PubMed]

38. Broeker, A.; Wicha, S.G. Assessing parameter uncertainty in small-n pharmacometric analyses: Value of the log-likelihood profiling-based sampling importance resampling (LLP-SIR) technique. *J. Pharmacokinet. Pharmacodyn.* **2020**, *47*, 219–228. [CrossRef] [PubMed]

3.4   Publication IV

Operational characteristics of full random effects modelling ('frem') compared to stepwise covariate modelling ('scm').

Lisa F. Amann[1], Sebastian G. Wicha[1]

[1]Dept. of Clinical Pharmacy, Institute of Pharmacy, University of Hamburg, Hamburg, Germany

Synopsis

Covariate analysis is an inherent part in pharmacometric analyses. So far, a comparison of the most often used stepwise covariate modelling procedure ('scm') to the full random effects modelling technique ('frem') was missing. This study introduced a 'frem' guided covariate selection, named 'frem$_{posthoc}$' standing for how 'frem' could be used to guide a covariate backward elimination. Both methods are different approaches to analyse and communicate a covariate analysis, so that this study compared on the one hand 'scm' with commonly used settings (scenario 1), but also in a 'head-to-head' comparison applying a statistically similar framework (scenario 2). Moreover 'frem' coefficients without a selection step were analysed in scenario 3. The scenarios were evaluated upon power to identify the true covariate, as well as precision, and accuracy of the estimated covariate coefficients. 'Frem$_{posthoc}$' had a up to three-fold higher power to detect the true covariate with lower bias in small N studies (N < 50) compared to 'scm' (scenario 1). This finding was vice versa in scenario 2 of note that the application of 'scm' does not represent common settings. For 'frem$_{posthoc}$', power, precision and accuracy of the covariate coefficient increased with higher number of individuals and covariate effect size. Moreover, 'frem' coefficients without a selection were unbiased and more accurate (scenario 3). We conclude that 'frem$_{posthoc}$' is also a suitable method to guide covariate selection, especially in small N datasets and that it is as reliable as 'scm' in large datasets (N >100).

ORIGINAL PAPER

Operational characteristics of full random effects modelling ('frem') compared to stepwise covariate modelling ('scm')

Lisa F. Amann[1] · Sebastian G. Wicha[1]

Abstract

An adequate covariate selection is a key step in population pharmacokinetic modelling. In this study, the automated stepwise covariate modelling technique ('scm') was compared to full random effects modelling ('frem'). We evaluated the power to identify a 'true' covariate (covariate with highest correlation to the pharmacokinetic parameter), precision, and accuracy of the parameter-covariate estimates. Furthermore, the predictive performance of the final models was assessed. The scenarios varied in covariate effect sizes, number of individuals (n = 20–500) and covariate correlations (0–90% cov-corr). The PsN 'frem' routine provides a 90% confidence intervals around the covariate effects. This was used to evaluate its operational characteristics for a statistical backward elimination procedure, defined as 'frem$_{posthoc}$' and to facilitate the comparison to 'scm'. 'Frem$_{posthoc}$' had a higher power to detect the true covariate with lower bias in small n studies compared to 'scm', applied with commonly used settings (forward p < 0.05, backward p < 0.01). This finding was vice versa in a statistically similar setting. For 'frem$_{posthoc}$', power, precision and accuracy of the covariate coefficient increased with higher number of individuals and covariate effect magnitudes. Without a backward elimination step 'frem' models provided unbiased coefficients with highly imprecise coefficients in small n datasets. Yet, precision was superior to final 'scm' model precision obtained using common settings. We conclude that 'frem$_{posthoc}$' is also a suitable method to guide covariate selection, although intended to serve as a full model approach. However, a deliberated selection of automated methods is essential for the modeller and using those methods in small datasets needs to be taken with caution.

Keywords Covariate analysis · Population pharmacokinetics · Simulation study · NONMEM®

Introduction

Over the past decades, population pharmacokinetic modelling with nonlinear mixed effects (NLME) approaches efficiently supported drug development. During model development covariates are analysed to establish a relationship between a model parameter and a patient specific variable. A covariate can be any variable on patient-level (not time varying) that influences the pharmacokinetics (PK) or pharmacodynamics (PD) of a drug. If informative, it reduces unexplained inter-individual PK or PD variability. To guide dose adjustments in special patient populations (e.g. elderly, adipose, hepatically or renally

impaired patients), a covariate analysis is also of interest to regulatory authorities [1]. To date, a number of automated covariate selection techniques are available [2]: these include e.g. stepwise covariate modelling ('scm') [3], or least absolute shrinkage and selection operator (lasso) [4]. The stepwise procedure tests predefined covariates on structural PK or PD parameters of interest. Automated covariate selection methods are statistically driven methods. The 'scm' includes covariates by the highest drop of objective function (dOFV) with a predefined p-value during the forward inclusion. In one of the more common implementations covariates are included until the likelihood ratio test identifies no significant covariate parameter relationship anymore. Afterwards, the backward elimination reduces the covariate model to obtain the final model, by applying a stricter p-value. This method has been evaluated on their properties and compared to other established methods before [5, 6]. In contrast to that, the 'frem' is a full model approach and includes all covariates

✉ Sebastian G. Wicha
   sebastian.wicha@uni-hamburg.de

[1] Department of Clinical Pharmacy, Institute of Pharmacy, University of Hamburg, Bundesstraße 45, 20146 Hamburg, Germany

of interest as observations (i.e., explicitly defining the likelihood of the covariate values) [7]. A full covariance matrix quantifies the random effects of PK parameters and describes parameter covariate relationships [8]. With the matrix, covariances of covariates can inform for other covariates so that this method is less sensitive to collinearity. Covariate coefficients are obtained from the ratio of covariance between parameter and covariate variability to the covariate variance [7].

The novel 'frem' method has not been applied to many clinical datasets yet [9–11]. Although 'scm' and 'frem' are techniques that are rather complementary in nature due their inherently different way to approach covariate modelling, a structured comparison of the operational characteristics using a simulation study is lacking. The aim of this study was to compare the 'scm' and 'frem' as automated covariate analysis methods. In order to enable a comparison, we here introduce the 'frem$_{posthoc}$' that offers a covariate selection step from the final 'frem' model using the confidence intervals around the estimated covariate effect sizes in the final 'frem' model. In the present study, the following aspects between 'scm', 'frem' and 'frem$_{posthoc}$' were compared: (1) the power to identify the true covariate (here defined as the covariate with the highest correlation with the PK parameter), (2) accuracy and precision of the estimated relationship, as well as (3) the predictive performance. To enable a thorough comparison, we investigated the impact of dataset size (n = 20–500), and covariate correlation (0–90%) for three covariate effect sizes in sparse simulated datasets using the commonly used ('scm') or predefined ('frem'/'frem$_{posthoc}$') settings of both approaches as well as statistically equal settings.

Methods

The workflow of this simulation study is shown in Fig. 1. The simulation dataset contained three covariates sampled from a multivariate normal distribution. The dataset was used to simulate with a one compartment model including the true covariate relationship on clearance. These simulated clinical datasets served for 'scm' and 'frem' analyses (n = 1000 for each scenario). Based upon the final models, power, precision, and accuracy were evaluated. The following section describes the single steps in detail.

Software

NLME modelling was applied with NONMEM® 7.5.0 [12], controlled through PsN 5.0.0 [13]. The software R (version 3.6.0) [14] was used for automated run executions

and data analysis. The NONMEM® models as well as relevant R code are provided in Supplement 1.

Generation of datasets and simulation of PK data

Continuous covariates

Three vectors of three covariates (i.e., covariate$_I$, covariate$_{II}$ and covariate$_{III}$) with defined means, and variances were drawn from a multivariate normal distribution (Supplement 3, Figure S3-1). The datasets included various correlations of covariate$_I$ (cov$_{true}$) and covariate$_{II}$ from 0 to 90%. Covariate$_{III}$ represented pure "noise" and was independent from cov$_{true}$ and covariate$_{II}$. All simulations used individually simulated datasets with 20, 50, 100 or 500 virtual patients (n) including 2 (sparse) concentration-time points per individual. The sparse sampling datasets included samples in the sixth and twelfth dosing interval (1 and 11.5 h time after last dose, respectively). PK profiles of the scenarios (1-CMT PK model, i.v. short infusion, linear elimination) were obtained via Monte Carlo simulations. The true PK model (run001) is described in Supplement 1.1. The simulated dose was 100 mg q12 h with 30 min infusion. The PK model parameters were clearance (CL) of 18 L/h with inter-individual variability on CL (IIV$_{CL}$: 0.1 variance, log-normal distribution), central volume of distribution (V1) of 400 L and a residual proportional error (%CV) of 15%. Cov$_{true}$ was implemented as an exponential covariate on CL (θ_{CL}) with the θ_{cov} as covariate coefficient (Eq. 1):

$$CL = \theta_{CL} \cdot e^{(\theta_{cov} \cdot (COV - COV_{mean}))} \cdot e^{\eta_i}. \tag{1}$$

The individual covariate value (cov) was normalized by the mean of the covariate distribution ($cov - cov_{mean}$). The remaining unexplained inter-individual variability (η_i) described the individual deviation from the typical parameter θ_{CL} for the ith individual (Eq. 1).

The observed concentration $Y_{observed,i,j}$ was calculated by the predicted concentration $Y_{predicted,i,j}$ multiplied by the proportional residual unexplained variance per individual i at each time point j (Eq. 2). No inter-occasion variability was included:

$$Y_{observed,i,j} = Y_{predicted,i,j} \cdot \left(1 + \varepsilon_{prop,i,j}\right). \tag{2}$$

The simulated covariate effect magnitudes varied between θ_{cov} = 0.026, 0.032 and 0.045, respectively. This resulted in relative effect sizes of − 18 to + 22%, − 22 to + 27% and − 29 to + 41% on CL at the 5th − 95th percentile of covariate values.

Fig. 1 Graphical workflow of the simulation study. *Scm* stepwise covariate modelling, *frem* full random effects modelling, *rrmse* relative root mean squared error, *rbias* relative bias, *mvrnorm* multivariate normal distribution
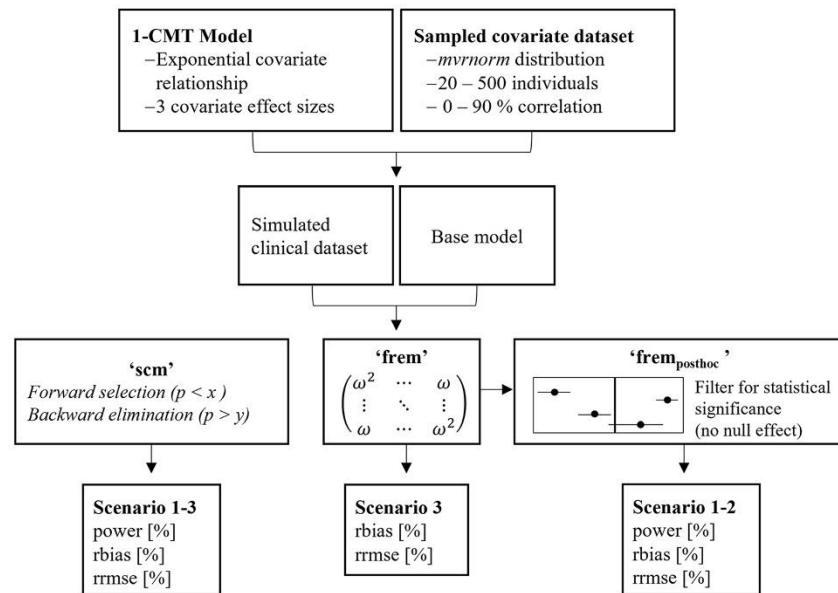
Evaluation using 'scm' or 'frem' models

Parameter estimation was performed using first order conditional estimation with interaction (FOCE+I), allowing three minimum retries on each simulated dataset (for each scenario, n = 1000). The structural model used for estimation is described in Supplement 1.2 (run002). The ADVAN 1 subroutine was used as analytical solution of the 1-CMT model. All three previously simulated covariates in the simulated dataset were provided to the 'scm', as well to 'frem' for analysis. The 'scm' and 'frem' were executed on each simulated dataset. The final 'scm' model results were either obtained in the last forward/backward step, or if the covariate identification failed, no covariate model was obtained. The 'frem' is a full model approach that includes all provided covariates simultaneously. Thereby, results cannot be compared to 'scm' without restrictions. To address the fundamental differences of these methods we evaluated the results in three settings:

(i) Scenario 1 evaluated the operational characteristics of 'frem$_{posthoc}$'. A covariate backward elimination from final 'frem' models was performed via the 90% confidence intervals of the estimated covariate effect and compared to final 'scm' models obtained with commonly used settings (forward inclusion, $p < 0.05$ and a backward elimination $p < 0.01$).

(ii) Scenario 2 assessed a statistical 'head-to-head' comparison of 'frem$_{posthoc}$' and 'scm' cov$_{true}$ coefficients with only forward inclusion ($p < 0.1$)

(iii) Scenario 3 showed a comparison of all estimated 'frem' cov$_{true}$ covariate coefficients without a selection step compared to 'scm' results of Scenario 1.

Scenario 1

A forward selection with a p-value of < 0.05 and a backward elimination ($p < 0.01$) was used reflecting the commonly used settings of the 'scm'. We compared those 'scm' runs, which selected cov$_{true}$ to those 'frem' runs that identified cov$_{true}$ with a covariate effect significantly different from zero. The significance was interpreted by the 90% confidence interval obtained from sampling importance resampling (SIR) [15]. The results were extracted from the PsN provided results files (PsN 5.0.0), and the effect sizes (5th – 95th percentile of the covariate effect, 90% confidence interval) reflect the default setting of the 'frem' PsN routine. Since this setting evaluated a backward elimination, we define this use case of the 'frem' as 'frem$_{posthoc}$'. We furthermore defined power (1–type II error) as the frequency of selecting cov$_{true}$ in the covariate model ('scm'), or as frequency to identify cov$_{true}$ as a covariate with the highest effect size different from zero and non-overlapping 90% confidence interval ('frem$_{posthoc}$'). For the 'frem$_{posthoc}$', the estimated univariate θ_{cov} coefficient was evaluated (PsN 'frem_results.csv'), which represents the effect of a single covariate in isolation [7]. Conditional accuracy and conditional precision,

expressed as rbias (Eq. 3) and rrmse (Eq. 4), were calculated as follows for significant cov_{true} coefficients:

$$rBIAS(\%) = \frac{1}{N} \cdot \sum_1^i \frac{(estimated_i - true_i)}{true_i} \cdot 100, \qquad (3)$$

$$rRMSE(\%) = \sqrt{\frac{1}{N} \cdot \sum_1^i \frac{(estimated_i - true_i)^2}{true_i^2}} \cdot 100. \qquad (4)$$

The denominator (N) was different across the simulated scenarios and methods, as the number of simulations for which cov_{true} coefficients was evaluated changed accordingly.

Moreover, true alpha values (Type-I error rate) were evaluated based on cov_{III} inclusion in the forward 'scm' models and the final 'frem$_{\text{posthoc}}$' models. Cov$_{\text{III}}$ is independent of the others and represents pure noise without having any simulated relationship between the pharmacokinetics and cov_{III}. The alpha values in the final 'frem$_{\text{posthoc}}$' models were defined as the frequency of runs in which the cov_{III} effect was not overlapping with zero.

According to Ribbing et al., we calculated the fraction of predictive models by assuming an estimated covariate coefficient between zero and two times cov_{true} to be likely to improve the predictive performance of a model [16]. For each scenario the fraction of predictive models was calculated (Eq. 5), where e represents the covariate effect size, c the correlation between cov_{true} and cov_{II} and N the dataset size varying from n = 20–500. S_{ecnN} represented the models which included cov_{true} ('scm') for the respective scenario. For 'frem$_{\text{posthoc}}$' coefficients, s_{ecnN} represented all runs or those including a significant cov_{true} relationship with the highest effect of all three covariates in the models for comparison to the 'scm'.

Fraction of predictive model:

$$s_{ecN} = 100 \cdot \frac{\sum_{n=1}^{1000}(P_{ecnN} \cdot s_{ecnN})}{\sum_{n=1}^{1000} s_{ecnN}}(\%), \qquad (5)$$

where,

$$P_{ecnN} = \begin{cases} 1 & if \left| \dfrac{\hat{\theta}_{ecnN} - \theta_{ecnN}}{\theta_{ecnN}} \right| < 1 \\ 0 & otherwise \end{cases}.$$

Scenario 2

For a comparison of equal selection criteria, 'scm' runs with only forward inclusion (p-value < 0.1) were compared to 'frem$_{\text{posthoc}}$' results (which evaluates overlap/nonoverlap with zero of the 90% confidence interval). Settings for 'frem$_{\text{posthoc}}$' were not changed compared to scenario 1. Power, conditional accuracy and precision were calculated

for those runs, where the included cov_{true} was statistically significant. Similar to scenario 1, the predictive performance of final 'scm' and frem$_{\text{posthoc}}$' models was evaluated according to Ribbing et al. [16]. As the number of significant runs changed across the simulated scenarios (e.g. n, covariate effect magnitude, cov-corr) the denominator to calculate these evaluation metrices changed between also between both methods.

Scenario 3

In this scenario, conditional accuracy, and precision, but also the predictive performance of all estimated 'frem' cov_{true} coefficients (i.e. no posthoc selection step from the final 'frem' model) were compared to 'scm' models obtained in scenario 1.

Categorical covariates

Additionally, a simulation study (n = 500) with a true dichotomous categorical covariate was performed. The dataset size varied from n = 20–500 and covariate correlation to a continuous covariate was 0% or 80%. The third covariate (continuous) was independent of the others. The true model included the categorical covariate as a fractional change of clearance with an effect size of either − 20% or − 40%. IIV$_{\text{CL}}$, but also inter individual variability on central volume of distribution (IIVV$_{\text{c}}$) was included in the model. More details on this study are described in Supplement 2.

Results

Power of cov_{true} inclusion for 'scm' and 'frem$_{\text{posthoc}}$'

The power to include the cov_{true} throughout the investigated scenarios was highly variable. Overall, the power to select cov_{true} increased with dataset size or covariate effect and decreased in presence of covariate collinearity.

In scenario 1, the simulations and estimations showed that 'frem$_{\text{posthoc}}$' power was higher compared to the 'scm' throughout all scenarios (Fig. 2), likely due to the higher value for alpha of 0.1 in the 'frem$_{\text{posthoc}}$' (non-overlapping 90% confidence interval of the covariate effect size) vs. 0.01 in the 'scm'. The dataset size (n = 20 to n = 100) strongly increased power for both methods. The presence of covariate correlation reduced the power of 'frem$_{\text{posthoc}}$' from 82 to 59% (n = 50, $\theta_{cov_{true}} = 0.032$) whereas the 'scm' power was less affected by correlation in the simulated scenarios (Table 1). Moreover, with an increasing covariate effect on clearance, we observed an increase of power from
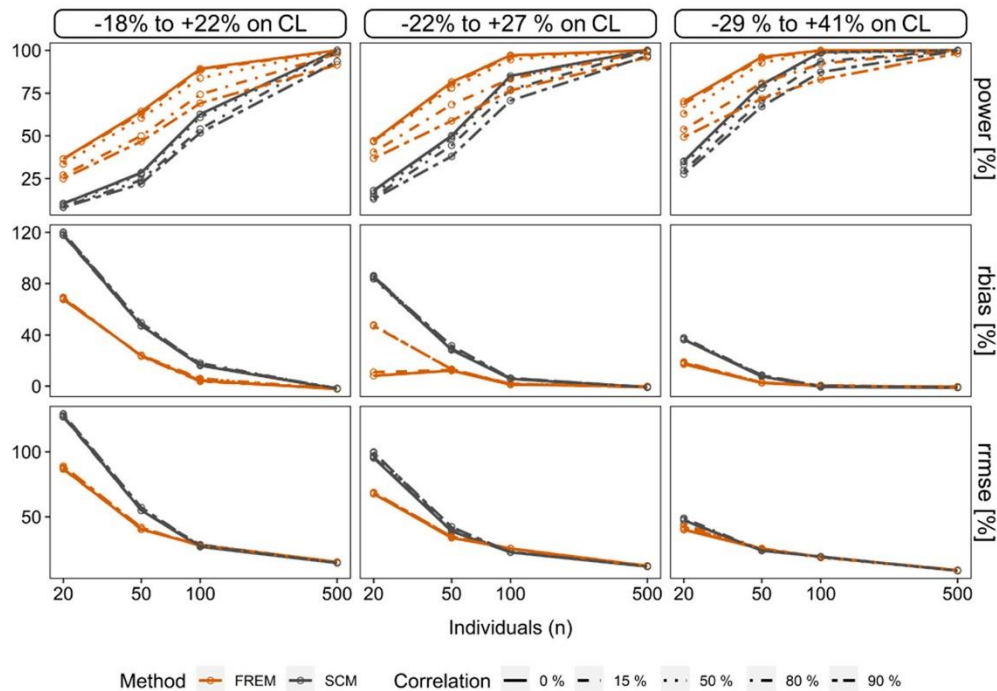
Fig. 2 'Scm' and 'frem$_{posthoc}$' results of scenario 1. Illustration of power (%), conditional relative bias (%) (*rbias*) and conditional relative root mean squared error (%) (*rrmse*) of *cov$_{true}$* estimates. Conditional accuracy and precision for the 'frem$_{posthoc}$' is shown for the univariate coefficients

28% ('scm', n = 50, 0% cov-corr, $\theta_{cov_{true}}$ = 0.026) to 80% ($\theta_{cov_{true}}$ = 0.045) and from 64 to 96% for 'frem$_{posthoc}$'. Scenarios with n = 500 showed a power of > 91%, independent of covariate effect magnitude and were less influenced by covariate collinearity (Fig. 2 and Table 1).

Moreover, the frequency of a significant cov$_{II}$ effect in the final 'frem$_{posthoc}$' models was > 77% in presence of $\geq$ 80% cov-corr (n $\geq$ 100). In contrast to that, cov$_{II}$ was significantly included in < 16% of 'scm' runs.

In scenario 2, a '*head-to-head*' comparison with a statistically similar setting was performed (same setting for the 'frem$_{posthoc}$' as in scenario 1 and 'scm' with sole forward inclusion using an alpha value of 0.1): the less strict alpha value in combination with only forward inclusion led to an increase of power for the 'scm', resulting in above 53% and with that being superior to 'frem$_{posthoc}$' (Fig. 3). More details are described in Supplement 3.

No comparison of power is possible for scenario 3 due to the missing selection step in the 'frem'.

Conditional accuracy and precision of $\theta_{cov_{true}}$ estimates

In scenario 1, an overestimation in small n datasets was more pronounced for 'scm' than for 'frem$_{posthoc}$' (Fig. 2). Thus, 'frem$_{posthoc}$' covariate coefficients were more accurate and precise. (Fig. 2, Supplement 3, Figure S3-2). We observed for both methods a power-dependent increase in conditional accuracy up to unbiased estimates, see Table 1 and Fig. 2. For example, the rbias of 'scm' coefficients was reduced from 50% ($\theta_{cov_{true}}$ = 0.026) to 8% ($\theta_{cov_{true}}$ = 0.045) in small datasets (n = 50) in presence of 90% cov-corr.

The conditional precision of the estimated coefficients in scenario 1 showed the same trend: Imprecision steeply decreased with increasing power (Table 1). With both methods, we obtained imprecise estimates in small n datasets (n = 50, $\theta_{cov_{true}}$ = 0.032, 'frem$_{posthoc}$': 35%, 'scm' 42%), independent of correlation.

In scenario 1, CL and V$_c$ were accurately (rrmse < 10%) and precisely (rbias < 3%) estimated in the final 'scm' as well as the 'frem$_{posthoc}$' model. The proportional error model estimate trended to underestimation (rbias > − 11%) and was less precise with rrmse < 27%.

Table 1 Simulation and estimation results of 'scm' and 'frem$_{posthoc}$' in scenario 1

N	Covariate correlation (%)	Method	$\theta_{COV} = 0.026$			$\theta_{COV} = 0.032$			$\theta_{COV} = 0.045$		
			power (%)	rbias (%)	rrmse (%)	power (%)	rbias (%)	rrmse (%)	power (%)	rbias (%)	rrmse (%)
20	0	frem	36.5	68.3	87.0	47.2	8.1	67.6	70.1	17.2	40.2
		scm	10.4	118	128	18.1	84.8	95.3	35.2	36.4	47.3
	50	frem	33.5	68.5	87.8	46.6	47.8	68.5	63.0	18.6	40.9
		scm	9.60	118	127	16.2	83.6	97.0	33.2	36.4	47.4
	90	frem	25.0	69.2	89.0	36.8	47.1	68.7	49.3	17.9	42.3
		scm	8.20	120	129	13.2	85.0	99.1	27.6	36.8	47.7
50	0	frem	64.2	23.8	40.5	81.5	12.5	33.9	96.0	2.50	25.3
		scm	28.4	47.3	54.9	50.1	28.3	39.0	80.0	7.60	24.2
	50	frem	60.4	23.7	40.6	78.0	12.8	34.4	92.6	3.00	25.2
		scm	27.5	47.2	54.8	48.4	28.8	39.6	78.0	8.00	24.2
	90	frem	46.5	23.4	41.8	58.8	13.2	34.9	71.8	2.70	25.8
		scm	22.1	49.5	57.1	38.0	31.6	42.2	67.2	8.30	24.2
100	0	frem	89.2	4.40	28.3	97.0	1.20	25.3	99.9	0.20	19.2
		scm	62.7	16.1	27.1	85.1	5.70	22.8	99.2	− 0.70	19.5
	50	frem	83.8	5.70	28.7	94.5	1.50	25.8	99.3	0.30	18.8
		scm	60.8	16.5	27.5	84.1	6.30	22.9	98.3	− 0.6	19.4
	90	frem	69.1	3.80	27.7	76.6	1.50	25.0	83.0	0.70	19.2
		scm	51.8	16.9	27.6	70.6	6.30	23.0	87.4	0.10	19.4
500	0	frem	99.2	− 2.2	15.4	99.9	− 0.2	12.4	100	− 0.50	8.80
		scm	100	− 2.1	14.6	100	− 1.0	11.9	100	− 1.2	8.60
	50	frem	99.2	− 2.3	15.3	100	− 0.2	12.4	100	− 1.0	8.70
		scm	100	− 2.0	14.6	100	− 1.0	11.9	100	− 1.1	8.60
	90	frem	91.96	− 1.8	15.1	95.8	− 0.7	12.1	98.1	− 1.0	9.10
		scm	93.5	− 1.7	14.6	96.7	− 0.8	11.9	99.6	− 1.1	8.60

The simulated relative covariate effect sizes were − 18 to + 22% ($\theta_{COV} = 0.026$), − 22 to + 27% ($\theta_{COV} = 0.032$) and − 29 to + 41% ($\theta_{COV} = 0.045$) on clearance at the 5th to 95th perc percentile of covariate values. Conditional accuracy and precision were expressed as rbias (%) and rrmse (%)

In scenario 2, the higher alpha value of 0.1 in scenario 1 for 'scm' forward selection strongly reduced overestimation of coefficients to a rbias below 48%. As a result, conditional accuracy was higher compared to 'frem$_{posthoc}$', whereas conditional precision of 'scm' coefficients was similar to 'frem' coefficients throughout the scenarios (Fig. 3, Supplement 3 Table S3-1). Additional details are described in Supplement 3.

Furthermore, scenario 3 compared all 'frem' cov$_{true}$ estimates without a selection step to those of the final 'scm' models obtained after backward elimination. This analysis quantitatively shows the effect of selection bias if compared to scenario 1 results. In sum all 'frem' coefficients were unbiased. Moreover we observed still a high imprecision of 'frem' coefficients in small n datasets (n < 100) which was independent of the selection step, but 'frem' showed a superior precision compared to 'scm' especially in small n datasets, (Fig. 4). Further details are described in Supplement 3.

The simulation study using a true categorical covariate showed the same trend of power, conditional rbias and rrmse for scenario 1 and scenario 2, whereas the differences of our evaluation criteria were smaller between 'scm' and 'frem$_{posthoc}$', if compared to the simulation study using a true continuous covariate. Supplement 2 provides a detailed description of all obtained results.

Predictive performance of 'scm' and 'frem$_{posthoc}$' models

Scenario 1 evaluated the estimated covariate coefficients of the final 'scm' and 'frem$_{posthoc}$' models for their predictivity, i.e., were termed predictive when estimated between zero and two times the true value. The results are shown in
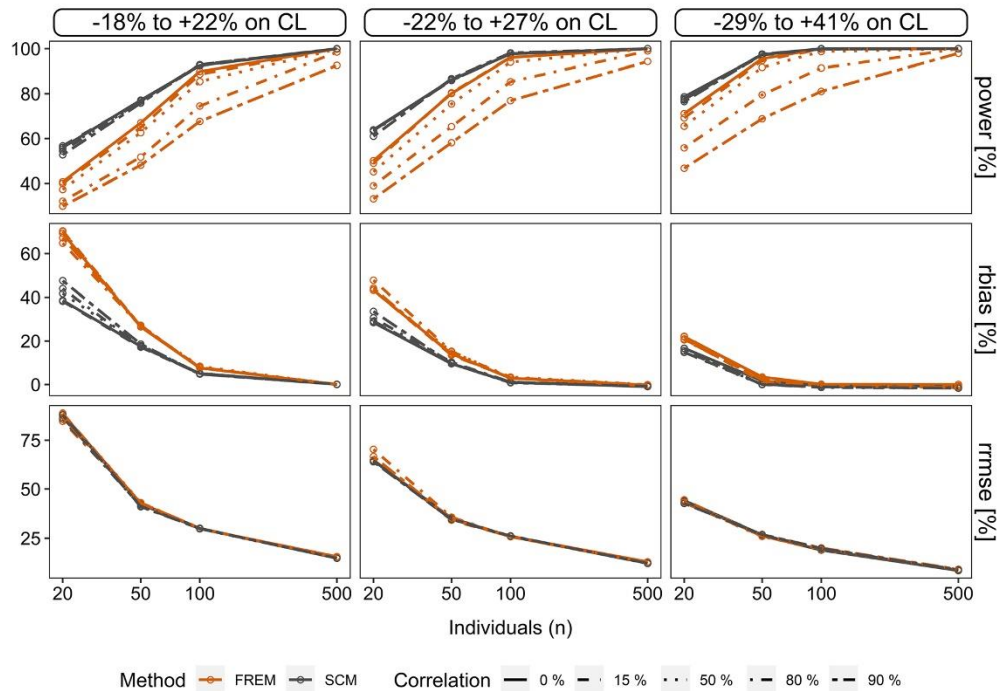
Fig. 3 'Scm' vs. 'frem$_{\text{posthoc}}$' in the scenario 2. Illustration of power (%), conditional relative bias (%) (*rbias*) and relative root mean squared error (%) (*rrmse*) of cov_{true} estimates in sparse datasets.

Conditional accuracy and precision for the 'frem$_{\text{posthoc}}$' is shown for the univariate coefficients

Fig. 5. The predictive performance of the cov_{true} estimates was a function of power for the 'scm', but also for 'frem$_{\text{posthoc}}$'. The 'frem$_{\text{posthoc}}$' showed a higher power in small n datasets, thus the fraction of predictive models was more than twice as high compared to 'scm'. On the other hand, the fraction of predictive 'scm' models increased more steeply with increasing power. At a power value of $> 28\%$ more than 90% of the final models were likely to improve the predictivity ('frem$_{\text{posthoc}}$' $> 47\%$ power).

As power is a composite of dataset size, covariate effect size and correlation, we analysed the individual components on their relation to influence the fraction of predictive models (Supplement 3 Figure S3-3). We observed that dataset size, covariate effect size, rbias and rrmse most influenced the fraction of predictive models and that predictive performance was less impacted by covariate correlation.

The fraction of predictive 'scm' and 'frem$_{\text{posthoc}}$' models in scenario 2 were similar (scm: 97.0% 'frem$_{\text{posthoc}}$': 97.5%, n = 50, cov-corr = 80%, $\theta_{cov_{true}} = 0.026$) and reached both 100% in the scenario with the highest simulated covariate effect magnitude, $\theta_{cov_{true}} = 0.045$, n > 50), see Supplement 3 Figure S3–4.

Overall, final 'frem' models (scenario 3) were providing highly predictive covariate coefficient estimates, which were mainly driven by covariate effect magnitude and independent of the dataset size (Supplement 3 Figure S3-6).

Type 1 error

For scenario 1, the true alpha values are displayed in Fig. 6. Overall, 'frem$_{\text{posthoc}}$' indicated a false significant covariate effect of the dummy covariate cov$_{\text{III}}$ in more cases, than the given 10% confidence intervals of the covariate effects would imply, i.e., an inflated type 1 error rate was observed. The 'scm' also displayed inflated type 1 error rates for small datasets. For n $\geq$ 100 both methods approached the set alpha value of 10% ('frem$_{\text{posthoc}}$') or 5% ('scm').

In scenario 2, the true 'scm' alpha values were between 6 and 11% and with that close to the expected 10% value.
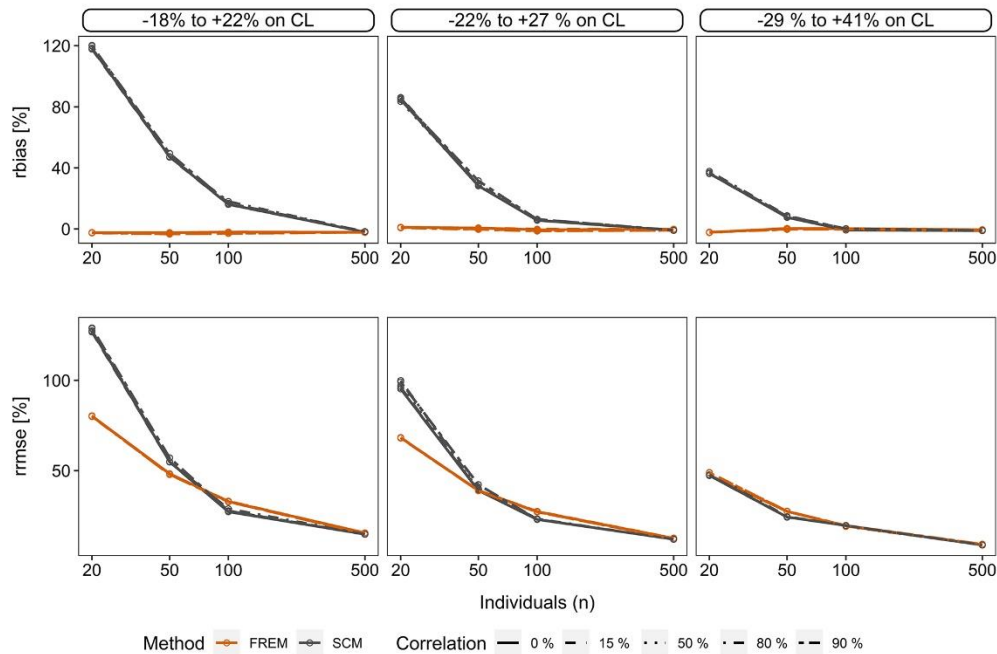
Fig. 4 'Scm' vs. 'frem' for scenario 3. Illustration of relative bias (%) (*rbias*) and relative root mean squared error (%) (*rrmse*) of cov_{true} estimates in sparse datasets. Accuracy and precision for the 'frem' is shown for the univariate coefficients

Discussion

In the present study, we compared operational characteristics of the novel 'frem' technique to 'scm' as automated covariate analysis methods. As the 'frem' method is a full model approach and does not originally comprise a selection step, we introduced the 'frem$_{posthoc}$' step to account for a covariate backward elimination based on significant covariate effect sizes. This reflects an additional application of a 'frem' model in an exploratory analysis. Overall, this study gave insights in operational characteristics of the 'frem' method, but also showed the ability of 'frem$_{posthoc}$' to guide covariate selection. Yet, for 'frem$_{posthoc}$' the same caution as for the 'scm' should be applied since this posthoc step also can introduce selection bias in scenarios with low power (i.e. small covariate effect size, small sample size). Of note, an evaluation of precision and accuracy of all cov$_{true}$ 'frem' estimates without a selection step showed that the covariate effect estimates were unbiased and showed lower imprecision as those determined using the 'scm', which were biased due to the selection step, in particular in scenarios with low power. This underlines the value of the 'frem' method. It has the additional advantage of interpreting the covariate effect simultaneously to statistical significance without the need for further evaluate the parameter uncertainty, which is

needed for 'scm' to evaluate clinical relevance (e.g. bootstrap, llp-sir [17]). In large datasets, both methods provided precise and accurate inference on covariate effects in our simulation study. Moreover, Yngman et al. described an advantage of 'frem' model, that it can provide covariate coefficients for any subset of the examined covariates and thus be applied to different covariate datasets [7]. In addition, a model reduction of the full model could be done in a stepwise manner, if a more parsimonious model is desired [2, 7]. This simulation study comprised an investigation of final 'frem' model subsets for the purpose of covariate backward elimination, presented in scenarios 1–2.

The statistical power to detect true covariate effects is important to guide clinical study design. Ribbing et al. described that dataset size, magnitude of collinearity, and covariate effect size influence the power of the 'scm' method [16]. Ahamadi et al. investigated the operating characteristics of 'scm' using different complexities of true models (i.e. 1–4 true covariates). Those scenarios with one true covariate (n = 300, cov-corr 32% or 89%, 250 simulations) reached a high power [18]. This is in line with our results in datasets n ≥ 100. Beyond that, our observed power increase, as a result of increased dataset- and covariate effect size, as well as a reduction of power caused by collinearity of covariates are in line with Ribbing et al.

Fig. 5 Fraction of models with high predictive performance for 'scm' and final 'frem$_{posthoc}$' models with significant true covariate relationships in scenario 1. Estimated coefficients between zero to two times the true value were assumed to improve the predictive performance
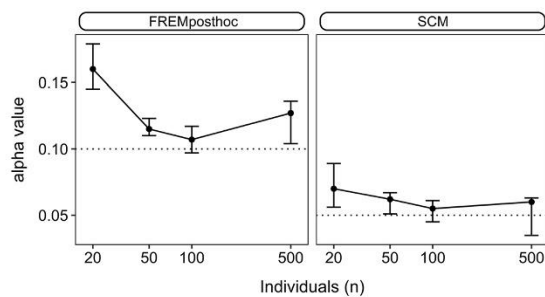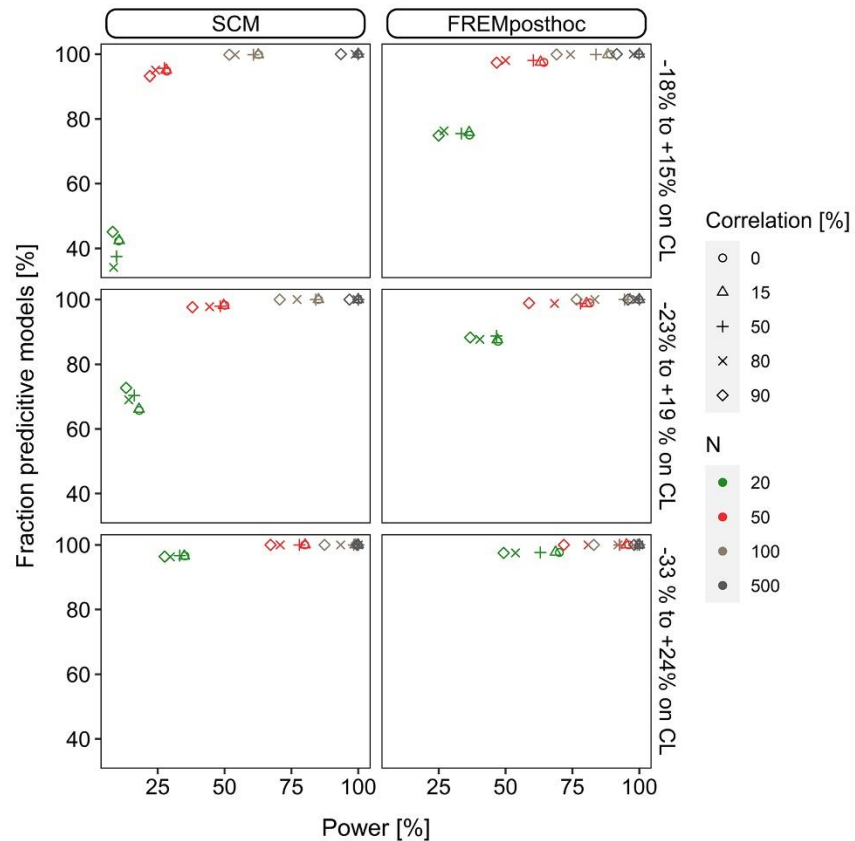
Fig. 6 True alpha-values for 'frem$_{posthoc}$' and 'scm' for scenario 1. Error bars shows min and maximum values, and points display median values

[19]. In comparison to that, the 'frem$_{posthoc}$' showed an up to three-fold higher power in the worst-case scenario with high correlation in small cohort studies (scenario 1, $\theta_{cov_{true}} = 0.026$), likely as a result of the different alpha values in the selection step. In scenario 2, power differences of the two methods were smaller, rather favouring 'scm'. We however think that 'scm' with only forward inclusion and an alpha value of 0.1 does not represent

common practice. Moreover, it is known that 'scm' suffers from multiple testing which is not the case of the 'frem$_{posthoc}$' method, which makes this an interesting comparison.

In this study cov$_{\Pi}$ carries up to 90% of the information of cov$_{true}$. 'Frem$_{posthoc}$' accounts for correlation and the high frequency significant cov$_{\Pi}$ inclusions in high correlation scenarios represents its ability to account for correlation. In contrast to that, 'scm' with forward selection (p value < 0.05) and backward elimination (p value < 0.01), but also with applying only forward inclusion (p-value < 0.1) is intrinsically not able to capture the true present correlation. However, the model prediction using a wrong, but highly correlated covariate, that carries information of the true covariate could be comparable to including the true covariate. One the one hand, the inclusion would lead to interpretation difficulties, on the other hand, an exclusion of correlated covariates could also cause confounded interpretation of covariate effect estimates, as the correlated covariate carries parts of the true covariate information. Thereby pharmacological understanding is key for decision making.

We also investigated a scenario with a true categorical covariate with and without an additional level of variability, the $IIVV_c$. The results showed a similar behaviour as observed for continuous covariates. Scenarios 1 and 2 showed only minor differences in power for 'scm' and 'frem$_{posthoc}$' in cases when the covariate has a strong effect size. The additional level of variability decreased power by up to ca. -5%. The simulation study using a true continuous covariate did not include $IIVV_c$, so we assume an overall worsening effect of the presented continuous covariate study results in presence of $IIVV_c$ here.

Moreover, conditional accuracy and precision of the covariate coefficients were investigated in case cov$_{true}$ was selected in the final models. In scenario 1 bias was present in both methods, however slightly lower when using the 'frem$_{posthoc}$' (especially in low power scenarios). In scenario 2 the findings were vice versa, so that overestimation was less pronounced for 'scm', resulting from a less strict alpha value in the selection step. According to Wahlby et al. selection bias is only moderate in typical PK modelling dataset [5], but this was only confirmed for covariates with high effect sizes [16]. In scenario 3 unbiased 'frem' estimates were obtained, as no covariates were selected, and all estimated coefficients were considered for the evaluation.

Conditional precision was more precise for 'frem$_{posthoc}$' compared to 'scm' in scenario 1 and equally high in scenario 2. Precision was improved by a less strict alpha value ('scm' in scenario 1 vs. scenario 2). As precision is a function of power, we assume that the increased precision is caused by increased 'scm' power.

Beyond that, in scenario 1 we evaluated the predictive performance of the final models and used the range of zero to two times the true coefficient value as a predictor for improvement of the model fit, according to Ribbing et al. [16]. The present study confirmed the predictive performance of 'scm' models being a function of power and we confirmed this for 'frem$_{posthoc}$' estimates. Compared to 'scm' models, the fraction of predictive 'frem$_{posthoc}$' models was higher, especially in scenarios which achieved power $< 50\%$. The predictive performance was positively correlated with rbias, rrmse and number of study individuals. Interestingly, covariate collinearity did not impact the predictive performance (Supplement 3 Figure S3-3).

The type 1 error rate was evaluated with cov$_{III}$ being independent from the other two available covariates. The previously described inflated type 1 error rate in the 'scm' approach [5] was confirmed in this study but was also observed for the 'frem$_{posthoc}$'. The 'frem$_{posthoc}$' alpha values were decreasing with increasing study size but were still slightly inflated. The confidence interval of the covariate effect is calculated by SIR in the PsN implementation of 'frem' [15]. The confidence interval served

for the calculation of the frequency in how many of the performed runs the cov$_{III}$ effect size was estimated to be significantly different from zero. Broeker et al. found, that especially in small n datasets the SIR-derived confidence interval tends to be underestimated, in particular for the omega values [17]. This underestimation might explain the inflated alpha values, as zero is less often included in the SIR-based confidence intervals if they are too narrow.

'Frem' is mathematically equivalent to FFEM, which has been suggested as an alternative to stepwise procedures [2]. Although a backward elimination is not originally intended by the full model approach, as this may curtail its benefits, a guidance for this backward elimination step has been proposed by Gastonguay et al. [2]. A model reduction based on covariate effect size, has also been applied to clinical data [20]. A reduction of a full model for predictive purposes can be done via exclusion of non-statistically significant (CI includes null value) and non-clinically important (entire CI contained within no effect range) covariate effects. Covariates which are clinically important and statistically significant, or are not statistically significant but may be clinically important should be retained in the model [2]. The clinical relevance criteria was not considered in our study evaluation, as this additional filter is subjective in a simulation study and driven by the pharmacological considerations. Furthermore, statistically significant effects are clearly defined, whereas the often used clinical relevance threshold of 20% is not. This threshold may apply for clearance; however, it can be different for other PK parameters related to a covariate effect. Moreover, this threshold can be dependent on the indication, pharmacometric question to be answered or substance itself, e.g. a narrow therapeutic window could reduce the threshold. These factors cannot be fully reflected in a simulation study.

A few more limitations shall be mentioned: the here evaluated scenarios only display a portion of the complexity of covariate analysis in real clinical datasets. The here simulated cov$_{true}$ effect magnitudes were chosen around the often-used clinical significance threshold of 20% on clearance [12] displaying a weak, moderate, and strong effect as it could be expected in a real clinical dataset. However, neither collinearity between more than one covariate, nor the presence of more than one true covariate carrying information was investigated.

To calculate the fraction of predictive models amongst the evaluated runs in each scenario, we assumed an estimated covariate coefficient between zero and two times cov$_{true}$ to be likely to improve the predictive performance of a model [16]. This in other words accounts for up to 100% overestimation, so that even in presence of a strong selection bias, coefficients were rated as predictive. Highly biased covariate coefficients make the model less adequate

for predictive purposes and could ultimately cause misleading clinical interpretation on e.g., clearance if the covariate coefficient originates from small n datasets ($< n = 100$). However, as 'frem$_{posthoc}$' has not been applied to clinical data yet, this needs to be further evaluated.

Besides that, this simulation study investigated only covariates on clearance, but usually clinical covariates are also found on other model parameters. Moreover, interindividual variability on central volume of distribution is very common in clinical datasets but was not included in the analysis using a true continuous covariate. Based on prior knowledge and confirmatory results obtained in the simulation study with categorical data, we assume a reduction of power in presence of more levels of variability. Moreover, the covariate coefficients directly obtained via the PsN 'frem' routine, represent exponential covariate parameterization in fixed effects models [8]. Other implementations might be of interest, too, and could be explored in subsequent studies.

Conclusion

Overall, this study contributed to the understanding of the 'frem' and showed properties and characteristics of the methods for continuous but also categorical covariates. We introduced with 'frem$_{posthoc}$' a possibility to guide covariate selection, mimicking how 'frem' could be additionally used in practise. With that, covariate effect size interpretation and selection can be done simultaneously and a predictive model with capturing correlation in the datasets can be obtained. Using the commonly applied settings of 'scm' and 'frem', in small n datasets the power of 'frem$_{posthoc}$' was substantially higher, leading to a lower bias, compared to 'scm' in scenario 1. In datasets with $n > 100$ power, precision, and accuracy of 'frem$_{posthoc}$' were comparable to 'scm'. However, the simulated scenarios still highlight the need for thoughtful choice of the method to answer the underlying pharmacometric question in small datasets.

Declarations

References

1. U.S. Food and Drug Administration. Guidance for industry: Pharmacokinetics in patients with impaired hepatic function: Study design, data analysis, and impact on dosing and labeling, U.S.Department of Health and Human Services Food and Drug Administration Center for Drug Evaluation and Research (CDER),Center for Biologics Evaluation and Research (CBER), May 2003.Clinical Pharmacology. Available from http://www.fda.gov/downloads/Drugs/GuidanceComplianceRegulatoryInformation/Guidances/ucm072123.pdf. Accessed 23 Jun 2022
2. Gastonguay MR. Full covariate models as an alternative tomethods relying on statistical significance for inferences aboutcovariate effects: a review of methodology and 42 case studies. Twentieth Meeting, Population Approach Group in Europe; 2011 Jun 7–10; Athens. Available at https://www.page-meeting.org/pdf_assets/1694-GastonguayPAGE2011.pdf. Accessed 06 Jan 2023
3. Jonsson EN, Karlsson MO (1998) Automated covariate model building within NONMEM. Pharm Res 15:1463–1468. https://doi.org/10.1023/a:1011970125687
4. Ribbing J, Nyberg J, Caster O, Jonsson EN (2007) The lasso—a novel method for predictive covariate model building in nonlinear mixed effects models. J Pharmacokinet Pharmacodyn 34:485–517. https://doi.org/10.1007/s10928-007-9057-1
5. Wahlby U, Jonsson EN, Karlsson MO (2002) Comparison of stepwise covariate model building strategies in population pharmacokinetic-pharmacodynamic analysis. AAPS PharmSci 4:1–12. https://doi.org/10.1208/ps040427
6. Hutmacher MM, Kowalski KG (2015) Covariate selection in pharmacometric analyses: a review of methods. Br J Clin Pharmacol 79:132–147. https://doi.org/10.1111/bcp.12451
7. Yngman G, Bjugård Nyberg H, Nyberg J et al (2022) An introduction to the full random effects model. CPT Pharmacomet Syst Pharmacol 11:149–160. https://doi.org/10.1002/psp4.12741
8. Karlsson MO (2004) A full model approach based on the covariance matrix of parameters and covariates. Aaps 20:207–253

9. Bruno R, Vivier N, Vergniol JC et al (1996) A population pharmacokinetic model for docetaxel (Taxotere®): model building and validation. J Pharmacokinet Biopharm 24:153–172. https://doi.org/10.1007/BF02353487

10. Brekkan A, Lopez-Lazaro L, Yngman G et al (2018) A population pharmacokinetic-pharmacodynamic model of pegfilgrastim. AAPS J 20:1–14. https://doi.org/10.1208/s12248-018-0249-y

11. Novakovic AM, Krekels EHJ, Munafo A et al (2017) Application of item response theory to modeling of expanded disability status scale in multiple sclerosis. AAPS J 19:172–179. https://doi.org/10.1208/s12248-016-9977-z

12. Boeckmann AJ, Sheiner LB, Beal SL, Bauer RJ (2011) NONMEM Users Guide. NONMEM Project Group, University of California at San Francisco, Ellicott City

13. Lindbom L, Pihlgren P, Jonsson N (2005) PsN-Toolkit—a collection of computer intensive statistical methods for non-linear mixed effect modeling using NONMEM. Comput Methods Programs Biomed 79:241–257. https://doi.org/10.1016/j.cmpb.2005.04.005

14. R Core Team (2019) R: A language and environment for statistical computing. R Foundation for Statistical Computing, Vienna

15. Dosne A-G, Bergstrand M, Harling K, Karlsson MO (2016) Improving the estimation of parameter uncertainty distributions in nonlinear mixed effects models using sampling importance resampling. J Pharmacokinet Pharmacodyn 43:583–596. https://doi.org/10.1007/s10928-016-9487-8

16. Ribbing J, Niclas Jonsson E (2004) Power, selection bias and predictive performance of the population pharmacokinetic covariate model. J Pharmacokinet Pharmacodyn 31:109–134. https://doi.org/10.1023/B:JOPA.0000034404.86036.72

17. Broeker A, Wicha SG (2020) Assessing parameter uncertainty in small-n pharmacometric analyses: value of the log-likelihood profiling-based sampling importance resampling (LLP-SIR) technique. J Pharmacokinet Pharmacodyn 47:219–228. https://doi.org/10.1007/s10928-020-09682-4

18. Ahamadi M, Largajolli A, Diderichsen PM et al (2019) Operating characteristics of stepwise covariate selection in pharmacometric modeling. J Pharmacokinet Pharmacodyn 46:273–285. https://doi.org/10.1007/s10928-019-09635-6

19. Bonate PL (1999) The effect of collinearity on parameter estimates in nonlinear mixed effect models. Pharm Res 16:709–717

20. Hu C, Adedokun O, Ito K et al (2015) Confirmatory population pharmacokinetic analysis for bapineuzumab phase 3 studies in patients with mild to moderate Alzheimer's disease. J Clin Pharmacol 55:221–229. https://doi.org/10.1002/jcph.393

Publisher's Note Springer Nature remains neutral with regard to jurisdictional claims in published maps and institutional affiliations.

4   Discussion

The presented publications I-IV cover various facets of the *in vitro* and clinical use of tigecycline, as well as the application of pharmacometric modelling techniques with the focus on tigecycline dose optimisation. Tigecycline remains a last resort antibiotic and its approved standard dose of 100 mg LD, followed by 50 mg q12h MD showed suboptimal microbial eradication and clinical cure over the past years[28]. Combined with increasing amount of (multi-) resistant bacteria causes difficulties to treat patients successfully. New treatment options are rare, so that finding new opportunities to optimise currently approved drugs is one strategy to tackle the current situation. Approved drugs can be optimized via e.g., escalated doses, new regimens or via patient individual covariate-based dose adjustment guided by pharmacometric approaches[67]. This work reflects the investigation of such an approach for the use of tigecycline. The following part provides an overarching discussion of the four articles in this work.

4.1   Tigecycline in *in vitro* experiments and clinical considerations

Tigecycline is an instable drug, particularly susceptible to dissolved oxygen in bacterial growth media. Thus, its handling *in vitro* is challenging. Previous studies observed a formation of an oxidative by-product, which increased from 3.5 % to 25 % in fresh vs. aged bacterial growth medium (containing dissolved oxygen), causing a strongly diminished antibacterial activity within 24 h[58]. This is of high relevance if the experiment duration lasts longer than the typical 24 h.

In **Publication I** it was hypothesized, that adding antioxidative agents (pyruvate, ascorbic acid) prevent tigecycline from *in vitro* degradation in the bacterial growth medium ca-MHB. Until now solely Oxyrase®, a costly supplement, or the use of freshly prepared broth enabled the use of stable tigecycline at bench side[58]. This, however, involved costly supplementation or increased daily working hours if the broth needs to be autoclaved on the same day as starting the *in vitro* experiment. Furthermore, the maximal duration of an experiment is limited. To tackle this, **Publication I** provided a cost and time saving alternative: The key outcome of **Publication I** was that ca-MHB supplemented with 2 % pyruvate prevented tigecycline from degradation while keeping its *in vitro* antibiotic activity.

By utilizing the results of **Publication I**, the execution of HFIM, as reported in **Publication II**, was feasible. This publication investigated tigecycline's *in vitro* dose optimization potential with variations of the daily dose and regimen up to continuous infusion. Alterations to continuous or prolonged infusions have shown benefits for drugs of the beta lactam family, as they have a time dependent antibiotic effect[90,91]. Benefits for tigecycline therapy by changing the regimen have been hypothesized but have not been tested *in vitro* yet[92]. **Publication II** is the first *in vitro* study that introduced new tigecycline regimens assessed in a dynamic HFIM. The experiments addressed the hypothesis that a change of the regimen or an increased dose could improve tigecycline's antibiotic activity *in vitro*. As shown in **Publication I** by the magnitude of tigecycline degradation over time an antioxidative supplementation would be necessary to enable continuous tigecycline infusions to humans. Therefore, safety aspects of the chemical agents need to be questioned. Pyruvate is a metabolic intermediate that engages in the production of energy in cells, such as glycolysis or gluconeogenesis. Jitkova et al have shown a high tolerability of 6 % pyruvate in mouse[93]. Thus, adding up to 2 % of this endogenous molecule to infusions applied to humans might be of low risk.

A key result of **Publication II** was that the clinically recommended and escalated doses were found ineffective against the investigated strains. This led to the conclusion that the optimization potential of tigecycline against the studied clinical *Klebsiella pneumoniae* isolates was limited. Neither intensified dosing, higher front loading, nor continuous infusion were able to suppress the regrowth and resistance development *in vitro* for strains > 0.125 mg/L. At clinically used doses, **Publication II** revealed a strong MIC increase of the regrowing resistant subpopulation. Additionally, the detected mutations were matching those previously described in patients undergoing tigecycline therapy[94].

According to literature doses of up to 200-400 mg loading dose, 100-200 mg q12h were well tolerated in humans. The most common side effects of tigecycline (nausea and vomiting) can be mitigated via comedication[95,92]. Thereby, it can be assumed that the investigated doses are in a tolerable range and practicable. However, case reports with severe liver associated side effects with an unidentifiable frequency were published and partly added to the prescribing information[96,97]. This might limit future dose increasements in patients, especially in patients with liver diseases.

Besides tolerability, the effectiveness of an antibiotic is the driver for a clinical cure and microbial eradication. In **Publication III**, no correlation between tigecycline drug exposure and survival was observed. The clinical failure rate was highest in patients with infections caused by gram negatives, which all had an MIC of 0.5 mg/L. This is consistent with the *in vitro* results of **Publication II** where tigecycline had no sustained antibiotic effect against the *Klebsiella pneumoniae* isolates with a MIC of 0.25 mg/L or 0.5 mg/L. Tigecycline's *in vitro* effectiveness was confined to an MIC of 0.125 mg/L, at which point the drug successfully kept the CFU/mL below the inoculum and prevented a re-growth of resistant subpopulations. Nevertheless, the MIC values of 0.125 mg/L is at the lower end of the ECOFF distribution of *Klebsiella pneumoniae*, therefore this MIC is less likely to be recommended for a clinical breakpoint. Beyond the limited *in vitro* efficacy **Publication II** has shown a tigecycline-induced resistance development. According to the FDA black box warning it is hypothesized that a progression of infection might explain clinical failure. This is in line with the strongly occurring regrowth of resistant subpopulation *in vitro* (determined via MIC increase) and might support this hypothesis and high failure rate observed in **Publication III**. Both, the high mortality of patients in **Publication III** but also the confirmatory *in vitro* results (e.g. limited antibiotic activity for *Klebsiella pneumoniae* with an MIC > 0.125 mg/L and drug-induced MIC increase) are in line with the current recommendations of the latest ESCMID Guideline (2022) for the treatment of infections caused by multidrug-resistant gram-negative bacilli[13]. In this guideline tigecycline is seldomly recommended given its lack of evidence to treat those infections.

For tigecycline a time but also an exposure dependent *in vitro, in vivo* and clinical effect has been previously discussed, whereas the AUC/MIC ratio is most commonly used as a PK/PD target [69,98,99,100,101,102]. **Publication II** showed that the continuous infusion of tigecycline did not improve its antibiotic activity, so we assumed that the time above the MIC is not a driver for tigecyclines effectiveness.

In the recruited study population of **Publication III** eight patients were infected with gram-negative bacteria (*E. coli*, *K. pneumoniae*, MIC 0.5 mg/L) of which only one showed clinical cure. This patient had an $f\text{AUC}_{0-24}/\text{MIC}$ of 11.3 while the observed mean $f\text{AUC}_{0-24}/\text{MIC}$ of these eight patients was 13.9. The HFIM experiments in **Publication II** revealed a $f\text{AUC}_{0-24}/\text{MIC}$ ratio of 38.5 to achieve stasis against *Klebsiella pneumoniae*, which is a multiple of the observed exposure in the investigated

patient population. Such an increase to a multiple of exposure however could increase the risk of side effects, e.g. coagulopathy[96,97,103]. The highest exposures were observed in the patients with Child Pugh C (n = 3, average fAUC$_{0-24}$/MIC = 17), whereas their exposure was still below half of the stasis target (fAUC$_{0-24}$/MIC of 38.5) obtained from **Publication II**. Of note, these patients had infections with gram-positive bacilli, thus a comparison to the HFIM results (all conducted using gram-negative bacteria) is limited. It needs to be considered that the PK/PD target for tigecycline varies across underlying type of bacteria that cause the infection, but also across indications, or site of infections[69,102,101]. Published clinical studies usually evaluate clinical cure or microbial eradication among types of infection, while a distinct evaluation of the outcome between infections caused by gram-positive and gram-negative is rare. Sevillano et al. observed that higher AUC/MIC values were needed for *Escherichia coli* (gram-negative), compared to *Staphylococcus aureus* or *Enterococcus faecium* (gram-positive) to achieve the same *in vitro* antibiotic effect[104]. In a clinical setting, Meagher et al. performed an exposure-response analysis of tigecycline in the treatment of cSSI infections, where *Staphylococcus aureus* and *streptococci* (both gram-positive bacteria) were the predominant pathogens[102]. Their analysis of microbiological response and clinical cure vs. AUC/MIC revealed a breakpoint of 17.9 for cSSI[102]. By applying the same factor for protein binding, as used in **Publication II**, this would correspond to an fAUC/MIC value of 11.3, being lower than the exposure which was seen in Child Pugh C patients in **Publication III**. Withal, the clinical outcome was inconclusive in these three patients (cure, intermediate, failure). Beyond that no correlation with tigecycline exposure and survival, but also no correlation between gram-type or pathogen causing the infections and survival was observed in **Publication III**: Overall, patients who died had an average fAUC$_{0-24}$/MIC of 13.3 and patients with clinical cure had an average fAUC$_{0-24}$/MIC of 13.4. Of note, these findings were based on a low patient count and must be taken with caution.

Tigecycline's effectiveness was shown to be influenced by the presence of an intact immune system, as demonstrated by Crandon et al[101]. This may also help to explain the absence of a correlation between drug exposure and survival in **Publication III**. In a murine thigh model, it was observed that the required drug exposure to achieve a maximal reduction of CFU/mL (decrease of approx. -1.7 log$_{10}$CFU/mL) was significantly reduced by a factor of 7, when comparing neutropenic mice (fAUC/MIC of 1.8) to immunocompetent mice (fAUC/MIC = 13)[101]. Thus, this might explain why clinically derived PK/PD targets are lower compared to targets derived from *in vitro* experiments. In

Publication III we saw a negative and significant correlation between survival and chronic liver disease, meaning that with the severeness of the underlying disease the survival probability was reduced. Critical health status, often associated with a lower activity of the immune system might explain the clinical failure of patients in **Publication III**. With this in conjunction to the strong occurring *in vitro* regrowth seen in **Publication II**, it was assumed that the presence of an intact immune system is a key factor for clinical cure undergoing tigecycline therapy. Consequently, an indication of tigecycline in immunocompromised patients is an alarming signal and must be carefully evaluated.

In **Publication II** no immune cells were included, so that these HFIM experiments represent rather worst-case scenarios. Despite the impact of the immune system, **Publication II** and **III** were probably different in their bacterial burden. Depending on the site and severeness of infections the bacterial burden at start of treatment could be lower than tested in the *in vitro* experiments of **Publication II**. Tsala et al. observed, that the required $f\text{AUC}_{0-24}$/MIC exposure were influenced by the size of inoculum (e.g. $f\text{AUC}_{0-24}$/MIC to achieve half maximal activity was 16 with 10^3 CFU/L and 28 with 10^5 CFU/mL)[105]. This shows that an antibiotic therapy with tigecycline could be optimised if the bacterial burden is known. However, a clinical determination of CFU at the site of infections is not practical as this would need a painful biopsy. Moreover, published information about bacterial burden at the site of infection are rather base on post-mortem studies[106].

By the nature of the HFIM model unbound concentrations are investigated, while the calculated AUC in **Publication III** referred to total concentrations. Overall, it can be assumed that only unbound concentrations can have a pharmacodynamic effect in the tissue. The conversion with a static factor for fraction unbound simplifies the complex protein binding behavior of tigecycline known to be nonlinear. Tigecycline has a high volume of distribution, showing a large apparent distribution into tissues. Nevertheless, the available information about unbound (i.e., active) concentrations at target sites is rare. Stein et al. observed a serum:soft tissue ratio of > 2.8, however being imprecise with a wide range from $0.7 - 5.5$[107]. Moreover, this ratio was derived from tissue biopsies. Those biopsy samples are usually homogenized and thus they represent a mixture of both free and bound concentrations from different compartments (interstitial fluid, cells, capillaries). Therefore, this ratio needs to be interpreted with great caution. Instead of determining total tissue concentration,

the state-of-the-art technique to measure active unbound drug concentrations is the microdialysis technique. Bulik et al. applied this method in patients with chronic wounds[108]. Here, the penetration ratio of thigh and wound fAUC to fAUC in plasma was 1 and no significant difference between infected and uninfected tissue was observed[108]. Beyond that a more recent study by Dorn et al. investigated tigecycline's penetration into soft tissue in obese vs. non-obese surgical patients using the microdialysis technique[109]. They also confirmed, that the concentrations in interstitial fluid of subcutaneous tissue were not higher compared to the free plasma concentrations[109]. Thereby we conclude that the mimicked PK profiles in **Publication II** were appropriate concentrations to derive an *in vitro* PK/PD relationship.

4.2   Covariate analysis in small N studies

'Covariate-based dose adjustment' refers to the process of adjusting the dose of a medication based on individual intrinsic or extrinsic factors (e.g., age, weight, organ function parameters). The goal is to maintain the drug exposure in a therapeutic range by considering factors that affect the drug's pharmacokinetics and pharmacodynamics. **Publication III** gives insights into tigecycline exposure in liver impaired critically ill patients and provides an in-depth covariate analysis using various parameters of the liver panel, such as liver enzymes or composite scores. Considering that tigecycline is mainly eliminated through the liver, we investigated alternatives to the recommended static Child Pugh score to allow for a covariate-based dose adjustment of the antibiotic.

For this purpose, the stepwise covariate analysis method was applied. This method was extensively evaluated in **Publication IV.** In an academic framework, as well as in early-stage clinical trials, small N study data are ubiquitous. Nonetheless, small N studies can provide valuable information about patient populations that are insufficiently represented in larger studies, just as the clinical trial of **Publication III**. Although this study recruited only thirty-nine patients, it represented the largest trial in this special patient population of liver impaired, critically ill patients. In general, small N studies potentially suffer from various sources of bias, e.g., the sample size is not representative of the larger population. Methods like 'scm' are known to overestimate the covariate effect in these types of data, which may lead to incorrect assumptions. **Publication IV** demonstrated a noticeable selection bias when the simulated population was smaller than N=50. Nevertheless, even with a

limited number of participants, these studies provide valuable insights and contribute to advancing scientific knowledge. But their limitations must be considered, and their results must be interpreted carefully. Therefore, it is important to acknowledge that the results of **Publication III** should only be interpreted within the observed population. This study can serve as a foundation for larger, more comprehensive studies that aim to confirm their results and deepen our understanding of tigecycline in special patient populations.

The 'frem' technique has not been widely applied to clinical data yet, although the method was developed a decade ago. Therefore, **Publication IV** aimed to increase knowledge about a novel 'frem' covariate analysis approach, while evaluating its potential for covariate selection against the benchmark 'scm' technique. This step was introduced in **Publication IV** as 'frem$_{posthoc}$', distinguishing from the original 'frem' idea to serve for a full model approach. 'Frem$_{posthoc}$' showed promising operational characteristics in small N datasets, being superior to 'scm' applied with commonly used settings. However, in **Publication III** the 'scm' technique was chosen to develop the covariate model based on data from thirty-nine study participants. For the sake of comparability with already published data, we used the standard 'scm' method for the model development in **Publication III**. 'Frem$_{posthoc}$' is a new application of the 'frem' and thereby not yet clinically established to develop a covariate-based dose adjustment strategy but a future application to clinical data in comparison to established methods is of interest.

5   Perspectives

The aim of this work was to investigate the dose optimization potential of tigecycline therapy by evaluating *in vitro* and clinical data supported by pharmacometric modelling. The results clearly showed that the use of tigecycline in monotherapy should be questioned. Therefore, the following paragraph highlights future perspectives and limitations:

The family of gram-negative bacteria is broad, and *Klebsiella pneumoniae* is only one representative. As mutational frequency and resistance genes can change across bacteria, and clinical tigecycline efficacy varied across pathogens, the extension of HFIM to other bacteria would be needed to broaden the picture and foster the findings. The approved standard dose monotherapy has only limited applications, hence an effective combination partner is needed to preserve the drug. To address this, the optimized experimental rhombic checkerboard experiment can serve as an efficient interaction screening tool to plan future HFIM with tigecycline combinations[110].
Furthermore, this work discussed the importance of a functioning immune system while undergoing tigecycline therapy. Therefore, an extension of HFIM including immune cells could give an even more realistic experiment design.

Overall, pharmacometric modelling has increased the informative value of *in vitro*, *in vivo,* and clinical data[111]. However, models rely on the quality of data. In the past years only small n studies evaluated tigecycline's clinical safety and efficacy. Across study populations tigecycline has shown a broad range of PK variability but also with respect to effectiveness. As these studies are limited in their informative value, an integration of all available data using an approach such as a model based meta-analysis could elucidate the picture of the current clinical situation a quantitative summary, which is also in the spirit of future 'Model Informed Drug Discovery and Development'.
Right now, patients suffer from severe and complicated infections and decisions need to be made at bedside. To overcome challenges to treat multi-drug resistant bacteria, programs such as antibiotic stewardships need to be emphasized and expert groups must update guidelines considering the current situation while academic institutions further investigate dose optimization strategies for approved drugs. Herewith pharmacometrics helps to quantitatively describe

individuals within populations to infer about clinically important measures like: What is the therapeutic dose range? How effective is the drug against different bacteria and what is the target we need to achieve to balance efficacy and safety? But to do so, pharmacometricians should be aware of technical advancement and new methodologies to perform state of the art analyses that help to get most out of the available data to improve antibacterial therapies in future.

6   References

1.   Van Wart SA, Cirincione BB, Ludwig EA, Meagher AK, Korth-Bradley JM, Owen JS. Population Pharmacokinetics of Tigecycline in Healthy Volunteers. *J Clin Pharmacol*. 2007;47(6):727-737. doi:10.1177/0091270007300263

2.   Van Wart SA, Owen JS, Ludwig EA, Meagher AK, Korth-Bradley JM, Cirincione BB. Population Pharmacokinetics of Tigecycline in Patients with Complicated Intra-Abdominal or Skin and Skin Structure Infections. *Antimicrob Agents Chemother*. 2006;50(11):3701-3707. doi:10.1128/AAC.01636-05

3.   CDC. *Antibiotic Resistance Threats in the United States, 2019*. Atlanta, Georgia; 2019. doi:10.15620/cdc:82532

4.   Smith PW, Watkins K, Hewlett A. Infection control through the ages. *Am J Infect Control*. 2012;40(1):35-42. doi:10.1016/j.ajic.2011.02.019

5.   Fischbach MA, Walsh CT. Antibiotics for emerging pathogens. *Science (80-)*. 2009;325(5944):1089-1093. doi:10.1126/science.1176667

6.   Bryan-Wilson J. No time to wait. *Artforum Int*. 2016;54(10):113-114.

7.   Martin SJ, Yost RJ. Infectious Diseases in the Critically Ill Patients. *J Pharm Pract*. 2011;24(1):35-43. doi:10.1177/0897190010388906

8.   Jovanović N, Jovanović J, Stefan-Mikić S, Kulauzov M, Aleksic-Dordević M, Cvjetković D. Mechanisms of bacterial resistance to antibiotics. *Med Pregl*. 2008;61 Suppl 1:9-14. doi:10.1128/9781555819316.part3

9.   Wright G. Mechanisms of resistance to antibiotics. *Curr Opin Chem Biol*. 2003;7(5):563-569. doi:10.1016/j.cbpa.2003.08.004

10.   Falagas ME, Koletsi PK, Bliziotis IA. The diversity of definitions of multidrug-resistant (MDR) and pandrug-resistant (PDR) Acinetobacter baumannii and Pseudomonas aeruginosa. *J Med Microbiol*. 2006;55(12):1619-1629. doi:10.1099/jmm.0.46747-0

11.   Magiorakos A-P, Srinivasan A, Carey RB, et al. Multidrug-resistant, extensively drug-resistant and pandrug-resistant bacteria: an international expert proposal for interim standard definitions for acquired resistance. *Clin Microbiol Infect*. 2012;18(3):268-281. doi:10.1111/j.1469-0691.2011.03570.x

12. Nordmann P, Naas T, Poirel L. Global Spread of Carbapenemase-producing Enterobacteriaceae. *Emerg Infect Dis*. 2011;17(10):1791-1798. doi:10.3201/eid1710.110655

13. Paul M, Carrara E, Retamar P, et al. European Society of Clinical Microbiology and Infectious Diseases (ESCMID) guidelines for the treatment of infections caused by multidrug-resistant Gram-negative bacilli (endorsed by European society of intensive care medicine). *Clin Microbiol Infect*. 2022;28(4):521-547. doi:10.1016/j.cmi.2021.11.025

14. Pankey GA. Tigecycline. *J Antimicrob Chemother*. 2005;56(3):470-480. doi:10.1093/jac/dki248

15. Mayne D, Dowzicky MJ. In vitro activity of tigecycline and comparators against organisms associated with intra-abdominal infections collected as part of TEST (2004–2009). *Diagn Microbiol Infect Dis*. 2012;74(2):151-157. doi:10.1016/j.diagmicrobio.2012.05.032

16. Biedenbach DJ, Beach ML, Jones RN. In vitro antimicrobial activity of GAR-936 tested against antibiotic-resistant gram-positive blood stream infection isolates and strains producing extended-spectrum β-lactamases. *Diagn Microbiol Infect Dis*. 2001;40(4):173-177. doi:10.1016/S0732-8893(01)00269-3

17. Bauer G, Berens C, Projan SJ, Hillen W. Comparison of tetracycline and tigecycline binding to ribosomes mapped by dimethylsulphate and drug-directed Fe2+ cleavage of 16S rRNA. *J Antimicrob Chemother*. 2004;53(4):592-599. doi:10.1093/jac/dkh125

18. Projan SJ. Preclinical pharmacology of GAR-936, a novel glycylcycline antibacterial agent. *Pharmacotherapy*. 2000;20(9 II). doi:10.1592/phco.20.14.219s.35046

19. Postier RG, Green SL, Klein SR, Ellis-Grosse E., Loh E. Results of a multicenter, randomized, open-label efficacy and safety study of two doses of tigecycline for complicated skin and skin-structure infections in hospitalized patients. *Clin Ther*. 2004;26(5):704-714. doi:10.1016/S0149-2918(04)90070-7

20. Babinchak T, Ellis-Grosse E, Dartois N, Rose GM, Loh E. The Efficacy and Safety of Tigecycline for the Treatment of Complicated Intra-Abdominal Infections: Analysis of Pooled Clinical Trial Data. *Clin Infect Dis*. 2005;41(s5):S354-S367. doi:10.1086/431676

21. Bergallo C, Jasovich A, Teglia O, et al. Safety and efficacy of intravenous tigecycline in treatment of community-acquired pneumonia: results from a double-blind randomized phase 3 comparison study with levofloxacin. *Diagn Microbiol Infect Dis*. 2009;63(1):52-61. doi:10.1016/j.diagmicrobio.2008.09.001

22.   Korth-Bradley JM, Baird-Bellaire SJ, Patat AA, et al. Pharmacokinetics and Safety of a Single Intravenous Dose of the Antibiotic Tigecycline in Patients With Cirrhosis. *J Clin Pharmacol*. 2011;51(1):93-101. doi:10.1177/0091270010363477

23.   Zhou C-C, Huang F, Zhang J-M, Zhuang Y-G. Population Pharmacokinetics of Tigecycline: A Systematic Review. *Drug Des Devel Ther*. 2022;Volume 16(June):1885-1896. doi:10.2147/DDDT.S365512

24.   De Pascale G, Montini L, Pennisi M, et al. High dose tigecycline in critically ill patients with severe infections due to multidrug-resistant bacteria. *Crit Care*. 2014;18(3):R90. doi:10.1186/cc13858

25.   Li MX, Li N, Zhu LQ, Liu W. Optimization of tigecycline dosage regimen for different infections in the patients with hepatic or renal impairment. *J Chemother*. 2020;32(8):420-428. doi:10.1080/1120009X.2020.1800318

26.   Deitchman AN, Singh RSP, Derendorf H. Nonlinear Protein Binding: Not What You Think. *J Pharm Sci*. 2018;107(7):1754-1760. doi:10.1016/j.xphs.2018.03.023

27.   Dorn C, Kratzer A, Liebchen U, et al. Impact of Experimental Variables on the Protein Binding of Tigecycline in Human Plasma as Determined by Ultrafiltration. *J Pharm Sci*. 2018;107(2):739-744. doi:10.1016/j.xphs.2017.09.006

28.   McGovern PC, Wible M, El-Tahtawy A, Biswas P, Meyer RD. All-cause mortality imbalance in the tigecycline phase 3 and 4 clinical trials. *Int J Antimicrob Agents*. 2013;41(5):463-467. doi:10.1016/j.ijantimicag.2013.01.020

29.   De Pascale G, Lisi L, Ciotti GMP, et al. Pharmacokinetics of high-dose tigecycline in critically ill patients with severe infections. *Ann Intensive Care*. 2020;10(1):94. doi:10.1186/s13613-020-00715-2

30.   Zha L, Pan L, Guo J, French N, Villanueva E V., Tefsen B. Effectiveness and Safety of High Dose Tigecycline for the Treatment of Severe Infections: A Systematic Review and Meta-Analysis. *Adv Ther*. 2020;37(3):1049-1064. doi:10.1007/s12325-020-01235-y

31.   Xia G, Jiang R. Clinical study on the safety and efficacy of high-dose tigecycline in the elderly patients with multidrug-resistant bacterial infections. *Medicine (Baltimore)*. 2020;99(10):e19466. doi:10.1097/MD.0000000000019466

32.   Muralidharan G, Micalizzi M, Speth J, Raible D, Troy S. Pharmacokinetics of Tigecycline after

Single and Multiple Doses in Healthy Subjects. *Antimicrob Agents Chemother*. 2005;49(1):220-229. doi:10.1128/AAC.49.1.220-229.2005

33. European Committee for Antimicrobial Susceptibility Testing (EUCAST) Guidance Document on Tigecycline Dosing, Dezember 2018. https://www.eucast.org/fileadmin/src/media/ PDFs/EUCAST_files/General_documents/Tigecycline_Guidance_document_20181223.pdf.

34. European Committee for Antimicrobial Susceptibility Testing (EUCAST), Guidance Document on Tigecycline Dosing, July 2022. https://www.eucast.org/fileadmin/src/media/ PDFs/EUCAST_files/Guidance_documents/Tigecycline_Guidance_document_v2_20220720 .pdf.

35. Xie J, Wang T, Sun J, et al. Optimal tigecycline dosage regimen is urgently needed: results from a pharmacokinetic/pharmacodynamic analysis of tigecycline by Monte Carlo simulation. *Int J Infect Dis*. 2014;18(1):62-67. doi:10.1016/j.ijid.2013.09.008

36. Yang T, Mei H, Wang J, Cai Y. Therapeutic Drug Monitoring of Tigecycline in 67 Infected Patients and a Population Pharmacokinetics/Microbiological Evaluation of A. baumannii Study. *Front Microbiol*. 2021;12(June):1-8. doi:10.3389/fmicb.2021.678165

37. Food and Drug Administration. Enhancing the Diversity of Clinical Trial Populations — Eligibility Criteria, Enrollment Practices, and Trial Designs Guidance for Industry. 2020;(November):November.

38. Vincent J-L. International Study of the Prevalence and Outcomes of Infection in Intensive Care Units. *JAMA*. 2009;302(21):2323. doi:10.1001/jama.2009.1754

39. Rhomberg PR, Fritsche TR, Sader HS, Jones RN. Antimicrobial susceptibility pattern comparisons among intensive care unit and general ward Gram-negative isolates from the Meropenem Yearly Susceptibility Test Information Collection Program (USA). *Diagn Microbiol Infect Dis*. 2006;56(1):57-62. doi:10.1016/j.diagmicrobio.2005.12.009

40. Roberts JA, Abdul-Aziz MH, Lipman J, et al. Individualised antibiotic dosing for patients who are critically ill: Challenges and potential solutions. *Lancet Infect Dis*. 2014;14(6):498-509. doi:10.1016/S1473-3099(14)70036-2

41. Rudd KE, Johnson SC, Agesa KM, et al. Global, regional, and national sepsis incidence and mortality, 1990–2017: analysis for the Global Burden of Disease Study. *Lancet*. 2020;395(10219):200-211. doi:10.1016/S0140-6736(19)32989-7

42. Delcò F, Tchambaz L, Schlienger R, Drewe J, Krähenbühl S. Dose adjustment in patients with liver disease. *Drug Saf*. 2005;28(6):529-545. doi:10.2165/00002018-200528060-00005

43. Spray JW, Willett K, Chase D, Sindelar R, Connelly S. Dosage adjustment for hepatic dysfunction based on Child-Pugh scores. *Am J Heal Pharm*. 2007;64(7):690-693. doi:10.2146/ajhp060287

44. Lindvig KP, Hansen TL, Madsen BS, et al. Diagnostic accuracy of routine liver function tests to identify patients with significant and advanced alcohol-related liver fibrosis. *Scand J Gastroenterol*. 2021;56(9):1088-1095. doi:10.1080/00365521.2021.1929450

45. Burra P, Masier A. Dynamic tests to study liver function. *Eur Rev Med Pharmacol Sci*. 2004;8(1):19-21.

46. Jara M, Bednarsch J, Valle E, et al. Reliable assessment of liver function using LiMAx. *J Surg Res*. 2015;193(1):184-189. doi:10.1016/j.jss.2014.07.041

47. Pugh RNH, Murray-Lyon IM, Dawson JL, Pietroni MC, Williams R. Transection of the oesophagus for bleeding oesophageal varices. *Br J Surg*. 1973;60(8):646-649. doi:10.1002/bjs.1800600817

48. Department of Health and Human Services Food and Drug Administration. Pharmacokinetics in Patients with Impaired Hepatic Function : Study Design , Data Analysis , and Guidance for Industry Pharmacokinetics in Patients with Impaired Hepatic Function. Study Design , Data Analysis , and Impact on Dosing and Labeling. 2003;(May).

49. Spray JW, Willett K, Chase D, Sindelar R, Connelly S. Dosage adjustment for hepatic dysfunction based on Child–Pugh scores. *Am J Heal Pharm*. 2007;64(7):690-693. doi:10.2146/ajhp060287

50. Broeker A, Wicha SG, Dorn C, et al. Tigecycline in critically ill patients on continuous renal replacement therapy: a population pharmacokinetic study. *Crit Care*. 2018;22(1):341. doi:10.1186/s13054-018-2278-4

51. Bastida C, Hernández-Tejero M, Aziz F, et al. Tigecycline population pharmacokinetics in patients with decompensated cirrhosis and severe infections. *J Antimicrob Chemother*. 2020;75(12):3619-3624. doi:10.1093/jac/dkaa362

52. Wiesner R, Edwards E, Freeman R, et al. Model for end-stage liver disease (MELD) and allocation of donor livers. *Gastroenterology*. 2003;124(1):91-96. doi:10.1053/gast.2003.50016

53. Cholongitas E, Marelli L, Shusang V, et al. A systematic review of the performance of the model for end-stage liver disease (MELD) in the setting of liver transplantation. *Liver Transplant*. 2006;12(7):1049-1061. doi:10.1002/lt.20824

54. Bastida C, Hernández-Tejero M, Aziz F, et al. Meropenem population pharmacokinetics in patients with decompensated cirrhosis and severe infections. *J Antimicrob Chemother*. 2020;75(12):3619-3624. doi:10.1093/jac/dkaa362

55. Stockmann M, Lock JF, Malinowski M, Niehues SM, Seehofer D, Neuhaus P. The LiMAx test: a new liver function test for predicting postoperative outcome in liver surgery. *HPB*. 2010;12(2):139-146. doi:10.1111/j.1477-2574.2009.00151.x

56. Wicha SG, Frey OR, Roehr AC, et al. Linezolid in liver failure: exploring the value of the maximal liver function capacity (LiMAx) test in a pharmacokinetic pilot study. *Int J Antimicrob Agents*. 2017;50(4):557-563. doi:10.1016/j.ijantimicag.2017.06.023

57. Petersen PJ, Bradford PA. Effect of Medium Age and Supplementation with the Biocatalytic Oxygen-Reducing Reagent Oxyrase on In Vitro Activities of Tigecycline against Recent Clinical Isolates. *Antimicrob Agents Chemother*. 2005;49(9):3910-3918. doi:10.1128/AAC.49.9.3910-3918.2005

58. Bradford PA, Petersen PJ, Young M, Jones CH, Tischler M, O'Connell J. Tigecycline MIC Testing by Broth Dilution Requires Use of Fresh Medium or Addition of the Biocatalytic Oxygen-Reducing Reagent Oxyrase To Standardize the Test Method. *Antimicrob Agents Chemother*. 2005;49(9):3903-3909. doi:10.1128/AAC.49.9.3903-3909.2005

59. Hope R, Warner M, Mushtaq S, Ward ME, Parsons T, Livermore DM. Effect of medium type, age and aeration on the MICs of tigecycline and classical tetracyclines. *J Antimicrob Chemother*. 2005;56(6):1042-1046. doi:10.1093/jac/dki386

60. CLSI. *M07-A10: Methods for Dilution Antimicrobial Susceptibility Tests for Bacteria That Grow Aerobically; Approved Standard*. Vol 35.; 2015. http://shop.clsi.org/site/Sample_pdf/M07A10_sample.pdf.

61. EUCAST. To clinical colleagues : On recent changes in clinical microbiology susceptibility reports - new interpretation of susceptibility categories S , I and R . Susceptible Resistant. 2020: 2020-2022. https://www.eucast.org/fileadmin/src/media/PDFs/EUCAST_files/Guidance_documents/To_clinical_colleagues_on_recent_changes_in_clinical_microbiolog

y_susceptibility_reports_9_July2021.pdf.

62.   European Committee on Antimicrobial Susceptibility Testing (EUCAST), Breakpoint tables for interpretation of MICs and zone diameters. *http://www.eucast.org/fileadmin/src/media/ PDFs/EUCAST_files/Breakpoint_tables/v_50_Breakpoint_Table_01.pdf*. 2024;v14.0. http://www.eucast.org/fileadmin/src/media/PDFs/EUCAST_files/Breakpoint_tables/v_5.0 _Breakpoint_Table_01.pdf.

63.   Blaser J, Stone BB, Zinner SH. Two compartment kinetic model with multiple artificial capillary units. *J Antimicrob Chemother*. 1985;15 (suppl A): 131-137. doi:10.1093/jac/ 15.suppl_A.131

64.   Pasipanodya JG, Nuermberger E, Romero K, Hanna D, Gumbo T. Systematic analysis of hollow fiber model of tuberculosis experiments. *Clin Infect Dis*. 2015;61(September 2003):S10-S17. doi:10.1093/cid/civ425

65.   Department PDSS. Qualification opinion: In vitro hollow fiber system model of tuberculosis (HSF-TB). *Eur Med Agency*. 2015;44(0):1-9.

66.   US FDA. Guidance for Industry Population Pharmacokinetics. *FDA Guid*. 2022;(February):31.

67.   Ambrose PG, Bhavnani SM, Rubino CM, et al. Antimicrobial Resistance: Pharmacokinetics-Pharmacodynamics of Antimicrobial Therapy: It's Not Just for Mice Anymore. *Clin Infect Dis*. 2007;44(1):79-86. doi:10.1086/510079

68.   Tuntland T, Ethell B, Kosaka T, et al. Implementation of pharmacokinetic and pharmacodynamic strategies in early research phases of drug discovery and development at novartis institute of biomedical research. *Front Pharmacol*. 2014;5 JUL(July):1-16. doi:10.3389/fphar.2014.00174

69.   Passarell JA, Meagher AK, Liolios K, et al. Exposure-Response Analyses of Tigecycline Efficacy in Patients with Complicated Intra-Abdominal Infections. *Antimicrob Agents Chemother*. 2008;52(1):204-210. doi:10.1128/AAC.00813-07

70.   Sheiner LB, Rosenberg B, Marathe V V. Estimation of population characteristics of pharmacokinetic parameters from routine clinical data. *J Pharmacokinet Biopharm*. 1977;5(5):445-479. doi:10.1007/BF01061728

71.   Aldrich J. R.A. Fisher and the making of maximum likelihood 1912-1922. *Stat Sci*. 1997;12(3):162-176. doi:10.1214/ss/1030037906

72. Bauer RJ. NONMEM Tutorial Part II: Estimation Methods and Advanced Examples. *CPT Pharmacometrics Syst Pharmacol*. 2019;8(8):538-556. doi:10.1002/psp4.12422

73. Steimer J-L, Mallet A, Golmard J-L, Boisvieux J-F. Alternative Approaches to Estimation of Population Pharmacokinetic Parameters: Comparison with the Nonlinear Mixed-Effect Model. *Drug Metab Rev*. 1984;15(1-2):265-292. doi:10.3109/03602538409015066

74. Owen JS, Fiedler-kelly J. *Mixed Effects Models Introduction To Population Pk/Pd Analysis*.

75. Jonsson EN, Karlsson MO. Automated covariate model building within NONMEM. *Pharm Res*. 1998;15(9):1463-1468. doi:10.1023/a:1011970125687

76. Yngman G, Bjugård Nyberg H, Nyberg J, Jonsson EN, Karlsson MO. An introduction to the full random effects model. *CPT Pharmacometrics Syst Pharmacol*. 2022;11(2):149-160. doi:10.1002/psp4.12741

77. Novakovic AM, Krekels EHJ, Munafo A, Ueckert S, Karlsson MO. Application of Item Response Theory to Modeling of Expanded Disability Status Scale in Multiple Sclerosis. *AAPS J*. 2017;19(1):172-179. doi:10.1208/s12248-016-9977-z

78. Brekkan A, Lopez-Lazaro L, Yngman G, et al. A Population Pharmacokinetic-Pharmacodynamic Model of Pegfilgrastim. *AAPS J*. 2018;20(5):1-14. doi:10.1208/s12248-018-0249-y

79. Abrantes JA, Solms A, Garmann D, Nielsen EI, Jönsson S, Karlsson MO. Bayesian Forecasting Utilizing Bleeding Information to Support Dose Individualization of Factor VIII. *CPT Pharmacometrics Syst Pharmacol*. 2019;8(12):894-903. doi:10.1002/psp4.12464

80. Yngman G, Bjugård Nyberg H, Nyberg J, Jonsson EN, Karlsson MO. An introduction to the full random effects model. *CPT Pharmacometrics Syst Pharmacol*. 2022;(July):1-12. doi:10.1002/psp4.12741

81. Nyberg J, Jonsson EN, Karlsson MO, Häggström J. Properties of the full random effect modelling approach with missing covariates. *bioRxiv*. 2019:656470. doi:10.1101/656470

82. Sheiner LB. Learning versus confirming in clinical drug development. In: *Clinical Pharmacology and Therapeutics*. Vol 61. ; 1997:275-291. doi:10.1016/S0009-9236(97)90160-0

83. Marshall S, Burghaus R, Cosson V, et al. Good Practices in Model-Informed Drug Discovery and Development: Practice, Application, and Documentation. *CPT Pharmacometrics Syst Pharmacol*. 2016;5(3):93-122. doi:10.1002/psp4.12049

84.   Duffull SB, Wright DFB, Winter HR. Interpreting population pharmacokinetic-pharmacodynamic analyses - a clinical viewpoint. *Br J Clin Pharmacol*. 2011;71(6):807-814. doi:10.1111/j.1365-2125.2010.03891.x

85.   Bonate PL. Pharmacokinetic-Pharmacodynamic Modelling. In: *Pharmacokinetics for the Pharmaceutical Scientist*. CRC Press; 2018:259-268. doi:10.1201/9780203743652-14

86.   Amann LF, Vicente ER, Rathke M, Broeker A, Riedner M, Wicha SG. Stability studies with tigecycline in bacterial growth medium and impact of stabilizing agents. *Eur J Clin Microbiol Infect Dis*. 2021;40(1):215-218. doi:10.1007/s10096-020-03970-0

87.   Amann LF, Broeker A, Riedner M, et al. Diagnostic Microbiology & Infectious Disease Pharmacokinetic / pharmacodynamic evaluation of tigecycline dosing in a hollow fiber infection model against clinical bla -KPC producing Klebsiella Pneumoniae isolates. *Diagnostic Microbiol Infect Dis*. 2024;108(2):116153. doi:10.1016/j.diagmicrobio.2023.116153

88.   Amann LF, Alraish R, Broeker A, Kaffarnik M, Wicha SG. Tigecycline Dosing Strategies in Critically Ill Liver-Impaired Patients. *Antibiotics*. 2022;11(4):479. doi:10.3390/antibiotics11040479

89.   Amann LF, Wicha SG. Operational characteristics of full random effects modelling ('frem') compared to stepwise covariate modelling ('scm'). *J Pharmacokinet Pharmacodyn*. 2023;0123456789. doi:10.1007/s10928-023-09856-w

90.   Falagas ME, Tansarli GS, Ikawa K, Vardakas KZ. Clinical outcomes with extended or continuous versus short-term intravenous infusion of carbapenems and piperacillin/tazobactam: A systematic review and meta-analysis. *Clin Infect Dis*. 2013;56(2):272-282. doi:10.1093/cid/cis857

91.   Bauer KA, West JE, O'Brien JM, Goff DA. Extended-infusion cefepime reduces mortality in patients with Pseudomonas aeruginosa infections. *Antimicrob Agents Chemother*. 2013;57(7):2907-2912. doi:10.1128/AAC.02365-12

92.   Falagas ME, Vardakas KZ, Tsiveriotis KP, Triarides NA, Tansarli GS. Effectiveness and safety of high-dose tigecycline-containing regimens for the treatment of severe bacterial infections. *Int J Antimicrob Agents*. 2014;44(1):1-7. doi:10.1016/j.ijantimicag.2014.01.006

93.   Jitkova Y, Gronda M, Hurren R, et al. A Novel Formulation of Tigecycline Has Enhanced Stability and Sustained Antibacterial and Antileukemic Activity. Sbarba P Dello, ed. *PLoS One*.

2014;9(5):e95281. doi:10.1371/journal.pone.0095281

94.   Sun Y, Cai Y, Liu X, Bai N, Liang B, Wang R. The emergence of clinical resistance to tigecycline. *Int J Antimicrob Agents*. 2013;41(2):110-116. doi:10.1016/j.ijantimicag.2012.09.005

95.   Baron J, Cai S, Klein N, Cunha B. Once Daily High Dose Tigecycline Is Optimal: Tigecycline PK/PD Parameters Predict Clinical Effectiveness. *J Clin Med*. 2018;7(3):49. doi:10.3390/jcm7030049

96.   Cui N, Cai H, Li Z, Lu Y, Wang G, Lu A. Tigecycline-induced coagulopathy: a literature review. *Int J Clin Pharm*. 2019;41(6):1408-1413. doi:10.1007/s11096-019-00912-5

97.   Rossitto G, Piano S, Rosi S, Simioni P, Angeli P. Life-threatening coagulopathy and hypofibrinogenaemia induced by tigecycline in a patient with advanced liver cirrhosis. *Eur J Gastroenterol Hepatol*. 2014;26(6):681-684. doi:10.1097/MEG.0000000000000087

98.   Conte JE, Golden JA, Kelly MG, Zurlinden E. Steady-state serum and intrapulmonary pharmacokinetics and pharmacodynamics of tigecycline. *Int J Antimicrob Agents*. 2005;25(6):523-529. doi:10.1016/j.ijantimicag.2005.02.013

99.   Van Ogtrop ML, Andes D, Stamstad TJ, et al. In vivo pharmacodynamic activities of two glycylcyclines (GAR-936 and WAY 152,288) against various gram-positive and gram-negative bacteria. *Antimicrob Agents Chemother*. 2000;44(4):943-949. doi:10.1128/AAC.44.4.943-949.2000

100.   Rubino CM, Bhavnani SM, Forrest A, et al. Pharmacokinetics-Pharmacodynamics of Tigecycline in Patients with Community-Acquired Pneumonia. *Antimicrob Agents Chemother*. 2012;56(1):130-136. doi:10.1128/AAC.00277-10

101.   Crandon JL, Banevicius MA, Nicolau DP. Pharmacodynamics of Tigecycline against Phenotypically Diverse Staphylococcus aureus Isolates in a Murine Thigh Model. *Antimicrob Agents Chemother*. 2009;53(3):1165-1169. doi:10.1128/AAC.00647-08

102.   Meagher AK, Passarell JA, Cirincione BB, et al. Exposure-Response Analyses of Tigecycline Efficacy in Patients with Complicated Skin and Skin-Structure Infections. *Antimicrob Agents Chemother*. 2007;51(6):1939-1945. doi:10.1128/AAC.01084-06

103.   Fan G, Jin L, Bai H, Jiang K, Xie J, Dong Y. Safety and Efficacy of Tigecycline in Intensive Care Unit Patients Based on Therapeutic Drug Monitoring. *Ther Drug Monit*. 2020;42(6):835-840. doi:10.1097/FTD.0000000000000784

104. Sevillano D, Aguilar L, Alou L, et al. Exposure–response analysis of tigecycline in pharmacodynamic simulations using different size inocula of target bacteria. *Int J Antimicrob Agents*. 2010;36(2):137-144. doi:10.1016/j.ijantimicag.2010.03.021

105. Tsala M, Vourli S, Daikos GL, et al. Impact of bacterial load on pharmacodynamics and susceptibility breakpoints for tigecycline and Klebsiella pneumoniae. *J Antimicrob Chemother*. 2017;72(1):172-180. doi:10.1093/jac/dkw354

106. Fabregas N, Ewig S, Torres A, et al. Clinical diagnosis of ventilator associated pneumonia revisited: comparative validation using immediate post-mortem lung biopsies. *Thorax*. 1999;54(10):867-873. doi:10.1136/thx.54.10.867

107. Stein GE, Smith CL, Missavage A, et al. Tigecycline Penetration into Skin and Soft Tissue. *Surg Infect (Larchmt)*. 2011;12(6):465-467. doi:10.1089/sur.2011.022

108. Bulik CC, Wiskirchen DE, Shepard A, Sutherland CA, Kuti JL, Nicolau DP. Tissue Penetration and Pharmacokinetics of Tigecycline in Diabetic Patients with Chronic Wound Infections Described by Using In Vivo Microdialysis. *Antimicrob Agents Chemother*. 2010;54(12):5209-5213. doi:10.1128/AAC.01051-10

109. Dorn C, Petroff D, Kratzer A, et al. Tigecycline Soft Tissue Penetration in Obese and Non-obese Surgical Patients Determined by Using In Vivo Microdialysis. *Eur J Drug Metab Pharmacokinet*. 2022;47(5):749-755. doi:10.1007/s13318-022-00789-2

110. Kroemer N, Aubry R, Couet W, Grégoire N, Wicha SG. Optimized Rhombic Experimental Dynamic Checkerboard Designs to Elucidate Pharmacodynamic Drug Interactions of Antibiotics. *Pharm Res*. 2022;39(12):3267-3277. doi:10.1007/s11095-022-03396-7

111. Rajman I. PK/PD modelling and simulations: utility in drug development. *Drug Discov Today*. 2008;13(7-8):341-346. doi:10.1016/j.drudis.2008.01.003

7 Appendix

7.1 Supplementary material of Publication I

LC-UV and LC-MS/MS methods

All samples (200 µL) were processed for protein precipitation by adding 200 µL of ice-cold acidic methanol to reduce adsorption to plastic labware, derived from Dorn et al [1]. The samples were centrifuged afterwards and 10 µL of the supernatant were injected. Calibration curve, quality control and samples were measured by UHPLC (Ultimate 3000 SD Dionex, Softron GmbH, Germering) equipped with a Nucleoshell RP 18 (100x3 mm, 2.7 µm particle size, Macherey Nagel, Dueren, Germany) using UV detection at 350 nm. As mobile phases (A) Milli-Q® water containing formic acid (95:5, v/v) and (B) methanol, acetonitrile, formic acid (47.5:47.5:5, v/v) were used in a gradient program. The gradient conditions were as follows: linear gradient starting at 1% B to 15% B within 3 min, then linear gradient to 70% B over 2 min and then isocratic at 70% B for 3 min. Afterwards, the pumps were programmed to 1% B over 1 min. A 4 min reconditioning time was used before injection of the next sample. Total run time was 13 min at a flow rate of 0.8 mL/min. The retention time of tigecycline was 3.4 min. A QTRAP 5500 (SCIEX, Framingham, Massachusetts, USA) electrospray ionisation mass spectrometer coupled with a 1290 Infinity HPLC II (Agilent Technologies, California, USA) was used for LC-MS/MS quantification of broth samples containing ascorbic acid, due to reaching the limit of quantification. For LC-MS/MS solvents were used in LC-MS grade. Separation was performed on a Nucleodur C18 Gravity-SB (100x3 mm, 3µm particle size, Macherey Nagel, Dueren, Germany). Solvents (A) water containing formic acid (99.9:0.1, v/v) and (B) methanol, acetonitrile, formic acid (49.9:49.9:0.1, v/v) were used in a gradient program. The gradient conditions were as follows: starting conditions 1% B, linear gradient starting at 1% B to 20% B within 4 min, then linear gradient to 70% B over 2 min and then isocratic at 70% B for 3 min. Afterwards, the pumps were programmed to 1% B over 1 min. A 4 min reconditioning time was used before injection of the next sample. Total run time was 15 min at a flow rate of 0.3 mL/min. The retention time of tigecycline was 6.3 min. LC–MS/MS data were acquired and analysed using Analyst 1.7 software (SCIEX, Framingham, Massachusetts, USA). The multiple reaction monitoring (MRM) transitions used were m/z 586.3/513.2 (quantifier) and 586.3/569.2 (qualifier).

7.2   Supplementary material Publication II

Supplement Text 1

The dynamic *in vitro* experiments were performed at 37 °C over 72 h with n=1 per scenario. A stirred central compartment was connected via a tubing to a FX-pead dialyser (Fresenius Medical Care AG & Co. KGaA, Bad Homburg, Germany)[104]. The dialyser served as bacterial compartment. An additional bacterial cycle (Supplement Figure 1), connected to a peristaltic pump, was used to keep the liquids in the cartridge moving. By this approach, we assumed rapid nutrient distribution and fast drug equilibrium between the central compartment and the cartridge. The total volume used in the HFIM was 200 mL and was kept constant over the experiment duration. Liquid flow was assured via peristaltic pumps: Drug elimination kinetics were controlled via inflow of drug-free Mueller-Hinton broth using an Ismatec Reglo ICC pump (Cole-Parmer GmbH, Wertheim, Germany) and circulation of the drug and the nutrients in the central compartment at a flow rate of 60 mL/min was assured via a Masterflex®L/S (Cole-Parmer GmbH, Wertheim, Germany). A Masterflex® syringe pump (Cole-Parmer GmbH, Wertheim, Germany) infused tigecycline into the central compartment.
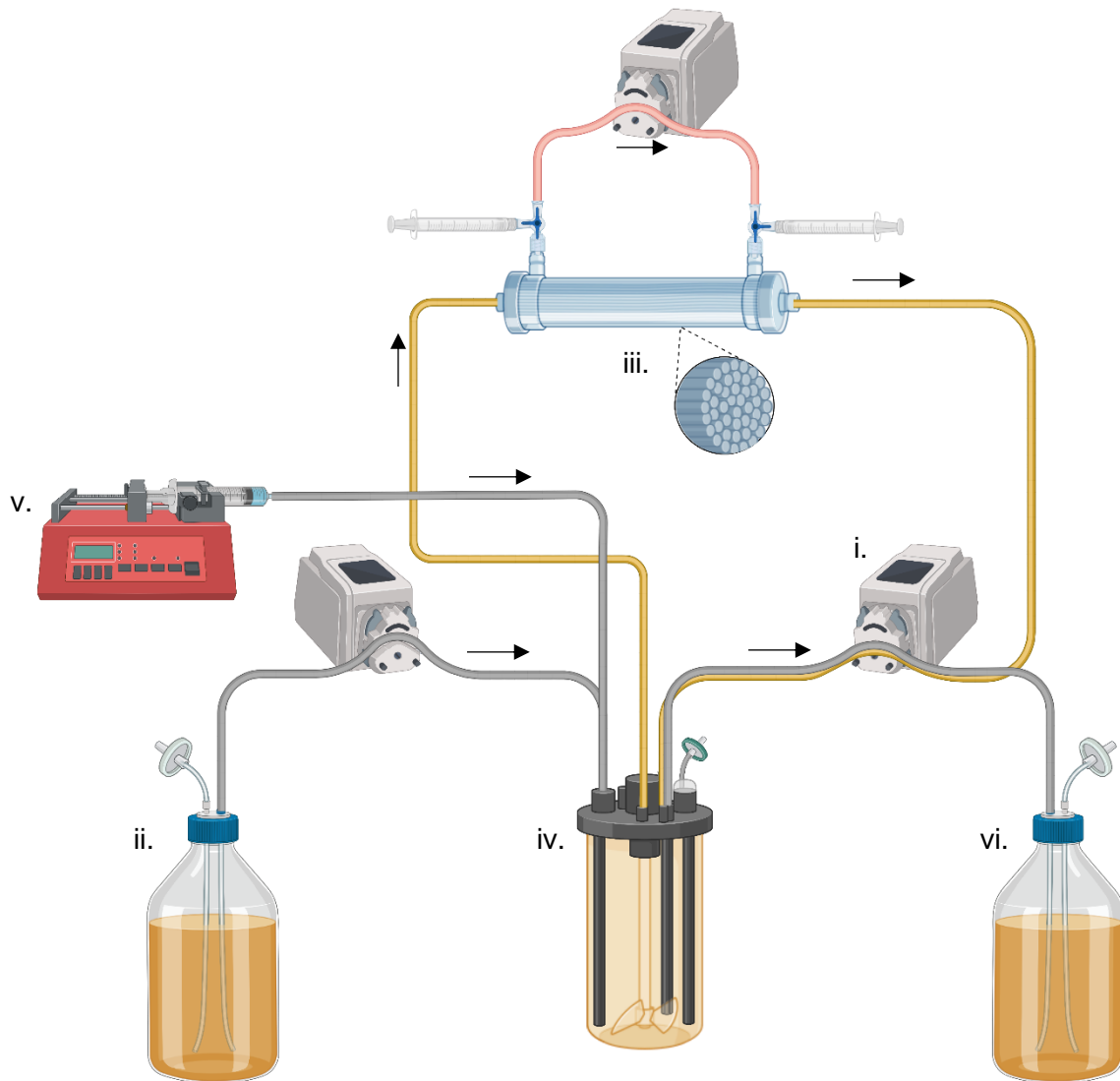
Supplement Figure S1 Schematic set up of the hollow fiber infection model. All liquid flows are guided via peristaltic pumps (i.). Continuous nutrient supply is guaranteed via drug-free bacterial growth medium (ii.). Bacteria are retained in the dialysis cartridge (iii.) and are circulating against the direction circulation of the central compartment to assure equal distribution of nutrients, drug and to prevent biofilm formation. The drug is infused into the central compartment (iv.) by a programmable syringe pump (v.) and eliminated drug and bacterial waste products are collected in a waste bin (vi.). The graphic was created with BioRender.com.
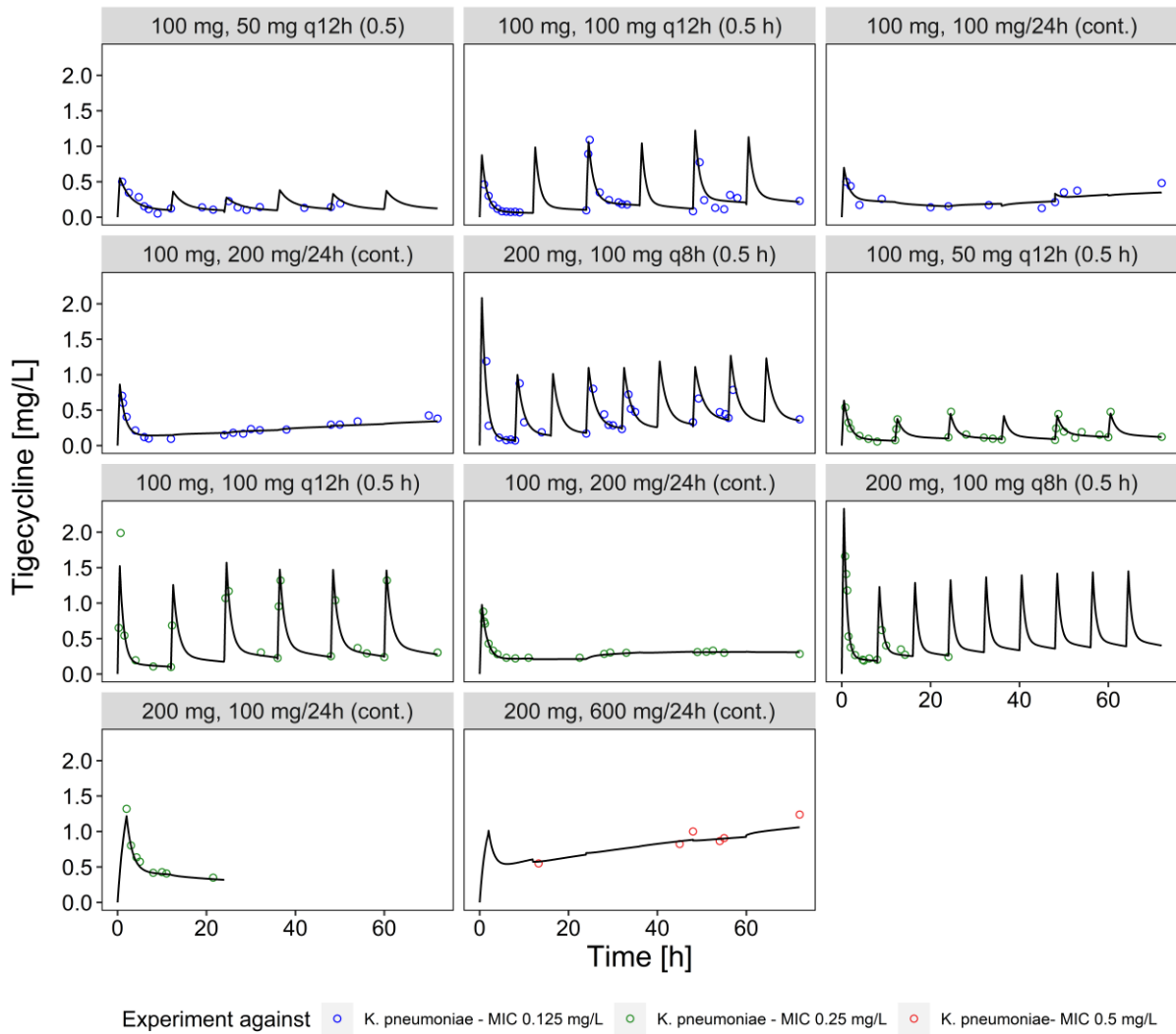
Supplement Figure S2 Measured tigecycline concentrations in the hollow-fiber infection model versus individual model predictions (IPRED) per experiment.
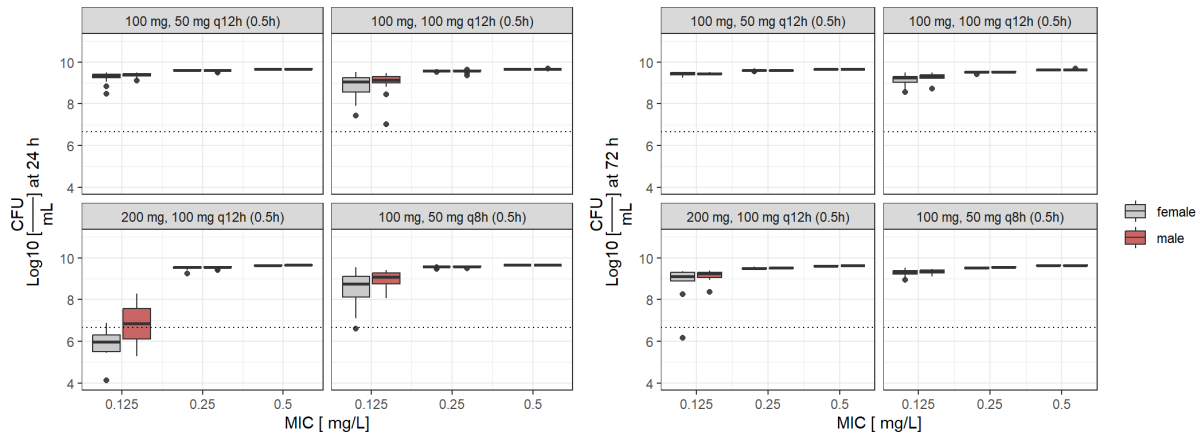
Supplement Figure S3 Clinical trial simulations of standard dose (100 mg loading dose (LD), 50 mg q12 h), high dose (100 mg q12 h), intensified standard dose (100 mg LD, 50 mg q8 h), as well as variation of the loading dose (200 mg LD, 100 q 12h). Colony forming units (CFU/mL) at 24 h and 72 h are displayed for each simulated dosing scenario, stratified by sex. Gray dashed y-intercept displays the estimated start inoculum (6.7 $\log_{10}$CFU/mL) of the pharmacometric PD model.

Supplement Table S1 Susceptibility information for *Klebsiella pneumoniae* isolates used in this study. *Klebsiella pneumoniae* 2977 (KPC-2, OXA-9, TEM-1; referred to as KP 2977), *Klebsiella pneumoniae* R307 (KPC-2, OXA-2, OXA-9, TEM-1, CTX-M-2; referred to as KP 307) and *Klebsiella pneumoniae* -N864 (KPC-3, OXA-9, TEM-1, referred to as referred to as KP N864) against beta-lactam class antibiotics.

Antibiotic	MIC of KP 2977 (mg/L)	MIC of KP 307 (mg/L)	MIC of KP N864 (mg/L)
Ceftazidime	>32	32	32
Ceftazidime/ Avibactam	≤ 0.5	1	1
Meropenem	4	> 16	2
Imipenem	4	> 32	8

Supplement Table S2 Comparative analysis of sampling in central vs. bacterial compartment.

Tigecycline concentration in bacterial compartment (mg/L)	Tigecycline concentration in central compartment (mg/L)	Deviation from central compartment (%)
1.18	1.25	-5.93
0.988	0.107	-8.29
0.792	0.736	-7.07
0.540	0.480	11.11
0.514	0.573	-11.4
0.378	0.389	-3.05
0.271	0.275	-1.48
0.205	0.193	5.85
0.189	0.191	-1.06

Supplement Table S3

CHROM	POS	REF	ALT	TYPE	150 wild-type	149 8x MIC TGC 2mg/L	148 KPR 307 32x MIC TGC 8mg/L	Effect	Impact	Functional Class	Codon change	Protein and Nucleotide change	Amino Acid Length	Gene name	Biotype	Protein	Function	Ass w/ TGC resistance	PMID
CP114785	11127	C	CG	INDEL	C	C	CG	Frameshift variant	HIGH		gcg/gGcg	p.Ala141fs/c.421dupG	811	htrE	protein coding	fimbrial usher gene	chaperon fimbria biosynthesis		
CP114785	103758	C	CG	INDEL	C	C	CG	Frameshift variant	HIGH		cgc/cCgc	p.Arg35fs/c.103dupC	194	ramR	protein coding	Transcriptional regulator	ramA regulator	ramA regulator	28368073
CP114785	294811	C	T	SNP	C	C	T	Missense variant	MODERATE	MISSENSE	Gtc/Atc	p.Val224Ile/c.670G>A	250	nagD	protein coding				
CP114785	546648	A	AG	INDEL	A	A	AG	Frameshift variant	HIGH		ctg/Gctg	p.Leu198fs/c.591dupG	490	resE	protein coding	two component sensor histidin kinase BACILLUS			
CP114785	556118	A	G	SNP	A	A	G	Missense variant	MODERATE	MISSENSE	cTg/cCg	p.Leu470Pro/c.1409T>C	480	O1G28_02780	protein coding				
CP114785	652818	T	C	SNP	T	T	C	Missense variant	MODERATE	MISSENSE	Tac/Cac	p.Tyr83His/c.247T>C	582	msbA	protein coding			mutations in adeS, rpsJ, rrf, msbA, and gnaA may contribute to emerging tige-cycline resistance mechanisms	PMID: 34170209

CHROM	POS	REF	ALT	TYPE	150 wild-type	149 8x MIC TGC 2mg/L	148 KPR 307 32x MIC TGC 8mg/L	Effect	Impact	Functional Class	Codon change	Protein and Nucleotide change	Amino Acid Length	Gene name	Biotype	Protein	Function	Ass w/ TGC resistance	PMID
CP114785	733031	A	G	SNP	A	A	G	Missense variant	MODERATE	MISSENSE	gTa/gCa	p.Val44Ala/c.131T>C	407	OIG28_03570	protein coding				
CP114785	1175584	C	T	SNP	C	C	T	missense variant	MODERATE	MISSENSE	Ccg/Tcg	p.Pro266Ser/c.796C>T	379	OIG28_05950	protein coding				
CP114785	1254330	A	AC	INDEL	A	A	AC	frameshift variant	HIGH		gtg/gGtg	p.Val6fs/c.18 1dupG	143	slyA	protein coding	Transcriptional regulator		Capsule expression, stress response hv phenotypes	
CP114785	1284353	C	T	SNP	C	C	T	missense variant	MODERATE	MISSENSE	gCc/gTc	p.Ala129Val/c.386C>T	548	fumA	protein coding				
CP114785	1416466	T	TG	INDEL	T	T	TG	frameshift variant	HIGH		gcc/gGcc	p.Ala665fs/c.1 993dupG	773	pys2	protein coding	Klebicin pyocin S HNH nuclease	Bacterioicin		
CP114785	1588886	C	T	SNP	C	C	T	missense variant	MODERATE	MISSENSE	gCc/gTc	p.Ala103Val/c.308C>T	232	mngR	protein coding				
CP114785	1692365	GT	G	INDEL	GT	GT	G	frameshift variant	HIGH		aaa/	p.Lys140fs/c.4 20delA	205	pspA	protein coding	phage shock protein			

CHROM	POS	REF	ALT	TYPE	150 wild-type	149 8x MIC TGC 2mg/L	148 KPR 307 32x MIC TGC 8mg/L	Effect	Impact	Functional Class	Codon change	Protein and Nucleotide change	Amino Acid Length	Gene name	Biotype	Protein	Function	Ass w/ TGC resistance	PMID
CP114785	1815070	A	AG	INDEL	A	A	AG	frameshift variant	HIGH		gtg/gGtg	p.Val353fs/c.1 057dupG	522	O1G28_0920 0	protein coding	hypothetical p	Putative sugar hydrolase		
CP114785	1830461	G	A	SNP	G	G	A	missense variant	MODERATE	MISSENSE	cGc/cAc	p.Arg88His/c. 263G>A	484	ansP2	protein coding				
CP114785	2028839	T	C	SNP	T	T	C	missense variant	MODERATE	MISSENSE	Acc/Gcc	p.Thr193Ala/c .577A>G	257	ssuB	protein coding				
CP114785	2205459	C	CT	INDEL	C	C	CT	frameshift variant	HIGH		agc/aAgc	p.Ser180fs/c.5 38dupA	451	O1G28_11215	protein coding	S-type pyocin domain-containing protein			
CP114785	2455873	G	T	SNP	G	T	G	missense variant	MODERATE	MISSENSE	gCa/gAa	p.Ala538Glu/c .1613C>A	721	O1G28_12490	protein coding				
CP114785	2646868	T	C	SNP	T	T	C	missense variant	MODERATE	MISSENSE	Aaa/Gaa	p.Lys235Glu/c .703A>G	556	menD	protein coding				
CP114785	2768458	G	A	SNP	G	G	A	missense variant	MODERATE	MISSENSE	Ccg/Tcg	p.Pro340Ser/ c.1018C>T	467	eutA	protein coding				

CHROM	POS	REF	ALT	TYPE	150 wild-type	149 8x MIC TGC 2mg/L	148 KPR 307 32x MIC TGC 8mg/L	Effect	Impact	Functional Class	Codon change	Protein and Nucleotide change	Amino Acid Length	Gene name	Biotype	Protein	Function	Ass w/ TGC resistance	PMID
CP114785	2826813	C	T	SNP	C	C	T	missense variant	MODERATE	MISSENSE	cGc/cAc	p.Arg47His/c.140G>A	525	guaA	protein coding				
CP114785	3272605	T	TG	INDEL	T	T	TG	frameshift variant	HIGH		ggc/ggGc	p.Asn36fs/c.104dupG	428	yesO	protein coding	Putative ABC transporter substrate-binding protein YesO			
CP114785	3292528	G	A	SNP	G	G	A	missense variant	MODERATE	MISSENSE	gCc/gTc	p.Ala76Val/c.227C>T	211	mrkF	protein coding				
CP114785	3293551	A	C	SNP	A	A	C	missense variant	MODERATE	MISSENSE	tgT/tgG	p.Cys67Trp/c.201T>G	327	mrkD	protein coding	Fimbria adhesin gene			virulence genes (29232167)
CP114785	3293642	C	CTGCCCACCACCA	INDEL	C	CTGCCCACCACCA	CTGCCCACCACCA	Conservative inframe insertion	MODERATE		agg/aTGGTGGTGGGCAgg	p.Asp36_Arg37insMetValIGl/c.109_110insTGGTGGTGGGCA	327	mrkD	protein coding	fimbria adhesin gene			virulence genes (29232167)
CP114785	3738095	T	C	SNP	T	T	C	Missense variant	MODERATE	MISSENSE	cTg/cCg	p.Leu28Pro/c.83T>C	333	msrP	protein coding				

CHROM	POS	REF	ALT	TYPE	150 wild-type	149 8x MIC TGC 2mg/L	148 KPR 307 32x MIC TGC 8mg/L	Effect	Impact	Functional Class	Codon change	Protein and Nucleotide change	Amino Acid Length	Gene name	Biotype	Protein	Function	Ass w/ TGC resistance	PMID
CP114785	3827944	C	CG	INDEL	C	C	CG	Frameshift variant	HIGH		gaa/gGaa	p.Glu312fs/ c.934dupG	457	cysG	protein coding	siroheme synthase CysG	Siroheme synthase CysG		
CP114785	4488277	T	C	SNP	T	T	C	Missense variant	MODERATE	MISSENSE	aTc/aCc	p.Ile481Thr/ c.1442T>C	491	ubiD	Protein coding				
CP114785	4576482	A	G	SNP	A	A	G	Missense variant	MODERATE	MISSENSE	aAg/aGg	p.Lys77Arg/ c.230A>G	429	lamB	Protein coding				
CP114785	4649692	TG	T	INDEL	TG	TG	T	Frameshift variant	HIGH		gct/	p.Ala82fs/ c.244delG	761	cckA	protein coding	sensory transduction histidine kinase/receiver protein CckA [Caulobacter vibrioides NA1000]			
CP114785	5161932	A	G	SNP	A	A	G	Missense variant	MODERATE	MISSENSE	gAg/gGg	p.Glu67Gly/ c.200A>G	574	ilvI	Protein coding				
CP114785	5188994	A	G	SNP	A	A	G	Missense variant	MODERATE	MISSENSE	Tcc/Ccc	p.Ser105Pro/ c.313T>C	206	coaE	protein coding				

CHROM	POS	REF	ALT	TYPE	150 wild-type	149 8x MIC TGC 2mg/L	148 KPR 307 32x MIC TGC 8mg/L	Effect	Impact	Functional Class	Codon change	Protein and Nucleotide change	Amino Acid Length	Gene name	Biotype	Protein	Function	Ass w/ TGC resistance	PMID
CP114785	5323150	C	T	SNP	C	C	T	Missense variant	MODERATE	MISSENSE	Gcc/Acc	p.Ala55Thr/c.163G>A	155	rnhA	Protein coding				
CP114785	5501062	C	G	SNP	C	C	G	Missense variant	MODERATE	MISSENSE	Gcc/Ccc	p.Ala194Pro/c.580G>C	491	ampG	Protein coding				resistance to β-lactam agents (34134705)
CP114785	5507200	T	TC	INDEL	T	T	TC	Frameshift variant	HIGH		gta/Cgta	p.Val13fs/c.36dupC	784	lon	Protein coding	endo-peptidase La		ramA regulation	27764207, 28368073
CP114785	5716529	A	AC	INDEL	A	A	AC	Frameshift variant	HIGH		ggg/ggggG	p.Cys92fs/c.273dupG	114	O1G28_28680	Protein coding	hypothetical p			
CP114785	5759886	G	GC	INDEL	G	G	GC	Frameshift variant	HIGH		ggg/ggggG	p.Leu120fs/c.357dupG	654	O1G28_28890	Protein coding	TraM recognition domain conatining protein			

7.3   Supplementary material Publication III
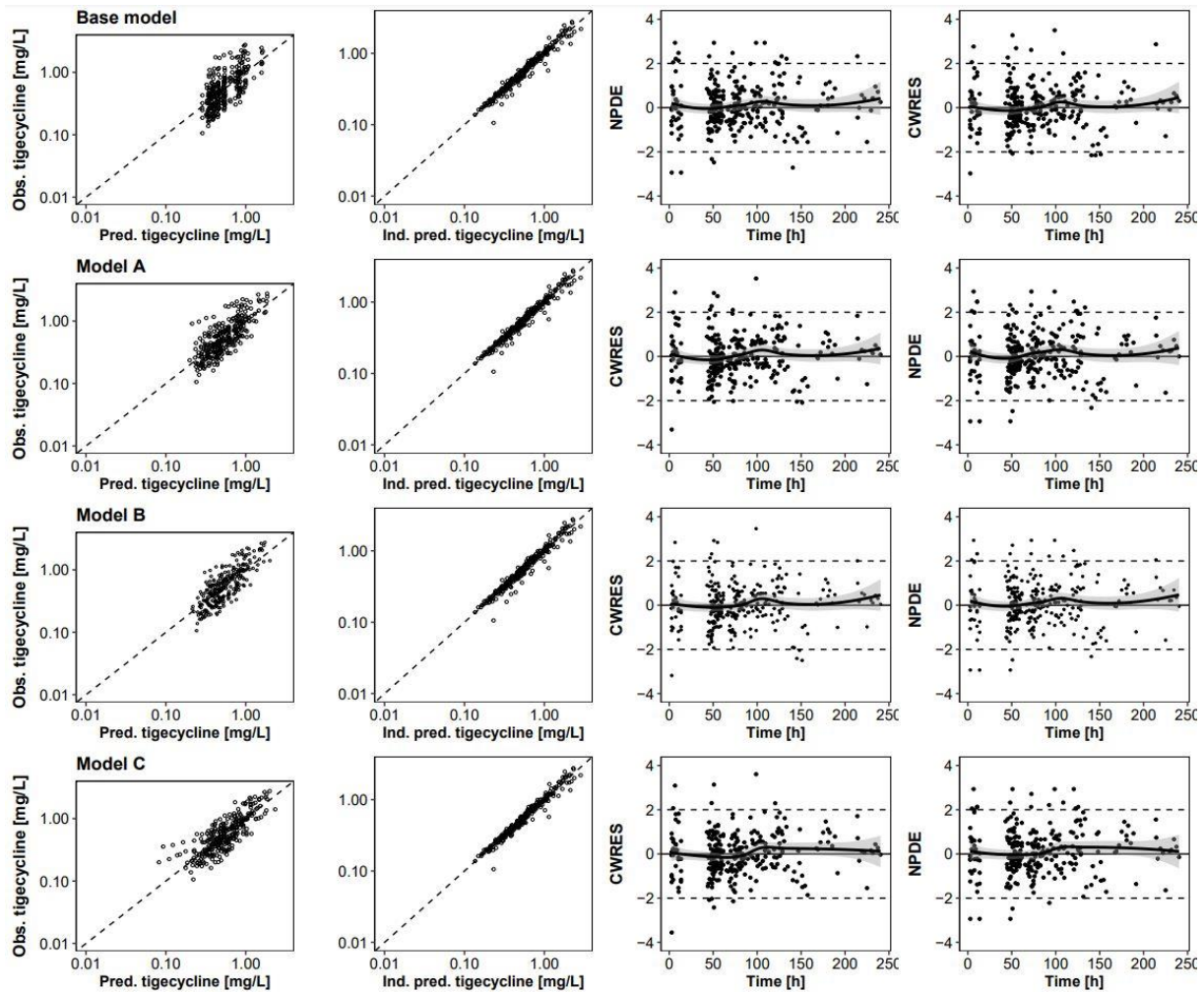
Supplement Figure 1 Population or individual tigecycline predicted vs. observed concentration (upper panel) and conditionally weighted residuals (CWRES) or normalized prediction distribution errors (NPDE) vs. time (lower panel); black line indicates the smoothed conditional mean incl. the 95th confidence interval (shaded area).
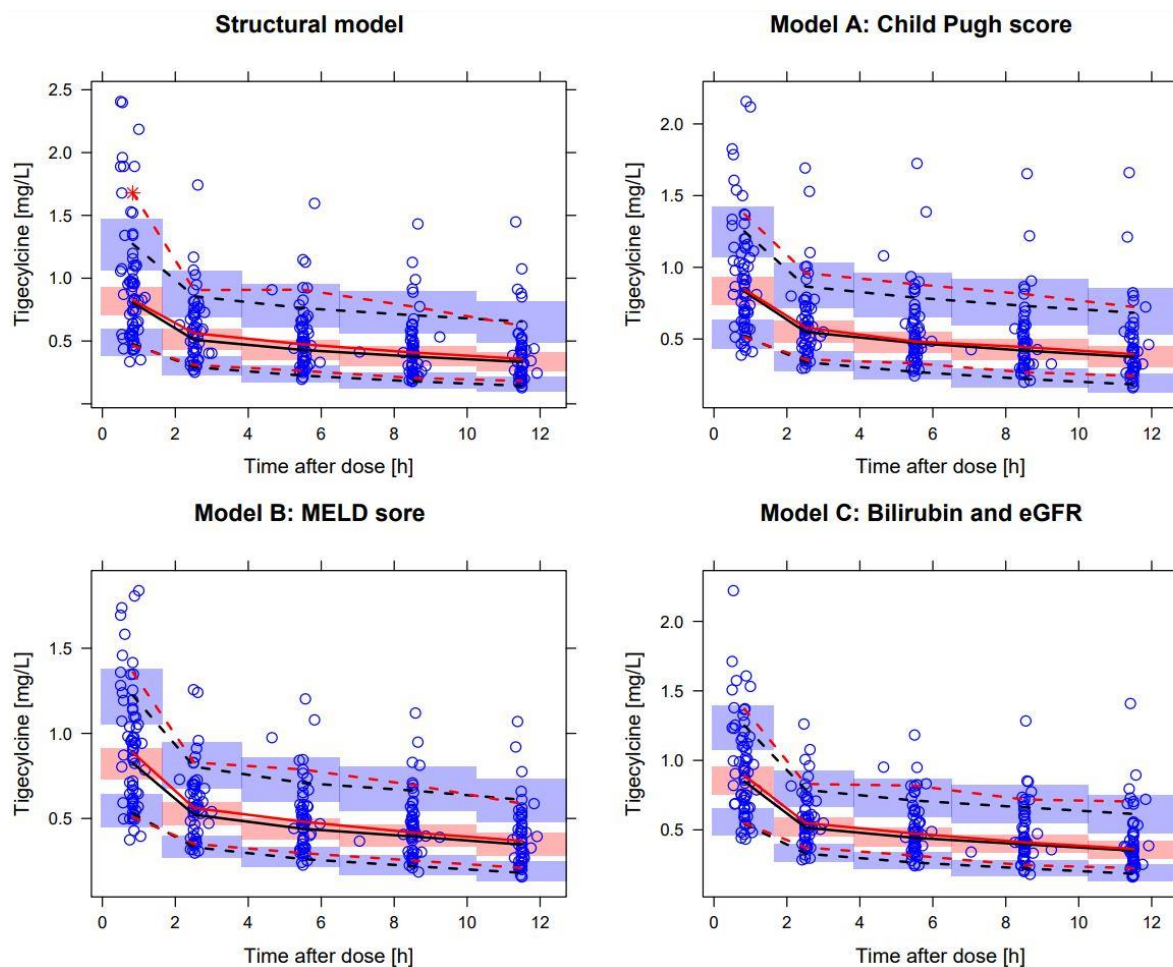
Supplement Figure 2: Visual predictive checks show prediction corrected observations of tigecycline versus time after dose of the structural 2 compartment base model and the covariate models (Model A-C). All covariate models include beside the described covariate on clearance weight on central volume of distribution. The red lines show median and 80 % interval of the prediction corrected observations, black dashed lines describe the 80 % interval of the simulated data's percentiles. Blue shaded area shows the 95 % confidence interval (CI) of the 5th and 95th prediction interval, red shaded area the 95 %-CI of the median prediction.

Supplement Table 1 Population pharmacokinetic model parameter estimates stratified by Child Pugh score as a categorical covariate on clearance (Model A) and weight as a covariate on central volume of distribution Vc (Eq. 1-2). Confidence intervals were determined by the log-likelihood profiling-based sampling importance resampling (llp-sir) method. Abbreviations: RUV: residual unexplained variability, TVVCL: Typical value of clearance. TVVc: Typical value of central volume of distribution.

Parameter	Explanation	Estimate	CI$_{95\%}$	RSE [%]
CL$_{CPS-A}$ [L/h]	Clearance of individuals with Child Pugh score A	11.3	$9.3 - 13.6$	9.71
CL$_{CPS-B}$ [L/h]	Clearance of individuals with Child Pugh score B	7.69	$6.61 - 9.16$	8.46
CL$_{CPS-C}$ [L/h]	Clearance of individuals with Child Pugh score C	4.81	$2.96 - 7.68$	25.0
V$_C$ [L]	Central volume of distribution	64.7	$49.6 - 85.0$	14.0
Q [L/h]	Intercompartmental clearance	48.4	$42.1 - 56.3$	7.46
V$_P$ [L]	Peripheral volume of distribution	119	$100 - 142$	9.08
Θ$_{Vc - weight}$	Linear covariate parameter estimate of weight on V$_c$	$2.44 \cdot 10^{-2}$	$1.87 \cdot 10^{-2} - 2.77 \cdot 10^{-2}$	9.46
IIV$_{CHP-CL}$ [%]	Interindividual variability of Child Pugh A, B, C individuals on clearance	41.8	$34.3 - 50.6$	20.3
IIV$_{Vc}$ [%]	Interindividual variability of central volume of distribution	70.0	$52.6 - 85.5$	24.6
IIV$_{Vp}$ [%]	Interindividual variability of peripheral volume of distribution	30.5	$19.7 - 40.6$	34.5
RUV [% CV]	Residual proportional variability	13.5	$12.2 - 15.0$	5.21

$$\text{IF(CPS = "A") TVCL} = CL_{CPS-A} \qquad \text{Eq. 1}$$

$$\text{IF(CPS = "B") TVCL} = CL_{CPS-B}$$

$$\text{IF(CPS = "C") TVCL} = CL_{CPS-C}$$

$$V_c = TVV_c \cdot (1 + \Theta_{Vc - weight} \cdot (WT - 80)) \qquad \text{Eq. 2}$$

Supplement Table 2 Population pharmacokinetic model parameter estimates using the MELD-score as a covariate on clearance as a power relationship and weight on V_c as a linear relationship (Model B) (Eq. 3-4). Confidence intervals were determined by the log-likelihood profiling-based sampling importance resampling (llp-sir) method. Abbreviations: RUV: residual unexplained variability. TVVCL: Typical value of clearance. TVV$_c$: Typical value of central volume of distribution.

Parameter	Explanation	Estimate	CI$_{95\%}$	RSE [%]
CL [L/h]	Clearance	8.57	$7.58 - 9.63$	6.11
V$_C$ [L]	Central volume of distribution	64.2	$50.8 - 83.4$	12.93
Q [L/h]	Intercompartmental clearance	48.7	$42.2 - 56.0$	7.23
V$_P$ [L]	Peripheral volume of distribution	119	100 - 141	8.75
$\Theta_{CL - MELD}$	Power relationship estimate of MELD-score on clearance	-0.453	$6.35 \cdot 10^{-1} -$ $2.78 \cdot 10^{-1}$	20.1
$\Theta_{Vc - weight}$	Linear covariate parameter estimate of weight on V_c	0.024	$0.019 - 0.028$	9.42
IIV$_{CL}$ [%]	Interindividual on clearance	37.9	$30.4 - 48.3$	25.1
IIV$_{Vc}$ [%]	Interindividual variability of central volume of distribution	69.1	$51.6 - 89.4$	28.5
IIV$_{VP}$ [%]	Interindividual variability of peripheral volume of distribution	29.1	$17.8 - 40.3$	39.4
RUV [% CV]	Residual proportional variability	13.9	$12.6 - 15.6$	5.59

$$CL = TVCL \cdot (\text{MELD-score}/18)^{\Theta_{CL - MELD}} \qquad \text{Eq. 3}$$

$$V_c = TVV_c \cdot (1 + \Theta_{Vc - weight} \cdot (WT - 80)) \qquad \text{Eq. 4}$$

Supplement Table 3: Population pharmacokinetic parameter estimates of the final backward elimination model using raw covariate values (Model C). Confidence intervals (CI$_{95\%}$) were determined by log-likelihood profiling-based sampling importance resampling (llp-sir); RSE: relative standard error. eGFR (CKD-EPI formula) and weight were included as a linear relationship bilirubin using a power function (Eq. 5-6).

Parameter	Explanation	Estimate	CI$_{95\%}$	RSE [%]
CL [L/h]	Total tigecycline clearance	7.52	6.68 – 8.46	6.03
V_c [L]	Central volume of distribution	63.4	49.8 – 83.0	13.4
Q [L/h]	Intercompartmental clearance	48.0	43.0 – 54.7	6.25
V_p [L]	Peripheral volume of distribution	120	102 – 144	8.84
IIV$_{CL}$ [%]	Inter-individual variability of clearance	38.3	31.4 – 45.8	19.4
IIV$_{(Vc)}$ [%]	Inter-individual variability of central volume of distribution	72.4	54.0 – 90.7	25.8
IIV$_{Vp}$ [%]	Inter-individual variability of peripheral volume of distribution	29.9	20.7 – 37.1	27.0
$\Theta_{CL\text{-}eGFR}$	eGFR on CL	$4.92 \cdot 10^{-3}$	$2.48 \cdot 10^{-3} - 7.83 \cdot 10^{-3}$	27.8
$\Theta_{CL\text{-}bilirubin}$	Bilirubin$_{tot}$ on CL	$2.12 \cdot 10^{-1}$	$3.09 \cdot 10^{-1} - 1.13 \cdot 10^{-1}$	23.7
$\Theta_{Vc\text{-}WT}$	Weight on V_c	$2.45 \cdot 10^{-2}$	$2.0 \cdot 10^{-2} - 2.8 \cdot 10^{-2}$	8.43
RUV [%]	Residual unexplained proportional variability	12.4	11.3 – 13.8	5.21

$$CL = TVCL \cdot (1 + \Theta_{CL\text{-}eGFR} \cdot (eGFR - 68.8)) \cdot (bilirubin_{tot}/2.64)^{\Theta_{CL\text{-}bilirubin}} \qquad \text{Eq. 5}$$

$$V_c = TVV_c \cdot (1 + \Theta_{Vc-weight} \cdot (WT - 80)) \qquad \text{Eq. 6}$$

7.4 Supplementary material Publication IV

7.4.1 Supplement 1

Run001

Run001 represents the true one compartment model with i.v. infusion and linear pharmacokinetics including the true covariate relationship on clearance.

```
$PROBLEM    SIM
$INPUT
ID, TIME, DV, AMT, RATE, EVID, MDV, CMT, OCC, COV1, COV2, COV3
$DATA       sim_temp.csv    IGNORE=@
$SUBROUTINE ADVAN1 TRANS2

$PK
;FREELINE1;
;FREELINE2;
;FREELINE3;
;FREELINE4;
; will be replaced in R by the mean of simulated cov values.
TVCL = THETA(1)* EXP(THETA(5)*(COV1- XXX ))
CL = TVCL*EXP(ETA(1))
TVV1 = THETA(2)
V  = TVV1
KE = CL/V
S1=V

$ERROR
IPRED = A(1)/V
W = SQRT( THETA(3)**2*IPRED**2 + THETA(4)**2)
Y = IPRED + W*EPS(1)
IRES = DV-IPRED
IWRES = IRES/W

$THETA
(18)    FIX  ; 1_CL
(400)   FIX  ; 2_V
(0.15)  FIX  ; 3_proportional error
(0.001) FIX  ; 4_add. Error
(0.026) FIX  ; 5_COV1
             ; 3 mod files for all different covariate effect size scenarios
             ;(0.032, 0.045)
;FREELINE5;  ; Placeholder
;FREELINE6;

$OMEGA
 0.1  FIX   ; 1_IIV_CL

$SIGMA  1  FIX

$SIM(20101994) (1234) ONLYSIM ;seed will be changed with R
NSUBPROBLEMS=1

$TABLE ID TIME AMT PRED IPRED RATE IPRED EVID MDV CMT CL V ETA1 OCC COV1 COV2
COV3 WRES CWRES  NPDE ONEHEADER NOPRINT FILE=sdtab001
```

Run002

Run002 represents the structural base model without a covariate relationship serving for 'scm' and 'frem' executions.

```
$PROBLEM  SCM vs FREM

$INPUT    ID, TIME, DV,AMT,RATE,EVID,MDV,CMT, OCC,COV1,COV2,COV3
; correct number of IDs adjusted via R code

$DATA    cov_temp.csv    IGNORE=@ IGNORE(ID>100)

$SUBROUTINE ADVAN1 TRANS2

$PK

TVCL = THETA(1)
CL = TVCL*EXP(ETA(1))
TVV = THETA(2)
V   = TVV
KE = CL/V
S1=V
PROP = THETA(3)
ADD = THETA(4)

$ERROR

IPRED = A(1)/V
W = SQRT( THETA(3)**2*IPRED**2 + THETA(4)**2)
Y = IPRED + W*EPS(1)
IRES = DV-IPRED
IWRES = IRES/W

$THETA

(0,21)           ; 1_CL
(0,400)          ; 2_V
(0,0.2)          ; 3_proportional error
(0.001) FIX      ; 4_add. Error

$OMEGA
 0.2
           ; 1_IIV_CL
$SIGMA  1  FIX

$EST METHOD=1 INTER MAXEVAL=9999 PRINT=20 NOABORT SIGL=3
$COV

$TABLE ID TIME MDV AMT EVID OCC CL V PROP ADD PRED ETA1 IPRED IWRES CWRES NPDE
ONEHEADER NOPRINT FILE=sdtab002

;XXTABLEXX          ; Placeholder to adjust output table via R
```

SCM configuration file

```
;;config_template_standard.scm
;;lines starting with ; are comments
;;if a line starts with ; it must not end with \ because that will
;;cause strange errors.
;;Some of the options in this file can also be given on the command-line,
;;but it is convenient to set them in the config file
;;Most of the options in this file are optional, but this file is a good
;;check-list. Not all scm options are listed here, see the user guide for
;;a complete list.
;;Edit as needed, comment/uncomment options to suit your run
;;model file without any of the covariate combinations in test_relations.
;;Other covariates may be included
model=run002.mod
;;search direction can be forward, backward or both
;;to be adjusted in case of 'head to head' comparison
search_direction=both

;;provided that the perl module Math::CDF is installed, any p-values can
;;be used. p_backward should be smaller than p_forward
;; backward elimination was not present in 'head to head' comparison
p_forward=0.05
p_backward=0.01

;;it is required to list the covariates to test
continuous_covariates=COV1,COV2,COV3
;;By default option parallel_states=0 and scm tries parameterizations
;;one at a time, in the order set in valid_states. Only if the covariate
;;is included in the model with the first parameterization is the next
;;parameterization tried.
;;if parallel_states is set to 1, scm will test all possible relation
;;forms for a parameter-covariate pair simultaneously.
parallel_states=1

;;These general PsN options that can be set in the configuration file.
;;Most general PsN options must however be set on the command-line
retries=3
threads=1
tweak_inits=1
picky=0
;;In the configuration file all single-line options must come BEFORE the
;;first bracket-header section, otherwise the options will be ignored by scm
;;Each bracket-header section can have many lines, but each header must
;;appear at most one time
[test_relations]
CL=COV1,COV2,COV3

;;valid_states (possibly in combination with [code]) tells scm which
;;parameterizations should be tested for the covariates
;;There are default meanings to numbers 1-5, but by adding a [code] section
;;new parameterizations can be defined, and numbers can be set to mean
;;different parameterizations for different parameter-covariate pairs
;;The first valid state must always be 1.

[valid_states]
continuous = 1,4
categorical = 1,2
```

Clinical dataset generation and study scenario creation

Run001 was used to simulate and Run002 for 'scm' and 'frem' executions.

```r
#-clear environment
rm(list=ls())
#-read in packages
library(data.table)
library(tidyverse)
require(zoo)
require(boot)
require(xpose4)
library(dplyr)
library(foreach)
library(doParallel)
library(tidyr)
library(MASS)
library(janitor)
library(stringr)


##############################################################
#                CREATE DATASET FUNCTION                     #
#'##############################################################
create.workingdata = function(regimen,  observations,  covariates.const,

          uncertainty.time.sd,    # additive sd in h - not used in this study
          uncertainty.RATE.sd,    # additive sd in h - not used in this study
          n_ID){                  # number of IDs to simulate

  #-combine dataset components into a list
  input.list = list(regimen, observations)
  #-eliminate NULL items before merge (required)
  input.list = input.list[which(!sapply(input.list,is.null))]
   dummy_out = NULL

for (i in 1:n_ID) {
  #-merge regimen, observations, and covariates
  dummy = Reduce(function(...) merge(..., all = TRUE, by = "TIME"), input.list)
  dummy = as.data.table(dummy)
  dummy$EVID = 0
  dummy$EVID[dummy$AMT > 0] = 1
  #dummy[dv >= 0, EVID := 0]

#-add uncertainty to sampling TIME if needed (not used in this study)
    dummy$TIME[dummy$EVID==0]=dummy$TIME[dummy$EVID== 0] +

    rnorm(n=length(dummy$TIME[dummy$EVID==0]),mean=0,sd=uncertainty.time.sd)

    dummy$RATE[dummy$EVID==1] = abs(dummy$RATE[dummy$EVID==1] +

    rnorm(n = length(dummy$RATE[dummy$EVID==1]),mean=0,sd=uncertainty.RATE.sd))

    dummy$RATE=dummy$AMT/(dummy[,"RATE",with = F])

    dummy$RATE[is.na(dummy$RATE)]=0

    dummy$AMT[is.na(dummy$AMT)]=0

    dummy$ID=i
```

```r
    dummy$CMT=1

    dummy = dummy[order(TIME),]
    dummy[EVID == 1, OCC := seq(1,length(dummy[EVID == 1]$TIME),by=1)]
    dummy[,OCC := na.locf(OCC)]
    dummy$MDV = 1
    dummy$MDV[dummy$EVID == 0] = 0
    dummy_out = rbind(dummy_out, dummy)
  }
  return(dummy_out)

}

###################################################################
#              CREATE   WORKING DATASET                          #
#'###################################################################

#-define max. number of IDs in dataset
n_ID = 500

#-define number of simulations
n_sim = seq(from = 0, to = 1000, by =1)

#-create seed numbers
seed=round(runif(1000,min=10000,max=99900),digits=0)

#-define dosing regimen
regimen1 = data.frame(TIME = c(0,12,24,36,48,60,72,84,96,108,120),
                      AMT = c(100, rep(50,10)),  RATE = c(0.5))
#-define timepoints of observations
#-per ID one trough sample, one sample 1h after peak concentration
observations1 = data.frame(TIME = c(71.5, 109),  DV = NA )
covariates.const1 = NULL


###################################################################
#                     LOOP  STARTS                              #
###################################################################
#-create lists for collecting simulation study data in loop

rep_list_data  = vector("list", length(n_sim))
rep_list_pop   = vector("list", length(n_sim))
frem_evaluation_out = vector("list", length(n_sim))

#-define covariate correlation, as well as dataset size (n) for the simulation
study
correlation = c(0, 0.15,0.5, 0.80, 0.90)
IDs =c(20,50,100,500)
#-define cores for parallelisation
n_cores=20

for( j  in IDs){

      for (z  in  correlation) {

      print(j, z)
      #-register on cluster for parallelisation of the n_simulation loop
      cl = makeCluster(n_cores)
      registerDoParallel(cl)
```

```r
#-start parallelization
simulations = foreach (a = unique(n_sim),
                       .errorhandling = "pass",
                       .verbose = T) %dopar% {

    library(data.table)
    require(zoo)
    require(xpose4)
    library(dplyr)
    library(tidyr)
    library(MASS)
    library(janitor)
    library(stringr)
    require(boot)
    #-create dataset for the scenario according to loop
    dataset1 = create.workingdata(
                        regimen = regimen1,
                    observations = observations1,
                    covariates.const = covariates.const1,
                    uncertainty.time.sd = 0, #-no uncertainty
                    uncertainty.RATE.sd = 0, #-no uncertainty
                    n_ID = n_ID)
    # "." for DV
    dataset1[,DV := as.character(DV)]
    dataset1[,DV := "."]
    dataset1$RATE[is.na(dataset1$RATE)] = "."
    #-setting sample size for multivariate
    #-normally distributed samples
    N <-500
    #-setting the means of covariates
    mu <- c(28,8, 5.8)
    #-create covariate-correlation matrix (3x3 matrix)
    #-desired variances: 15,1.2,0.3 of the covariates
    #-z defines correlation between covariate 1 and 2
    sigma <- matrix(c(15, z*sqrt(15*1.2), 0,
                         z*sqrt(15*1.2), 1.2,0,
                                    0,0, 0.3),3,3)

    #-setting the seed value
    set.seed(seed[a])
    #-simulate the data, as specified above
    df1 <- mvrnorm(n=N,mu=mu,Sigma=sigma)
    #-extract simulated covariate values
    COV1 = as.data.frame(df1)
    #-create covariate dataset
    data = data.frame(ID=c(1:n_ID))
    data$COV1 = COV1$V1
    data$COV2 = COV1$V2
    data$COV3 = COV1$V3
    data_out = left_join(dataset1,data, by="ID")
    data_out = dplyr::select(data_out,ID, TIME, DV, AMT, RATE,
    VID, MDV, CMT, OCC, COV1, COV2, COV3)
    #-provide simulated dataset for NONMEM simulation with "true
    model" to obtain DV values; each dataset is individual for the
    respective scenario and simulation
    write.csv(data_out,
                paste("Datasets_SIM/sim_temp", j, "IDs",
                z*100, "corr_sim", a, ".csv", sep= "" ),
                row.names = F, quote = F)
```

```r
################################################################
#                     SIM WITH TRUE MODEL                      #
################################################################
#-read in "true model" modfile
modfile = scan("run001.mod", sep = "\n", what = character(),
                 quiet = TRUE)
#-change seed
seed_n_sim=seed[a]
modfile_train=gsub("20101994",
                      as.character(seed_n_sim),
                      modfile, ignore.case=T)
#-normalize to mean of covariate (as automated in FREM)
modfile_seed_train=gsub("XXX",
                      round(mean(COV1$V1), digits=3),
                      modfile_train, ignore.case=T)
#-navigate to simulated dataset
modfile_seed_train[19]= paste(
                          "$DATA   Datasets_SIM/sim_temp",
                           j, "IDs",z*100, "corr_sim", a,
                        ".csv     IGNORE=@ ","  IGNORE(ID >",j,  ")",
                        sep = "")
#-Create unique sdtabs for each execution with NONMEM simulations
modfile_seed_train=gsub("FILE=sdtab001",
                        as.character(paste("FILE=  sdtab_train_",
                        j, "IDs_", z*100,"corr_sim", a, sep = "")),
                        modfile_seed_train, ignore.case=T)


#-save changes in "true model"
write(modfile_seed_train,
      file = paste("run001seed_train_",
               j, "IDs_", z*100, "corr_sim", a, ".mod" , sep = ""))
#-execute NONMEM model for simulations
system(paste("execute ","run001seed_train_",
       j, "IDs_", z*100, "corr_sim", a, ".mod",
       " -model_dir_name -silent -clean=3", sep = ""),
        wait = T, intern = F)


#-read in simulated sdtab
#-dataset  for FREM and SCM runs for training
dataset1.sim_train = read.table(
                          paste("sdtab_train_",
                          j, "IDs_", z*100,"corr_sim",
                          a, sep = ""),
                          skip = 1, header = T)
#-copy simulated DV into simulated dataset1 and filter dataset
size according to j
dataset2 = copy(data_out) %>%  dplyr::filter(ID <= j)
dataset2[,DV := dataset1.sim_train$DV[dataset1.sim_train$ID <= j]]
dataset2$DV[dataset2$MDV == 1] = "."

#create "clinical dataset" including DV and covariates for use in
scm and frem executions
write.csv(dataset2,
          paste("Datasets_SIM/cov_temp",
                j, "IDs", z*100, "corr_sim", a, ".csv",
          sep= "" ),
       row.names = F, quote = F)
```

```
###############################################################
#                      START SCM AND FREM                     #
###############################################################
#-read in structural base model to change it individually
#-according to the study scenario
run002 = scan("run002.mod", sep = "\n", what = character()
        quiet = TRUE)
#-provide clinical dataset and edit IDs according to the scenario
run002[20] = paste("$DATA        ",
              "Datasets_SIM/cov_temp",j, "IDs",z*100,"corr_sim",
               a, ".csv","   IGNORE=@ IGNORE(ID>", j, ")", sep = "")
#-save changes in mod file
write(run002,file = paste("run002_",j,
                     "IDs_", z*100, "corr_sim",a,".mod",sep = ""))
#-change scm configuration file according to the study scenarios
#-(change of IDs and modfile name)
scm.file = scan("scm_run002.scm", sep = "\n",
                 what = character(), quiet = TRUE)
# edid SCM config file
scm.file = gsub("model=run002.mod",
                   as.character(paste("model= run002_",j, "IDs_",
                   z*100, "corr_sim",a,".mod", sep = "")),scm.file)
write(scm.file, file = paste("scm_run002_",j,
       "IDs_", z*100, "corr_sim", a, ".scm",
       sep = ""))
#-execute structural base model (without a covariate relationship)
system(paste("execute ", "run002_",j, "IDs_", z*100,
              "corr_sim", a, ".mod",
              " -model_dir_name -min_retries=3
              -silent -clean=3",sep =""), wait = T, intern = F)
#-start SCM
system(paste("scm ","run002_",j, "IDs_", z*100, "corr_sim",
              a, ".mod"," -dir=SCM_RUN_",j, "IDs_",
              z*100, "corr_sim",a, " -silent -config_file=
              scm_run002_",j,"IDs_",z*100, "corr_sim", a,
              ".scm -clean=3",sep =""),wait = T, intern = F)
#-start FREM
system(paste("frem ", "run002_",j, "IDs_",z*100, "corr_sim", a,
              ".mod", " -dir=FREM_RUN_", j,IDs_",*100,"corr_sim",a,
              " -silent -covariates=COV1,COV2,COV3 -run_sir
              -check -rplots=2 -clean=3", sep =""),
               wait = T, intern = F)
#-check if frem output was completely created - if not delete and
#-restart – manual "retries" of frem method
x = 1
while(length(list.files(path = paste("FREM_RUN_", j, "IDs_",
z*100,"corr_sim", a, sep=""), pattern = "*.html")) == 0 && (x <=3
)){
x= x+1
#-delete not successful frem run and start new one with same
directory
system(paste("rm -r FREM_RUN_", j,"IDs_", z*100, "corr_sim", a,
sep=""), wait = T, intern = F)
system(paste("frem","run002_",j,"IDs_",z*100,"corr_sim",a,".mod",
" -dir=FREM_RUN_", j, "IDs_", z*100, "corr_sim",a,
" -silent -covariates=COV1,COV2,COV3 -run_sir -check -rplots=2 -
clean=3", sep =""),
wait = T, intern = F)
  }
```

```r
            #-Print information about status of simulation estimation via
            #-R out data
              print(paste("SCM FREM Cycle", dir," completed at", Sys.time()))

              }

            stopCluster(cl) #stop parallelisation for that loop

            } #-close 'correlation' loop

            } #-close 'ID' loop


            ##########################################################
            #                   END OF EXECUTIONS                    #
            ##########################################################
```

R code for 'frem' results extraction

```r
#-clear environment
rm(list=ls())
#-load R packages
library(data.table)
library(tidyverse)
library (zoo)
library (boot)
library (xpose4)
library(stringr)
library(janitor)
#-define scenarios
IDs = c(20,50,100,500)
CORR = c(0,0.15,0.5,0.8,0.9)
SIM = seq(1,1000)
#-create folder names to navigate into frem folders
loop1 = list()
loop2 = list()
loop3 = list()

for( i in IDs){
   for(c in CORR){
    for(s in SIM){
       loop1[[s]]  = paste("FREM_RUN_",i, "IDs_", c*100, "corr_sim", s, sep ="")
      }
      loop2[[which(CORR == c)]] = as.character(unlist(loop1))
  }
  loop3[[which(IDs == i)]]  = as.character(unlist(loop2))
}
fremruns = unique(as.character(unlist(loop3)))

###################################
#           FREM   ANALYSIS       #
###################################
#-prepare lists for collection of frem output results
rep_list_coeff        = list()
rep_list_cov          = list()
rep_list_pop          = list()
rep_list_coeff.loop   = list()
rep_list_cov.loop     = list()
rep_list_pop.loop     = list()
#-directories for covariate effect size scenarios. For that three different
true models were used
for (d in c("COV0026")){# ', "COV0032", "COV0045"'
        #-define coefficient for true covariate
        true = ifelse(d == "COV0026",0.026,
               ifelse(d == "COV0032", 0.032, 0.045))

    for (b in fremruns){
            #live tracking for analysis via Rout data file
          print(paste(d, "FREM data Cycle",b, Sys.time()))
          #-define patterns to extract the files
          #-of interest in the respective folder
          pattern  = paste(d,"/FREM/", b,"/frem_results.csv", sep="")
          pattern2 = paste(d,"/FREM/", b,"/results.csv", sep="")
          pattern3 = paste(d,"/FREM/", b,"/final_models/sdtab002", sep="")
```

```
####################################
#    PSN created frem_results.csv    #
####################################

#-results.csv was not created, no output of frem
    if(file.exists(pattern2) == FALSE){
      print(paste(pattern2, "does not exsist"))
      frem_cov = data.frame(  parameter = NA,
                              covariate = NA,
                              condition = NA,
                              p5 = NA,
                              mean = NA,
                              p95 = NA,
                              RUN = b,
                              IDs = NA,
                              CORR = NA,
                              SIM = NA,
                              DIR = d,
                              SIGCOV = 0,
                              INFO = "FAILED"  )

    rep_list_cov[[which(fremruns == b)]] = frem_cov
    }

    #-results.csv was created and information is extracted
    if(file.exists(pattern2) == TRUE){
            frem_cov_results = as.data.table(read.csv(paste(d,"/FREM/",
                                b,"/results.csv", sep = ""),
                                header = FALSE, stringsAsFactors = F))

    #-extract table of interest
    index3 = which(frem_cov_results$V1  == "covariate_effects")+1
    index4 = which(frem_cov_results$V1  == "individual_effects")-1
    frem_cov =  filter(frem_cov_results[index3:  index4, ])

    frem_cov = frem_cov %>%
      mutate_all(funs(na_if(., ""))) %>%
      remove_empty("cols") %>%
      row_to_names(row_number = 1) %>%
      mutate("RUN" = b)

    #-use folder name to add scenario information to dataset
    matches.cov <- regmatches(frem_cov$RUN,
                  gregexpr("[[:digit:]]+", frem_cov$RUN))

    runID.cov = as.numeric(unlist(matches.cov))[1:3]
    frem_cov$IDs = runID.cov[1]
    frem_cov$CORR = runID.cov[2]
    frem_cov$SIM = runID.cov[3]
    frem_cov$DIR = d
    #-Check for percentile overlapping with 1
    #-(no effect on clearance) to identify which covariate
    #-was significant in frem run

    covariates= c("COV1", "COV2", "COV3")
```

```r
for(c in covariates){

      #-Note: The effect at the 5th percentile covariate value can be smaller
      #-or higher than the effect at the 95th percentile covariate value. Based
      #-on that, significance is flagged by non-overlapping confidence
      #-intervals at either the upper or lower end of the uncertainty band.

      if(( frem_cov$mean[frem_cov$covariate == c &
                         frem_cov$condition == "5th"] <
          frem_cov$mean[frem_cov$covariate == c &
                         frem_cov$condition == "95th"]) == TRUE){

           frem_cov$SIGCOV[frem_cov$covariate == c] =
                  ifelse(frem_cov$p95[frem_cov$covariate == c &
                  frem_cov$condition == "5th"] < 1 , 1,
                  ifelse(frem_cov$p5[frem_cov$covariate == c &
                  frem_cov$condition == "95th"] > 1, 1,0))}

      if(( frem_cov$mean[frem_cov$covariate == c &
          frem_cov$condition == "5th"] >
          frem_cov$mean[frem_cov$covariate == c &
          frem_cov$condition == "95th"]) == TRUE){

            frem_cov$SIGCOV[frem_cov$covariate == c]  =
           ifelse(frem_cov$p5[frem_cov$covariate == c &
                  frem_cov$condition == "5th"] > 1 , 1,
           ifelse(frem_cov$p95[frem_cov$covariate == c &
                  frem_cov$condition == "95th"] < 1, 1,0))}
           }
#-identify how many covariates were significant per frem run.Note: We define a
#-significant covariate only in cases where the effect at the 5th and 95th
#-percentile of covariate value was not overlapping with 1

#-2 covariates significant
if(length(frem_cov$SIGCOV[frem_cov$SIGCOV == 0]) == 2 & # 4x SIGCOV == 1
   length(unique(frem_cov$covariate[frem_cov$SIGCOV == 1])) == 2){

   frem_cov$INFO =  "2 covariates significant"

}

if(length(frem_cov$SIGCOV[frem_cov$SIGCOV == 0]) == 1 &
   length(unique(frem_cov$covariate[frem_cov$SIGCOV == 1])) == 3){

   frem_cov$INFO =  "2 covariates significant"

     }

#-all covariates significant
if(length(frem_cov$SIGCOV[frem_cov$SIGCOV == 0]) == 0 ){
   frem_cov$INFO = "all covariates significant"
}
```

```r
#-no covariate significant
if (length(frem_cov$SIGCOV[frem_cov$SIGCOV == 0]) == 6 |
    length(frem_cov$SIGCOV[frem_cov$SIGCOV == 0]) == 5) {
    frem_cov$INFO =  "no significant covariate"           }

if (length(frem_cov$SIGCOV[frem_cov$SIGCOV == 0]) == 4 &
    length(unique(frem_cov$covariate[frem_cov$SIGCOV == 1])) > 1) {
    frem_cov$INFO =  "no significant covariate"                      }

if (length(frem_cov$SIGCOV[frem_cov$SIGCOV == 0]) == 3 &
    length(unique(frem_cov$covariate[frem_cov$SIGCOV == 1]))  ==3 ) {
    frem_cov$INFO =  "no significant covariate"                      }

#-one covariate significant
if(length(frem_cov$SIGCOV[frem_cov$SIGCOV == 0]) >= 3 &
   length(frem_cov$SIGCOV[frem_cov$SIGCOV == 0]) <= 4 &
   length(unique(frem_cov$covariate[frem_cov$SIGCOV == 1])) == 1 ){
   frem_cov$INFO = "1 covariate significant" }

if (length(frem_cov$SIGCOV[frem_cov$SIGCOV == 0]) == 2 &
    length(unique(frem_cov$covariate[frem_cov$SIGCOV == 1]))  > 2)  {
    frem_cov$INFO =  "1 covariate significant"
}
if (length(frem_cov$SIGCOV[frem_cov$SIGCOV == 0]) == 3 &
          length(unique(frem_cov$covariate[frem_cov$SIGCOV == 1]))  == 2 ) {
       frem_cov$INFO =  "1 covariate significant"
}
if (length(frem_cov$SIGCOV[frem_cov$SIGCOV == 0]) == 4 &
    length(unique(frem_cov$covariate[frem_cov$SIGCOV == 1]))  == 1)  {
    frem_cov$INFO =  "1 covariate significant"
}
#-flag the runs, that identified only COV1 (true) with  significant effect on
clearance
frem_cov$COV1SIG[frem_cov$SIGCOV == 1 & frem_cov$covariate == "COV1" &
                 frem_cov$INFO   == "1 covariate significant"]  = 1
#-calculate total covariate effect on clearance
effect.diff = frem_cov %>%
     mutate(mean = as.numeric(mean) ) %>%
     group_by(covariate) %>%
     summarise_at(vars(mean), diff) %>%
     pivot_wider(names_from = covariate , values_from = c(mean))

frem_cov$COV1effect = effect.diff$COV1
frem_cov$COV2effect = effect.diff$COV2
frem_cov$COV3effect = effect.diff$COV3
#-flag which covariate had the biggest effect, FLAG them with 1
frem_cov = frem_cov %>%
    mutate("cov1_highest" =
            ifelse(COV1effect > COV2effect&
                   COV1effect > COV3effect,1,0)) %>%
    mutate("cov2_highest" =
            ifelse(COV2effect > COV1effect &
                   COV2effect > COV3effect, 1, 0)) %>%
    mutate("cov3_highest" =
             ifelse(COV3effect > COV2effect &
                    COV3effect > COV1effect, 1, 0))
      rep_list_cov[[which(fremruns == b)]] = frem_cov
}
```

```r
if(file.exists(pattern3) == TRUE){
      #-sdtab is present (created with model_4)
      #-use .lst file to select population PK values in final frem model
      #-(by default called model_4) or each frem run
      lst_frem   = read.lst(
                          paste(d, "/FREM/", b,
                          "/final_models/model_4.lst", sep= ""))

      frem_theta =  data.frame(unlist(lst_frem["thetas"]))

      frem_theta =  frem_theta %>%
        mutate("NUM"=seq(1:length(frem_theta$'unlist.lst_frem..thetas...')))%>%
        mutate("PARAMETER" = c("CL","V",
                              "PROP","ADD",
                              "CLCOV1","CLCOV2","CLCOV3")) %>%
       #-Number 1- 3 are PK parameters,
       #-number 4 is the fixed additive error,
       #-higher numbers are related to covariates
       filter(NUM<4) %>%
       mutate("RUN" = b)  %>%
       mutate("NUM" = NULL) %>%
       rename("est" = "unlist.lst_frem..thetas...")
      #-extract information from folder name about simulation scenario
      matches.theta <- regmatches(frem_theta$RUN,
                                  gregexpr("[[:digit:]]+",
                                  frem_theta$RUN))

      runID.cov = as.numeric(unlist(matches.theta))[1:3]

      frem_theta$IDs = runID.cov[1]
      frem_theta$CORR = runID.cov[2]
      frem_theta$SIM = runID.cov[3]
      frem_theta$DIR = d
      frem_theta$true = ifelse(frem_theta$PARAMETER == "CL", 18,
                        ifelse(frem_theta$PARAMETER == "V", 400,
                        ifelse(frem_theta$PARAMETER == "PROP", 0.15,-99)))

      frem_theta = frem_theta %>%
            group_by(RUN,DIR) %>%
            mutate(RUNDIR=paste(RUN, DIR)

      rep_list_pop[[which(fremruns == b)]] <- frem_theta
    }
  }

  #-collect the information for each covariate effect directory

  rep_list_coeff.loop[[d]] <- bind_rows(rep_list_coeff)
  rep_list_cov.loop[[d]] = bind_rows(rep_list_cov)
  rep_list_pop.loop[[d]] <- bind_rows(rep_list_pop)
}

#-estimated frem coefficients
data_out_frem                  = dplyr::bind_rows(rep_list_coeff.loop)
data_out_frem_cov              = dplyr::bind_rows(rep_list_cov.loop)
data_out_frem_cov$parameter = NULL
```

```r
data_out_frem= data_out_frem %>%
        group_by(RUN, DIR) %>%
        mutate(RUNDIR=paste(RUN, DIR))

data_out_frem_cov = data_out_frem_cov %>%
        group_by(RUN,DIR) %>%
        mutate(RUNDIR=paste(RUN, DIR))

data_out_frem_cov$COV1SIG[is.na(data_out_frem_cov$COV1SIG)] = 0

#-set same names, as in scm
data_out_frem_cov$covariate[data_out_frem_cov$covariate == "COV1"] = "CLCOV1"
data_out_frem_cov$covariate[data_out_frem_cov$covariate == "COV2"] = "CLCOV2"
data_out_frem_cov$covariate[data_out_frem_cov$covariate == "COV3"] = "CLCOV3"

names(data_out_frem_cov)[1] = "PARAMETER"

data_out = left_join(data_out_frem_cov,
                     data_out_frem,
                     by= c("RUN","IDs","CORR","SIM","DIR","RUNDIR","PARAMETER"))
#save frem run data
write.csv(data_out, file= "FREM.csv", row.names = F)

data_out_frem_pop1 = dplyr::bind_rows(rep_list_pop.loop)

data_out_frem_pop = dplyr::bind_rows(data_out_frem_pop1, data_out_frem)

write.csv(data_out_frem_pop, file="FREM_PK_parameter.csv", row.names = F)
```

R code for 'scm' results extraction

```r
rm(list=ls())
library(data.table)
library(tidyverse)
library(zoo)
library(boot)
library(xpose4)
library(stringr)
library(MASS)
library(janitor)
library(stringr)


IDs = c(20,50,100,500)              #- IDs of simulation study
CORR = c(0,0.15,0.5,0.8,0.9)        #-define correlations tested in the study
SIM = seq(1,1000)                   #-define number of simulations

#-name lists to collect folder names for each scenario
loop1 = list()
loop2 = list()
loop2a= list()

#-get folder names for each scenario
for( i in IDs){
  for(c in CORR){
    for(s in SIM){
      loop1[[s]] = paste("SCM_RUN_",i, "IDs_", c*100, "corr_sim", s, sep ="")
    }
    loop2[[which(CORR == c)]]= as.character(unlist(loop1))
  }
  loop2a[[i]] =as.character(unlist(loop2))
}
scmruns = unique(as.character(unlist(loop2a)))

#-define names of lists for the analysis loop
rep_list_scm_tab_pop.loop = list()
rep_list_scm_tab_pop = list()
vector.is.empty <- function(x) return(length(x) ==0 )

for (d in c("COV0026", "COV0032" and "COV0045" )){
    true =  ifelse(d == "COV0026", 0.026,
            ifelse(d == "COV0032", 0.032, 0.045))
for(l in scmruns){
   print(l)
   pattern4 = paste( d,"/SCM/", l,"/final_models/final_backward.lst",sep="")
   pattern5 = paste( d,"/SCM/", l,"/final_models/final_forward.lst" ,sep="")


   #-define pattens to search for in mod file
   cov_pattern =";;; CLCOV"
   FILE_pattern = "FILE=/home/YOUR_DIRECTORY/"
   cov_def =  ") ; CLCOV"
   cov1 = "CLCOV11"
   cov2 = "CLCOV21"
   cov3 = "CLCOV31"
```

```r
#####################################
#        NO COVARIATE  FOUND        #
#####################################


if(file.exists(pattern4) == FALSE & file.exists(pattern5) == FALSE) {
  matches <- regmatches(l, gregexpr("[[:digit:]]+", l))
  runID = as.numeric(unlist(matches))[1:3]

  mod.rerun = scan(paste("run001_est.mod",sep=""),
               sep = "\n", what = character(), quiet = TRUE)

  #-run model with COV1 relationship included to obtain
  #-a coefficient for the "all to all" comparison
  #-navigate to dataset used for scm

  mod.rerun[19] = paste("$DATA       cov_temp",
                        runID[1], "IDs", runID[2],
                        "corr_sim", runID[3] ,
                        ".csv   IGNORE=@",sep = "")

  #-adjust initial estimate to simulated covariate effect size
  if(d == "COV0026"){ mod.rerun[46] = "(0.026)                 ; 5_CL-COV1" }
  if(d == "COV0032"){ mod.rerun[46] = "(0.032)                 ; 5_CL-COV1" }
  if(d == "COV0045"){ mod.rerun[46] = "(0.045)                 ; 5_CL-COV1" }

  #-write modfile
  write(mod.rerun, paste( d, "/SCM/" ,l,"/run001_est.mod",sep=""))

  #-execute runs
  system(paste("execute -model_dir ",
          d, "/SCM/" ,l,"/run001_est.mod",
          " -clean=3 -silent",sep=""),
          wait = T , intern = F)
  #-read thetas in .lst file
  lst_scm_rerun = read.lst(paste(d, "/SCM/", l,
                    "/run001_est.lst", sep= ""))["thetas"]

  #-extract estimated coefficient of true covariate
  scm_theta =  data.frame(unlist(lst_scm_rerun["thetas"]))
  scm_pop =  scm_theta %>%
    mutate("NUM" = seq(1:length(scm_theta$unlist.lst_scm_rerun..thetas...
    ))) %>%
    mutate("PARAMETER" = c("CL", "V", "PROP", "ADD", "CLCOV11")) %>%
    mutate("RUN" = l)  %>%
    mutate("NUM" = NULL) %>%
    rename("est" = "unlist.lst_scm_rerun..thetas...")

  scm_pop$SIG = 0
  scm_pop$model = "no covariate selected"
  scm_pop$IDs = runID[1]
  scm_pop$CORR = runID[2]
  scm_pop$SIM = runID[3]
  scm_pop$DIR = d
  scm_pop$true[scm_pop$PARAMETER == "CL"] = 18
   scm_pop$true[scm_pop$PARAMETER == "V"] = 400
  scm_pop$true[scm_pop$PARAMETER == "PROP"] = 0.15
  scm_pop$true[scm_pop$PARAMETER == "CLCOV11"] =
               ifelse(d=="COV0026",  0.026,
               ifelse(d == "COV0032",  0.032, 0.045))
```

```r
      #-assure numeric columns
      scm_pop$est = as.numeric(scm_pop$est)
      scm_pop$IDs = as.numeric(scm_pop$IDs)
      scm_pop$CORR = as.numeric(scm_pop$CORR)
      scm_pop$SIM = as.numeric(scm_pop$SIM)
      scm_pop$true= as.numeric(scm_pop$true)
      scm_pop$SIG= as.numeric(scm_pop$SIG)
      scm_pop$METHOD = "SCM"
      scm_pop$RUNDIR = paste(scm_pop$RUN, scm_pop$DIR)

      rep_list_scm_tab_pop[[which(scmruns == l)]]  <- scm_pop
} #-close "no covariate found"

#################################################
#             BACKWARD MODEL PRESENT                     #
#        EITHER WITH OR WITHOUT COVARIATE      #
#################################################
if(file.exists(pattern4) == TRUE){ #check if final  backward file is
present
      print("final backward model present")
      mod = scan(paste(
d,"/SCM/",l,"/final_models/final_backward.mod",sep=""),
            sep = "\n", what = character(), quiet = TRUE)
#-search for covariate relationship
      search_cov_rel = grep(cov_pattern, mod)
      matches <- regmatches(l, gregexpr("[[:digit:]]+", l))
      runID = as.numeric(unlist(matches))[1:3]

###########################################
#        BACKWARD MODEL PRESENT        #
#            WITHOUT COVARIATE           #
###########################################
#-empty backward model
if(vector.is.empty(search_cov_rel) == TRUE){
        mod.rerun= scan(paste("run001_est.mod",sep=""),
                    sep = "\n", what = character(), quiet = TRUE)

#-navigate to simulated dataset, which was used in the scm run
        mod.rerun[19] = paste("$DATA      cov_temp", runID[1], "IDs",
runID[2],
                              "corr_sim", runID[3] ,".csv  IGNORE=@", sep
                = "")

if(d == "COV0026"){ mod.rerun[46] = "(0.026)               ; 5_CL-COV1" }
if(d == "COV0032"){ mod.rerun[46] = "(0.032)               ; 5_CL-COV1" }
if(d == "COV0045"){ mod.rerun[46] = "(0.045)               ; 5_CL-COV1" }
#-write modfile
write(mod.rerun, paste( d, "/SCM/" ,l,"/run001_est.mod",sep=""))

#-execute run
system(paste("execute -model_dir ",  d, "/SCM/" ,l,"/run001_est.mod",  "
-clean=3 -silent",sep=""), wait = T , intern = F)

#-read thetas in lst file
lst_scm_rerun = read.lst(paste(d, "/SCM/", l,
                            "/run001_est.lst",sep= ""))["thetas"]
scm_theta = data.frame(unlist(lst_scm_rerun["thetas"]))
```

```
        scm_pop = scm_theta %>%
            mutate("NUM"=seq(1:length(
            scm_theta$unlist.lst_scm_rerun..thetas...))) %>%
            #-use the name of the cov relation
            mutate("PARAMETER" = c("CL", "V", "PROP", "ADD", "CLCOV11")) %>%
            mutate("RUN" = l)  %>%
            mutate("NUM" = NULL) %>%
            rename("est" = "unlist.lst_scm_rerun..thetas...")

        scm_pop$model = "backward_NOCOV"
        scm_pop$SIG = 0

        } #close "final backward model without covariate"


        ####################################################
        #       BACKWARD MODEL WITH COVARIATE             #
        ####################################################
        #-if vector includes a number, a covariate was selected

        if(vector.is.empty(search_cov_rel) == FALSE){
          mod_scm = gsub("IPRED IWRES CWRES",
                      as.character("COVCOEFF IPRED IWRES CWRES"), mod,
                      ignore.case=T)

          mod_scm2 = gsub(";FREELINE1;",
                      as.character("COVCOEFF = THETA(5)"),
                      mod_scm,
                      ignore.case=T)

          file_repl = grep(FILE_pattern, mod_scm2)

        #pop-PK data in one table per scm run
        lst_scm   = read.lst(paste( d,"/SCM/", l,
                          "/final_models/final_backward.lst", sep= ""))

        scm_theta = data.frame(unlist(lst_scm["thetas"]))

        # need to know which covariate was selected
        search_scm = grep(cov_def, mod_scm2)
        mod_search_scm = mod_scm2[search_scm]

        scm_pop =  scm_theta %>%
           mutate("NUM" =
                      seq(1:length(scm_theta$'unlist.lst_scm..thetas...'))) %>%
           #-as PK parameter names and use the name of the selected covariate
           mutate("PARAMETER" = c("CL", "V", "PROP",
                                    "ADD", word(mod_search_scm, -1))) %>%
           filter(NUM!=4) %>% # num. 4 is add error, which is fixed
           mutate("RUN" = l)  %>%  mutate("NUM" = NULL) %>%
           rename("est" = "unlist.lst_scm..thetas...")

        scm_pop$model = "backward"
        scm_pop$SIG = 1
```

```
#########################################################
#        BACKWARD MODEL WITH WRONG COVARIATE           #
#########################################################

if(scm_pop[4,2] %in% c("CLCOV21", "CLCOV31")){
   matches <- regmatches(scm_pop$RUN, gregexpr("[[:digit:]]+",
scm_pop$RUN))
   runID = as.numeric(unlist(matches))[1:3]

   #-read in model file with $ESTIMATION
   mod.rerun = scan(paste("run001_est.mod",sep=""),
                    sep = "\n", what = character(),
                    quiet = TRUE)

   #-use simulated dataset, which was used in the scm run
   mod.rerun[19] = paste("$DATA    cov_temp", runID[1], "IDs"
                         runID[2], "corr_sim", runID[3] ,".csv
IGNORE=@",
                  sep = "")

if(d == "COV0026"){ mod.rerun[46] = "(0.026)            ; 5_CL-COV1" }
if(d == "COV0032"){ mod.rerun[46] = "(0.032)            ; 5_CL-COV1" }
if(d == "COV0045"){ mod.rerun[46] = "(0.045)            ; 5_CL-COV1" }

#-write modfile
write(mod.rerun, paste( d, "/SCM/" ,l,"/run001_est.mod", sep="" ))
#-execute runs
system(paste("execute -model_dir ",  d, "/SCM/",l,
       "/run001_est.mod -clean=3 -silent",sep=""),
       wait = T , intern = F)

#-read thetas out of  .lst file
lst_scm_rerun   = read.lst(paste( d,"/", l,
                 "/run001_est.lst", sep= ""))["thetas"]

#-extract estimated coefficient of true covariate
coeff.cov1 = unlist(lst_scm_rerun)[5]
#-add row to scm_pop data frame with estimate,
#-parameter name, folder name,
#-non-significance Information
#-add coefficient for true covariate
scm_pop[nrow(scm_pop)+1, ] = c(coeff.cov1, "CLCOV1", l, 0,
                                "backward_wrong cov")


 }
} # close "final backward model with covariate"

#-add additional information in scm_pop data.frame
scm_pop$IDs  = runID[1]
scm_pop$CORR = runID[2]
scm_pop$SIM  = runID[3]
scm_pop$DIR = d
scm_pop$true[scm_pop$PARAMETER == "CL"] = 18
scm_pop$true[scm_pop$PARAMETER == "V"] = 400
scm_pop$true[scm_pop$PARAMETER == "PROP"] = 0.15
scm_pop$true[scm_pop$PARAMETER == "CLCOV11"] =
            ifelse(d == "COV0026",  0.026,
            ifelse(d == "COV0032",  0.032, 0.045))
```

```
        scm_pop$true[scm_pop$PARAMETER == "CLCOV21"] = 0
        scm_pop$true[scm_pop$PARAMETER == "CLCOV31"] =  0
        scm_pop$est = as.numeric(scm_pop$est)
        scm_pop$IDs = as.numeric(scm_pop$IDs)
        scm_pop$CORR = as.numeric(scm_pop$CORR)
        scm_pop$SIM = as.numeric(scm_pop$SIM)
        scm_pop$true= as.numeric(scm_pop$true)
        scm_pop$SIG= as.numeric(scm_pop$SIG)
        scm_pop$METHOD = "SCM"
        scm_pop$RUNDIR = paste(scm_pop$RUN, scm_pop$DIR)

        rep_list_scm_tab_pop[[which(scmruns == 1)]] <- scm_pop

        } #close "final backward model"

        ###########################################
        #        FORWARD  MODEL PRESENT         #
        ###########################################

        #-check if final forward file is present,
        #-use the forward model only if this is the final model
        #-(no backward model present)


        if(file.exists(pattern5) == TRUE & file.exists(pattern4) == FALSE){
            mod = scan(paste( d,"/SCM/",l,
                       "/final_models/final_forward.mod",
                     sep=""),
                  sep = "\n", what = character(), quiet = TRUE)

        #-search for covariate relationship
        search_cov_rel = grep(cov_pattern, mod)
        matches <- regmatches(l, gregexpr("[[:digit:]]+", l))
        runID = as.numeric(unlist(matches))[1:3]


        #######################################
        #  FORWARD MODEL,  NO COVARIATE      #
        #######################################


        if(vector.is.empty(search_cov_rel) == TRUE) {
            mod.rerun= scan(paste("run001_est.mod",sep=""),
                      sep = "\n", what = character(), quiet = TRUE)
        #-navigate to simulated dataset, which was used in the scm run
        mod.rerun[19] = paste("$DATA      cov_temp", runID[1], "IDs",  runID[2],
                            "corr_sim", runID[3] ,".csv    IGNORE=@",
                          sep = "")

        if(d == "COV0026"){ mod.rerun[46] = "(0.026)                ; 5_CL-COV1" }
        if(d == "COV0032"){ mod.rerun[46] = "(0.032)                ; 5_CL-COV1" }
        if(d == "COV0045"){ mod.rerun[46] = "(0.045)                ; 5_CL-COV1" }

        #-write modfile
        write(mod.rerun, paste( d, "/SCM/" ,l,"/run001_est.mod",sep=""))
        #-execute run
        system(paste("execute -model_dir ",  d, "/SCM/" ,l,
                   "/run001_est.mod", " -clean=3 -silent",sep=""),
             wait = T , intern = F)
```

```
      #-read thetas in lst file
lst_scm_rerun   = read.lst(paste(d, "/SCM/", l,"/run001_est.lst",
                           sep= ""))["thetas"]
#-extract estimates coefficient of true covariate
coeff.cov1 = unlist(lst_scm_rerun)[5]

#-add row to scm_pop data frame with estimate,
#-parameter name, folder name, non-significance information
scm_theta =  data.frame(unlist(lst_scm_rerun["thetas"]))

scm_pop =  scm_theta %>%
      mutate("NUM" = seq(1:length(
            scm_theta$unlist.lst_scm_rerun..thetas...))) %>%
      #-use the name of the cov relation
      mutate("PARAMETER" = c("CL", "V", "PROP", "ADD", "CLCOV1")) %>%
      mutate("RUN" = l)  %>%
      mutate("NUM" = NULL) %>%
      rename("est" = "unlist.lst_scm_rerun..thetas...")

      scm_pop$SIG = 0
      scm_pop$model = "forward_NOCOV"
      } #close "final forward, no covariate"

##############################################
#       FORWARD MODEL WITH COVARIATE     #
##############################################

#if vector includes a number, a covariate was selected

if(vector.is.empty(search_cov_rel) == FALSE) {
      #-pop-PK data per scm run
      lst_scm  =  read.lst(paste( d,"/SCM/",
                         l,"/final_models/final_forward.lst",
                          sep= ""))
      scm_theta     =  data.frame(unlist(lst_scm["thetas"]))
      search_scm    = grep(cov_def, mod)  # need to know the position
      mod_search_scm = mod[search_scm]

      scm_pop =  scm_theta %>%
        mutate("NUM" = seq(1:length(
                      scm_theta$'unlist.lst_scm..thetas...'))) %>%
        #-use the name of the cov relation
        mutate("PARAMETER" = c("CL", "V", "PROP",
                             "ADD", word(mod_search_scm, -1))) %>%
        #-num. 4 is add error, which is fixed higher numbers
        #-are covariate related
        filter(NUM!=4) %>%
        mutate("RUN" = l)  %>%
        mutate("NUM" = NULL) %>%
        rename("est" = "unlist.lst_scm..thetas...")
        scm_pop$SIG = 1
        scm_pop$model = "forward"
        #-In cases a wrong covariate (COV2 or COV3)
        #-was included in the final model, use the model with
        #-covariate relationship to obtain a COV1 coefficient for the
        #-'all to all' comparison.
```

```
##########################################################
#        FORWARD MODEL   WITH WRONG COVARIATE           #
##########################################################
#-read in model file with $ESTIMATION (true model with $EST instead of
$SIM)

if(scm_pop[4,2] %in% c("CLCOV21", "CLCOV31")){
      mod.rerun = scan(paste("run001_est.mod",sep=""),
                  sep = "\n", what = character(),
                  quiet = TRUE)
#-navigate to simulated dataset, which was used in the scm run

mod.rerun[19] = paste("$DATA      cov_temp",
                      runID[1], "IDs",  runID[2], "corr_sim",
                      runID[3] ,".csv   IGNORE=@",
                      sep = "")
#-set the initial estimate to the true value according to the d
if(d == "COV0026"){ mod.rerun[46] = "(0.026)                 ; 5_CL-COV1" }
if(d == "COV0032"){ mod.rerun[46] = "(0.032)                 ; 5_CL-COV1" }
if(d == "COV0045"){ mod.rerun[46] = "(0.045)                 ; 5_CL-COV1" }

#-write modfile
write(mod.rerun, paste(d, "/SCM/",l,"/run001_est.mod",sep=""))
#-execute runs
system(paste("execute -model_dir ",  d , "/SCM/",
             l,"/run001_est.mod  -clean=3",sep=""),
       wait = T , intern = F)

#-read thetas in .lst file
lst_scm_rerun  = read.lst(paste(d,"/SCM/", l,"/run001_est.lst",
                          sep= ""))["thetas"]
#-extract coefficient of true covariate
coeff.cov1 = unlist(lst_scm_rerun)[5]
#-add row to scm_pop data frame with estimate,
#-parameter name, folder name, non-significance information
scm_pop[nrow(scm_pop)+1, ] = c(coeff.cov1, "CLCOV1", l, 0,
                               "forward_wrong_cov")
    } #close "final forward with wrong covariate"

  }#close "final forward with covariate"


matches <- regmatches(scm_pop$RUN, gregexpr("[[:digit:]]+", scm_pop$RUN))
runID = as.numeric(unlist(matches))[1:3]

scm_pop$IDs  = runID[1]
scm_pop$CORR = runID[2]
scm_pop$SIM  = runID[3]
scm_pop$DIR  = d

scm_pop$true[scm_pop$PARAMETER == "CL"] = 18
scm_pop$true[scm_pop$PARAMETER == "V"] = 400
scm_pop$true[scm_pop$PARAMETER == "PROP"] = 0.15
scm_pop$true[scm_pop$PARAMETER == "CLCOV11"] =
             ifelse(d == "COV0026",  0.026,
             ifelse(d == "COV0032",  0.032, 0.045))
```

```r
        scm_pop$true[scm_pop$PARAMETER == "CLCOV1"] =
                    ifelse(d == "COV0026",  0.026,
                    ifelse(d == "COV0032",  0.032, 0.045))

        scm_pop$true[scm_pop$PARAMETER=="CLCOV21"|scm_pop$PARAMETER == "CLCOV31"
        ] = 0
        scm_pop$est = as.numeric(scm_pop$est)
        scm_pop$IDs = as.numeric(scm_pop$IDs)
        scm_pop$CORR = as.numeric(scm_pop$CORR)
        scm_pop$SIM = as.numeric(scm_pop$SIM)
        scm_pop$true= as.numeric(scm_pop$true)
        scm_pop$SIG= as.numeric(scm_pop$SIG)
        scm_pop$METHOD = "SCM"
        scm_pop$RUNDIR = paste(scm_pop$RUN, scm_pop$DIR)
        rep_list_scm_tab_pop[[which(scmruns == l)]] <- scm_pop
        } #close "final forward model"
 } #close  l loop

rep_list_scm_tab_pop.loop[[d]] = bind_rows(rep_list_scm_tab_pop)

} # close d loop

scm_pop_out = bind_rows(rep_list_scm_tab_pop.loop)

scm_pop_out$PARAMETER[scm_pop_out$PARAMETER == "CLCOV11"] = "CLCOV1"
scm_pop_out$PARAMETER[scm_pop_out$PARAMETER == "CLCOV21"] = "CLCOV2"
scm_pop_out$PARAMETER[scm_pop_out$PARAMETER == "CLCOV31"] = "CLCOV3"

scm_pop_out$PARAMETER = as.character(scm_pop_out$PARAMETER)
scm_pop_out$RUN = as.character(scm_pop_out$RUN)
scm_pop_out$model = as.character(scm_pop_out$model)
scm_pop_out$true[scm_pop_out$PARAMETER == "ADD"] = 0.001
write.csv(scm_pop_out, file= paste("SCM_DATA ",Sys.Date(),
                                    sep =""),
         row.names = F)
```

7.4.2 Supplement 2

Simulation study using a true categorical covariate

In this simulation sub study, we investigated 0 % and 80 % correlation between the true dichotomous categorical covariate and covariate$_{II}$. Covariate$_{III}$ was independent of the other two covariates and represents pure noise. Covariate values were sampled with the code below.

```
#-define number of samples
N <-500
#-set the means
mu <- c(28,8)

#-define correlation matrix between the two continuous covariates,
#-here correlation 0 %
sigma <- matrix(c(15, 0, 0, 1.2 ),2,2)

#-set a seed number
set.seed(seed[a])
#-sample
df <- as.data.frame(mvrnorm(n=N, mu=mu, Sigma=sigma))

#-set up the data frame with a categorical covariate correlated by 80 % to
#-one of the continuous covariates
df1<-df%>%
  mutate(CATEGORICAL = case_when(
      V1<quantile(V1,0.25) ~ sample(c(1,0), n(),replace = TRUE, p = c(1,0)),
      V1<quantile(V1,0.5) ~ sample(c(1,0), n(), replace = TRUE, p = c(1,0)),
      V1>quantile(V1,0.5) ~ sample(c(1,0), n(), replace = TRUE, p = c(0,1)),
      V1>quantile(V1,0.75) ~ sample(c(1,0), n(), replace = TRUE, p = c(0,1))))

#Check correlation
round(cor(df1)[3,1], digits= 3)
```

All simulations used individually simulated datasets with 20, 50, 100, 500 virtual patients (n) including 2 (sparse) observations per individual. PK profiles of the scenarios (1-CMT PK model, i.v. short infusion, linear elimination) were obtained via Monte Carlo simulations. The true model included the categorical covariate as fractional change on clearance (Eq. 1)

IF(CATEGORICAL.COV == 0) CL = THETA(1)   Eq. 1

IF(CATEGORICAL.COV == 1) CL = THETA(1) * (1+$\theta_{\text{cat-cov}}$)

Simulated coefficients represented a covariate effect of -20 % or -40 % (-0.2, -0.4) on clearance. In cases that a categorical covariate of 1 was identified as the 'reference' value, the true value is +0.25 or +0.67.

Beside interindividual variability on clearance (IIV$_{CL}$: 0.1 variance, log-normal distribution), this sub study compared simulations in presence with and without inter individual variability on central volume of distribution (IIV$_{V}$: 0.2 variance, log-normal distribution). PK parameter estimation was performed with first order conditional estimation with interaction (FOCE+I),

using the simulated datasets (n = 1000) and a structural model without any covariates included. From here 500 'scm' and 'frem' runs were executed. Scenario 1 simulated a comparison applying 'scm' forward selection ($p < 0.05$) and a backward elimination ($p < 0.01$), as well as applied only 'scm' forward selection (p< 0.1) as comparison to 'frem$_{posthoc}$' (scenario 2). We evaluated the power to select/identify the true categorical covariate, but also conditional accuracy (Eq. 2) and precision (Eq. 3) of the estimates. For 'frem$_{posthoc}$' the mean effect of '*other*' compared to '*reference*' served for calculation of the fractional change coefficient. Whether 0 or 1 was the reference in the datasets was extracted from the PSN provided 'results.csv' file.

$$rBIAS \ [\%] = \ \frac{1}{N} \cdot \sum_{1}^{i} \frac{(estimated_i - \ true_i)}{true_i} \cdot 100 \hspace{3cm} \text{Eq. 2}$$

$$rRMSE \ [\%] = \sqrt{\frac{1}{N} \cdot \sum_{1}^{i} \frac{(estimated_i - true_i)^2}{true_i^2}} \ \cdot 100 \hspace{2cm} \text{Eq. 3}$$

Scenario 1 (categorical covariate)

The results of scenario 1 are displayed in Figure S2-1. For 'frem$_{posthoc}$' models with a significant cov$_{true}$ effect were evaluated. The power to identify the true categorical covariate was 47 % ('frem$_{posthoc}$') vs. 28 % ('scm') in the scenario with n = 20, cov-corr 80 % and the covariate effect being -20 % on clearance. With increasing the covariate effect size to -40 % we revealed a power of 89 % using the 'frem$_{posthoc}$' and 74 % in 'scm' (n = 20, cov-corr: 80 %). Thus, the observed behavior of power was similar as in the study handling continuous covariates. Power increased with increasing covariate effect size and was reduced in presence of 80 % cov-corr. In large datasets (n= 500), both methods approached 100 % power.

Additionally, we investigated the presented scenarios without inter individual variability on central volume of distribution (IIVV) to investigate its impact. The power of the 'frem$_{posthoc}$' method increased from e.g., from 89 % to 95 % (n = 20, cov-corr: 80 %, -40 % on clearance). For 'scm' power was increased in this scenario from 74 % to 78 %.

Besides that, the correlated continuous covariate (80 %) had a significant effect in ≥ 79 % of the 'frem$_{posthoc}$' models and in ≥ 95 % in large datasets (n = 500). In contrast to that, 'scm' included the true categorical covariate together with covariate$_{II}$ in none of the models. As a single covariate, 'scm' selected covariate$_{II}$ at a maximum of 15 %.

Moreover, the independent, non-correlated covariate (covariate$_{III}$) had a significant effect in 10 % (n=500) - 16 % (n = 20) of 'frem' runs and between 4 – 9 % in 'scm' runs.

Conditional accuracy and precision were functions of power. Rbias was strongly reduced with increasing power and the effect of correlation had only minor impact, regardless of the method. 'Scm' (-5.3 to 7 %) and 'frem$_{posthoc}$' (-4 to 0.2 %) estimates were slightly biased in small n datasets, if the covariate effect was strong (-40 %). In the simulations without IIVV rbias was comparable (9 % to 12 %, covariate effect:-40 %).

The rrmse of the true covariate coefficient estimated, obtained via 'scm' was reduced from 110 % to 15 % (n = 20 − 500, - 20%) or with increasing effect size from 110 % to 43 % (n=20, 80 % correlation). Without IIVV, rrmse was reduced from 108 % to 13 % ('scm', n= 20-500, 80 % corr, - 20 %) and from 108 % to 39 % with increasing effect size of the covariate ('scm', n= 20, 80 % corr, -20 %). Across all simulated scenarios, 6/16000 'frem' models provided an estimated true covariate effect of >2500 % on clearance, so that these models were excluded for the evaluations as these outliers would blur the statistics.
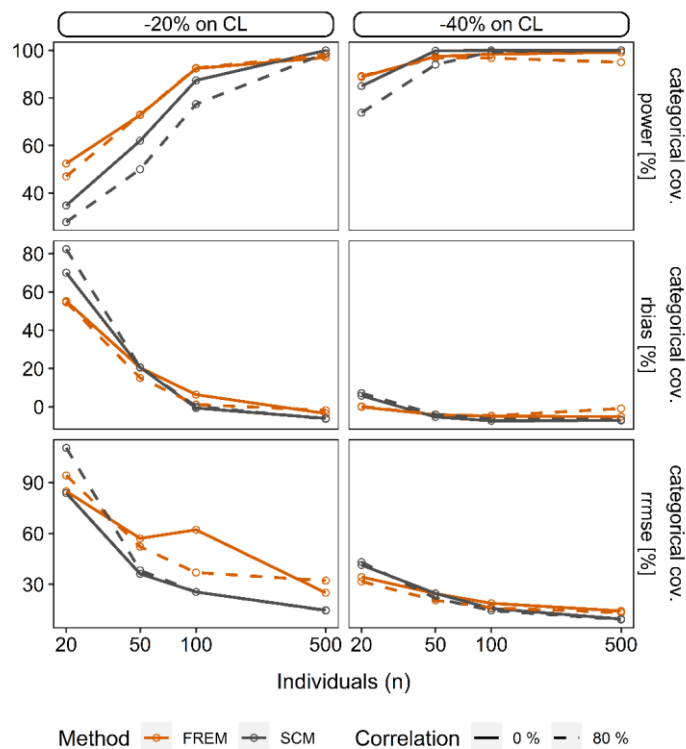
Figure S2-1 Power precision and accuracy of the true categorical covariate (cat. cov) in the comparison of 'scm' (forward selection, p<0.05; backward elimination p>0.01) vs. 'frem$_{posthoc}$' for two covariate effect sizes (scenario 1).

Scenario 2 (categorical covariate)

For this comparison, the scm was performed with forward selection only (p<0.1), as a direct comparison to the 90 % confidence interval of the covariate effects in the 'frem$_{posthoc}$' method.

The overall results followed the same trend as observed for the true continuous covariate but were also comparable to scenario 1 (Figure S2-2). Power increased from 40 % to 100 % ('scm', n=20-500, cov-corr: 0 %, covariate effect: -20 %) and from 40 % to 89 % with increasing covariate effect size.

Rbias decreased from 57 %/48 % to -5.8 %/-1.4 % and rrmse from 94 %/84 % to 14 %/29 % ('scm'/'frem', n=20-500, cov-corr: 0 %, covariate effect: -20 %), as a function of power. In the scenarios with -40 % covariate effect size, power was strongly increased (> 74 %) and rbias was between 2.2 % and -7.4 %. The correlated continuous covariate$_{II}$ was statistically significant in 39 % of simulated small n datasets (n=20, covariate correlation 80 %, covariate effect: -20 %) and in 95 % in large datasets (n=500). In contrast to that, none of the final forward 'scm' models included both covariates. The independent covariate$_{III}$ had a significant effect in 15 − 10 % (n = 20 − 500) of the final 'frem' models with a mean error between -0.017 - 0.02. The alpha value for 'scm' was between 6 and 12 %.
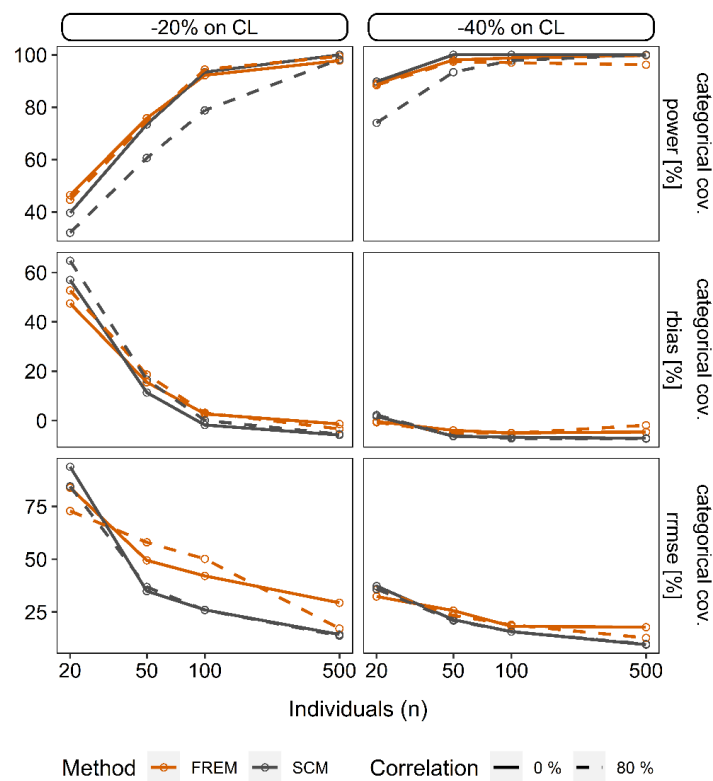

Figure S2 -2 Power, precision, and accuracy of the true categorical in scenario 2 of 'scm' (forward selection, p <0.1) and 'frem$_{posthoc}$'. The covariate effect on clearance was -20 %, -40 % respectively.
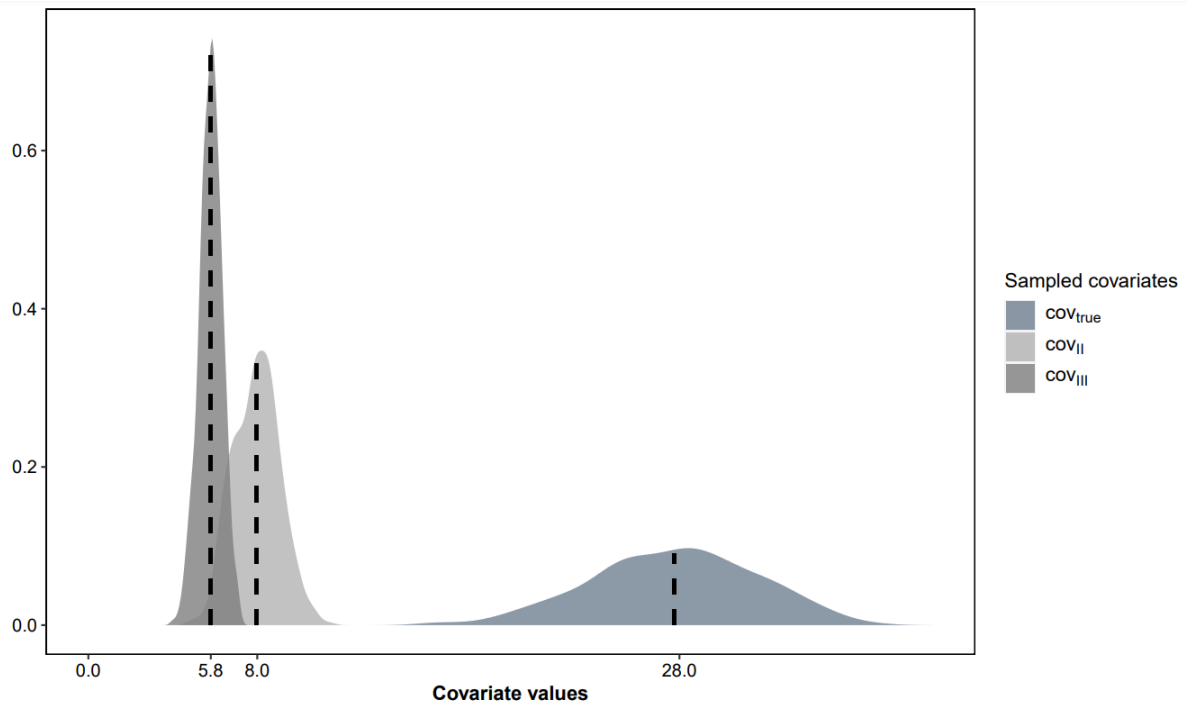
7.4.3 Supplement 3

Figure S3 - 1 Multivariate normal distribution of continuous covariate values with the mean displayed as vertical lines
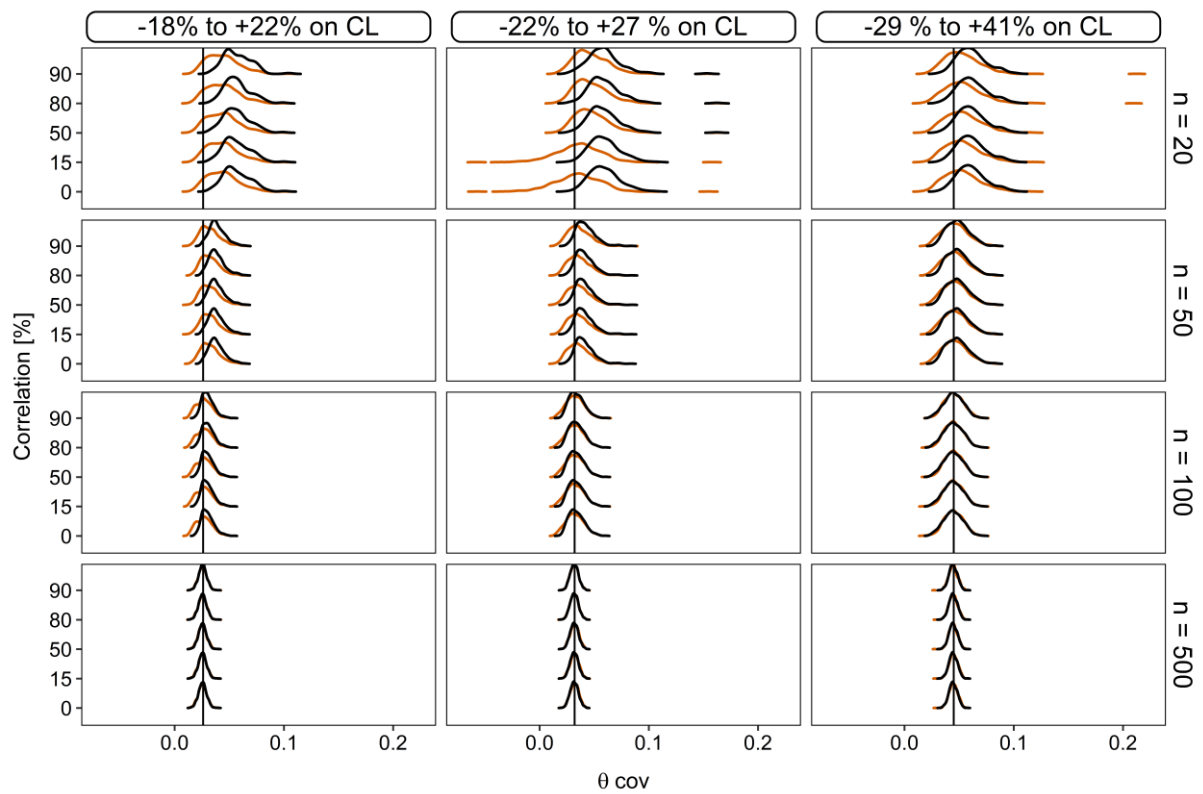
Results for Scenario 1

Figure S3 - 2 Density plot with estimated covariate coefficients for scenario 1 with three different covariate relative effect sizes on clearance (CL). The vertical line denotes the true covariate coefficient.
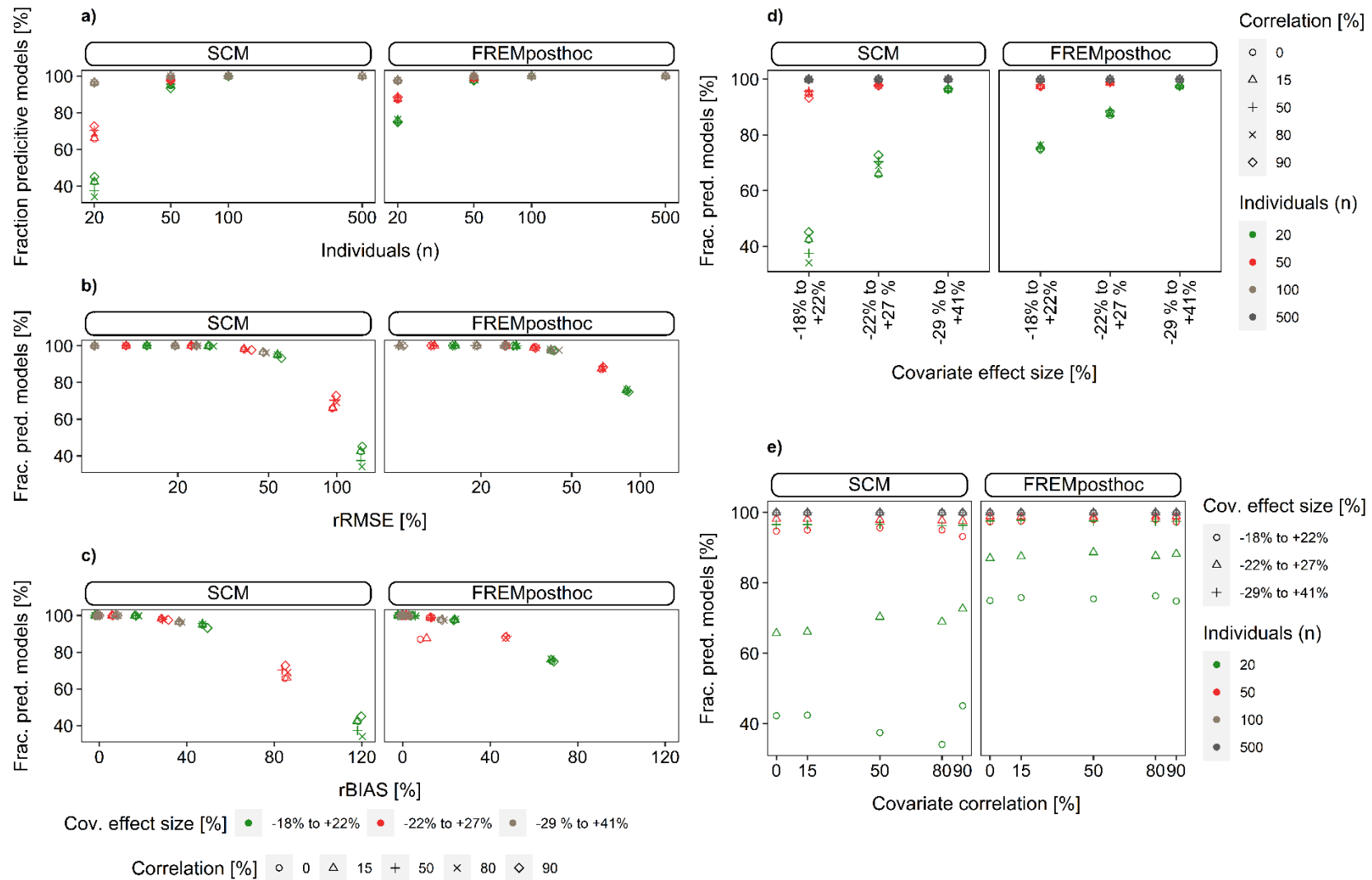
Figure S3 - 3: Fraction of predictive performance of 'scm' and 'fremposthoc' (scenario 1, continuous covariates) against single components (a: N, b: relative root mean squared error (rrmse), c: relative bias (rbias), d: covariate effect size, e: covariate correlation) of this simulation study. Covariate coefficient estimates between zero and two times the true value were termed predictive.

Results for Scenario 2

'Frem$_{posthoc}$' results were compared to 'scm' forward inclusion models (p-value <0.1) to provide a statistically similar 'head-to-head' comparison. Throughout scenario 2, the 'scm' power to include cov$_{true}$ was less affected by correlation compared to 'frem$_{posthoc}$' (Figure 3 and Table S3-1). In small n datasets, the 'scm' performed slightly better with a maximum difference in power of +23 % (n = 20, $\theta_{cov_{true}} = 0.026$).

For 'frem$_{posthoc}$', the frequency of significant cov$_{II}$ inclusions in the final 'frem$_{posthoc}$' models was > 74 % in presence of ≥ 80 % correlation between the covariates (n ≥ 100). In contrast to that, cov$_{II}$ was significantly included in < 23 % of 'scm' runs with a maximum mean error (me) of cov$_{II}$ estimate of 0.2 (n=20, $\theta_{cov_{true}} = 0.045$, cov-corr 90 %). The highest mean error of 'frem$_{posthoc}$' cov$_{II}$ estimates was 0.18 (n=20, $\theta_{cov_{true}} = 0.045$, cov-corr 90 %).

Overestimation of the $\theta_{cov_{true}}$ was observed for 'frem$_{posthoc}$' and 'scm', favouring 'scm' in small n datasets. The rbias of frem$_{posthoc}$ $\theta_{cov_{true}}$ coefficients were reduced with an increasing number of study subjects, but also with increasing relative covariate effect size (Table S3-1). In large datasets, estimated covariate coefficients were unbiased. Although power differences were observed, the fraction of predictive models in scenario 2 were similar (scm: 97.0 % 'frem$_{posthoc}$':97.5 %, n = 50, cov-corr = 80 %, $\theta_{cov_{true}} = 0.026$) and reached both 100 % in the scenario with the highest simulated covariate effect magnitude ($\theta_{cov_{true}} = 0.045$, n > 50), see Figure S3 - 4. Conditional accuracy and precision for each method is presented in Table S3-1.

The direct comparison of the estimated 'frem$_{posthoc}$' and 'scm' coefficients (based on the same dataset) is displayed in Figure S3 - 5. This representation of the results shows that 'frem$_{posthoc}$' estimates are similar to 'scm' in case both methods found a significant cov$_{true}$ relationship based on the same dataset.

Table S3 - 1: 'Scm' and 'fremposthoc' simulation results of scenario 2. The relative covariate effect sizes were -18 - +22 % ($\theta_{cov_{true}}$_true) 0.026), -22 to +27 % ($\theta_{cov_{true}}$ 0.032) and -29 to +41 % ($\theta_{cov_{true}}$ 0.045) on clearance.

| N	Covariate correlation [%]	Method	$\theta_{cov_{true}}0.026$			$\theta_{cov_{true}}\ 0.032$			$\theta_{cov_{true}}\ 0.045$		
			power [%]	rbias [%]	rrmse [%]	power [%]	rbias [%]	rrmse [%]	power [%]	rbias [%]	rrmse [%]
20	0	'frem'	40.7	69.3	88.4	50.1	43.1	64.7	71.1	21.9	43.9
		'scm'	56.0	38.6	88.0	63.9	28.4	64.5	78.6	16.7	44.1
	50	'frem'	40.0	70.3	88.5	45.1	43.5	64.7	65.5	20.5	43.0
		'scm'	56.7	41.7	87.9	63.2	28.9	64.3	77.9	14.8	43.5
	90	'frem'	29.9	67.3	86.9	33.2	44.1	66.6	46.7	20.7	43.1
		'scm'	52.7	47.6	87.9	61.0	33.6	64.0	76.5	16.5	42.7
50	0	'frem'	67.0	26.5	42.7	80.1	14.4	34.4	95.5	3.40	26.2
		'scm'	77.1	17.5	42.2	86.2	9.5	35.1	97.3	1.70	26.7
	50	'frem'	62.6	26.5	43.1	75.4	15.3	34.9	91.7	2.30	25.9
		'scm'	76.1	18.0	41.9	86.2	9.90	34.6	97.5	0.10	26.7
	90	'frem'	48.1	27.2	43.0	58.1	13.7	34.6	68.8	2.10	26.8
		'scm'	75.8	18.6	41.0	86.7	9.60	34.5	97.5	0.10	26.9
100	0	'frem'	89.9	7.60	29.8	96.1	2.90	25.9	100	0.13	18.9
		'scm'	92.5	5.10	30.1	97.7	1.00	25.9	100	-0.7	18.9
	50	'frem'	85.4	8.4	29.9	94.0	3.40	25.8	98.7	0.05	19.3
		'scm'	92.5	5.10	29.8	97.7	1.10	26.0	99.8	-1.0	19.6
	90	'frem'	67.6	7.50	30.0	76.9	3.00	25.8	81.0	-0.5	20.1
		'scm'	92.9	4.80	30.0	98.1	0.80	26.2	99.9	-1.1	19.8
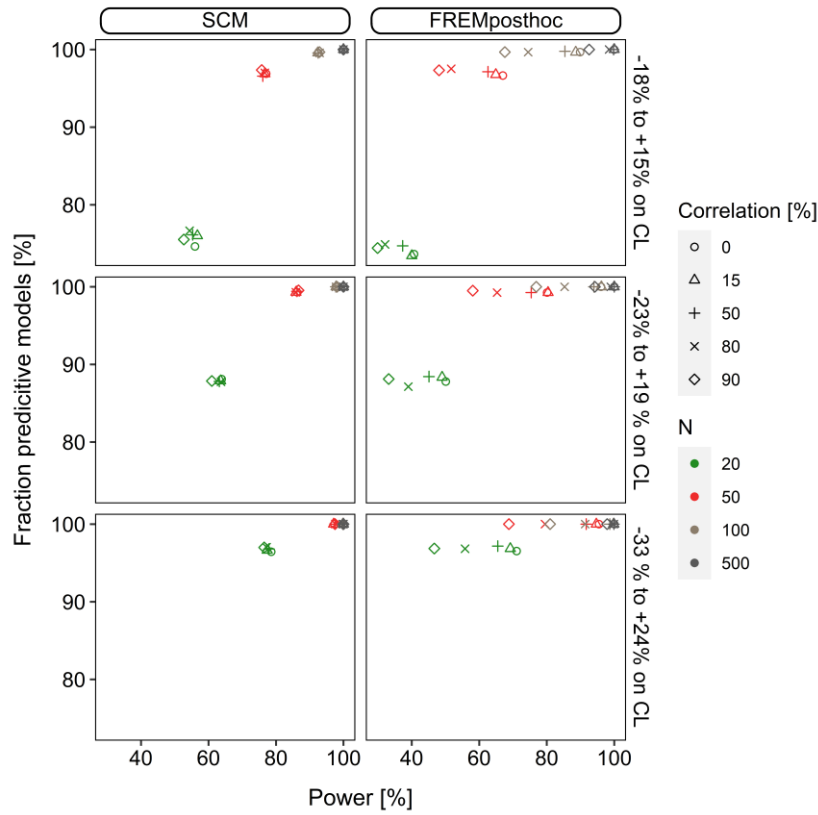
Figure S3 - 4 Fraction of models with high predictive performance for scm and final 'frem_posthoc' models with significant true covariate relationships in scenario 2. Estimated coefficients between zero to two times the true value were assumed to improve the predictive performance.
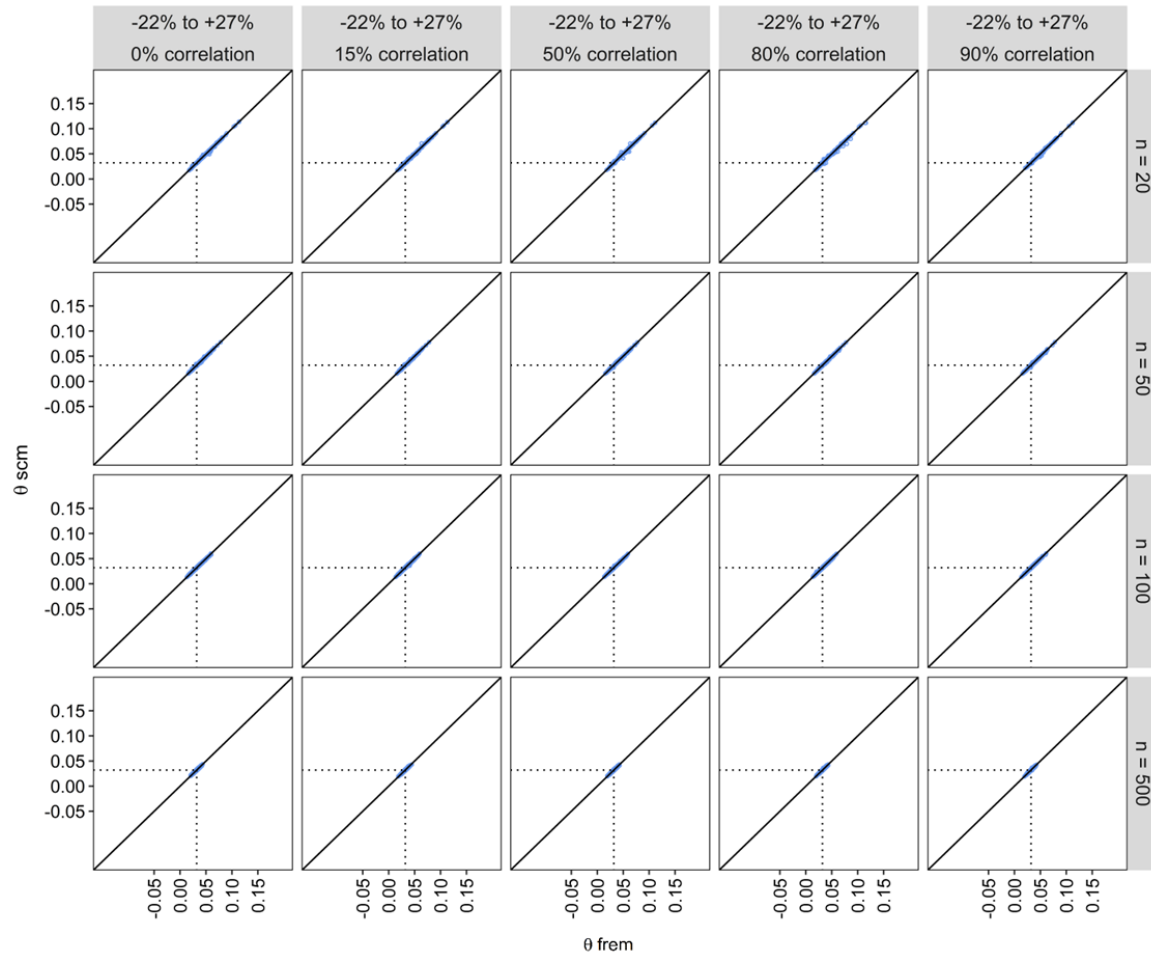
Figure S3 - 5 Estimated 'scm' vs. 'frem$_{posthoc}$' coefficients per study scenario (θ = 0.032). Dotted lines represent the true coefficient value.

Results for scenario 3

Scenario 3 compared all estimated 'frem' cov_{true} coefficients without a posthoc selection against those of the final 'scm' model obtained after forward inclusion ($p < 0.05$) and backward elimination ($p < 0.01$). In sum all 'frem' coefficients are unbiased (-1.4 – 3.7 %) compared to the 'scm' where a selection is default. Even if unbiased, the estimated 'frem' coefficients are highly imprecise, especially in datasets n < 100. Nevertheless 'frem' provides cov_{true} coefficients with a higher precision in small n datasets. Rrmse was reduced from 48 % to 27 % from weakest to strongest covariate effect scenario (n = 50) and from 80 % to 8 % with increasing dataset size (n = 20 – 500). In sum final 'frem' model provide a high faction of predictive models (> 87 %), mostly impacted by covariate effect magnitude as shown in Figure S3 - 6.
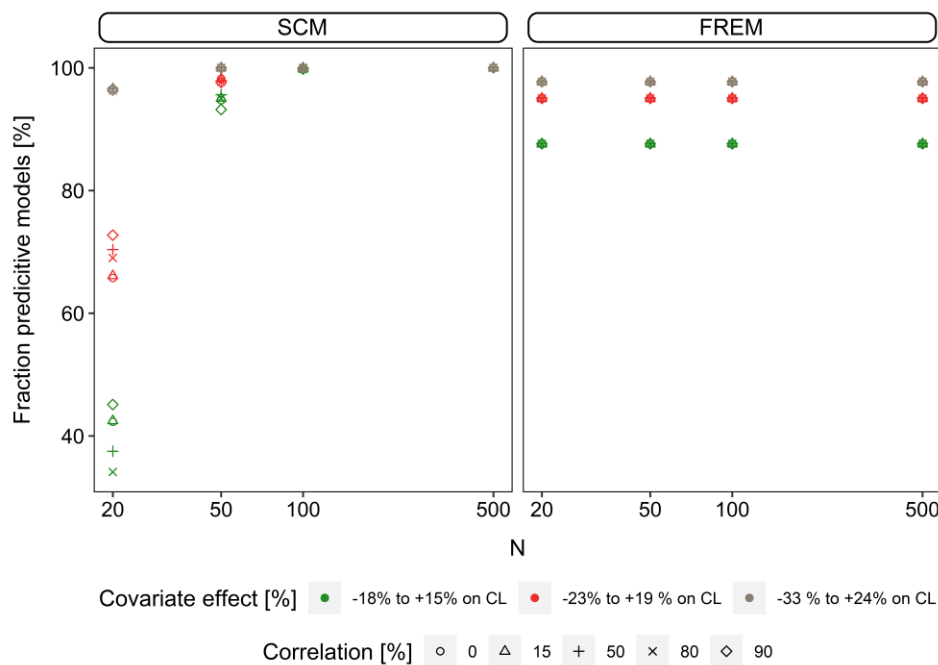
Figure S3 - 6 Fraction of models with high predictive performance for final scm and 'frem' models in scenario 3. Estimated coefficients between zero to two times the true value were assumed to improve the predictive performance.

8   Hazardous materials

Chemicals	CAS-Nr.:	Pictogram	H statement	P statement
Acetonitrile	75-05-8		H225, H302, H312, H332, H319	P210, P280, P303+P361+P353, P403+P235
Formic acid	64-18-6		H226, H290, H302, H331, H314, H314, H318	P210, P280, P303+P361+P353, P304+P340, P305+P351+P338, P310
Hydrochloric acid	7647-01-0		H290, H314, H335, H318	P280, P310, P303+P361+P353, P304+P340, P305+P351+P338
Methanol	67-56-1		H225, H301, H311, H331, H370	P210, P280, P301+P310, P303+P361+P353, P308+P311
Sodium hydroxide	1310-73-2		H290, H314, H318	P233, P280, P303+P361+P353, P305+P351+P338, P310
Tigecycline	220620-09-7		H319, H360	P201, P202, P264, P280, P305+P351+P338, P308+P313, P337+P313, P405, P501

8.1   Hazard statements

H225	Highly flammable liquid and vapour
H290	Substance or mixture corrosive to metals
H302+H312+H332	Harmful if swallowed, in contact with skin or if inhaled
H 314	Skin corrosion/irritation
H318	Serious eye damage/eye irritation
H319	Causes serious eye irritation
H331	Toxic if inhaled
H335	Specific target organ toxicity - single exposure (respiratory tract irritation)
H360	May damage fertility or the unborn child

8.2   Precautionary statements

P201	Obtain special instructions before use
P202	Do not handle until all safety precautions have been read and understood.
P233	Keep container tightly closed
P264	Wash thoroughly after handling
P280	Wear protective gloves/protective clothing/eye protection/face protection.
P301+P310	If swallowed: Immediately call a poison center/doctor.
P303+P361+P353	If on skin (or hair): Take off immediately all contaminated clothing. Rinse skin with water or shower.
P308+P313	If exposed or concerned: Get medical advice/attention.
P308+P310	If exposed or concerned: Call poison center/doctor.
P337+P313	If eye irritation persists: Get medical advice/attention
P304+P340.	If inhaled: Remove person to fresh air and keep comfortable for breathing
P305+P351+P338	IF in eyes: Rinse cautiously with water for several minutes. Remove contact lenses, if present and easy to do. Continue rinsing.
P310	Immediately call a poison center/doctor.
P405	Store locked up
P403+P235	Store in a well-ventilated place. Keep cool
P501	Dispose of contents/container in accordance with local/regional/national/international regulations

9   Acknowledgements

The field of pharmacometrics captivated me instantly, and the establishment of a new clinical pharmacy research group in Hamburg was a fortunate stroke of luck, allowing me to do my PhD in my cherished hometown. The challenge of delving into programming, modelling, and simulation—areas that appeared rather unfamiliar at that timepoint—was made surmountable by great people around me. My journey was undoubtedly a mix of highs and lows, but I am profoundly grateful for the consistent and unwavering support that accompanied me from the very outset.

And therefore, I would like to express my gratitude first and foremost to my supervisor *Prof. Dr. Sebastian Wicha*. Dear *Sebastian*, thank you for your exceptional supervision and mentoring, your consistent optimism, inspiration, and motivating words throughout the past years. I am grateful for your guidance, which has led me to my passion for pharmacometrics.

Additionally, I extend my gratitude to *Niklas Krömer* for the exchange of knowledge and the problem-solving scientific discussions. I am indebted to you for creating an environment in office 201 that I looked forward to going to ever day. Thank you for taking the time to review this thesis.
I thank *Dr. Astrid Broeker* and *Dr. David Uster* for making it possible to get off a smooth start as a new member in the group and their patient, collegial, helpful learning environment to on which my knowledge is based today. I especially thank you *David* for providing his layout for this dissertation and reviewing the thesis.

Furthermore, without my colleagues in the group and institute, my time as a doctoral student would certainly have been less entertaining. I would like to thank *Khalid, Christoph, Aneeq, Christine, Emily* for the great coffee breaks, Pizza-Fridays, and gaming evenings over the past years. Furthermore, I would like to thank *Eilika Zorn* for always having time for a chat when a break from the lab was needed.

My sincere thanks to *Dr. Maria Riedner* and *Gaby Graak* for your extensive analytical support and advises. Moreover, I would like to thank my BTA interns *Marina, Eileen, Jana, Kirstin, Hisham, Isabell, Hilal*, and *Thomas* for doing a great job in the lab.

I would like to thank our collaborators and clinical partners *Dr. Rawan Alraish* and *Dr. Magnus Kaffarnik* for providing clinical tigecycline dataset and Prof. Holger Rode and team for their bioinformatical analysis.

I would like to thank *Prof. Dr. Charlotte Kloft* and *Prof. Dr. Wilhelm Huisinga* for including me in the PharMetrX Research Training[+] program. This gave me a unique opportunity to network with my peers in the field. And I thank *Dr. Valerie Nock* for giving the internship at Boehringer Ingelheim that made me willing to stay and offering me a great opportunity to start as a clinical pharmacometrician in industry.

My exceptional heartfelt thank goes to my family and friends, being the perfect balance to the 'work-life' and your moral support. *Nicholas Bungert*, I thank you for your unwavering love, and optimism. You've been a consistent pillar of support, especially during the last stretch where stamina and perseverance were essential. I am looking forward to our path ahead.

And above all I deeply thank *my mother*. You imparted upon me strength, endurance, and diligence, which empowered me to accomplish this achievement.

As I pen down these words, I am filled with immense gratitude for each one of you who has contributed to this milestone in my academic journey. Your support has been invaluable, and I will always cherish the memories and lessons learned during this phase of my life.

10 Eidesstattliche Versicherung

Hiermit versichere ich an Eides statt, die vorliegende Dissertation selbst verfasst und keine anderen als die angegebenen Hilfsmittel benutzt zu haben. Die eingereichte schriftliche Fassung entspricht der auf dem elektronischen Speichermedium. Ich versichere, dass diese Dissertation nicht in einem früheren Promotionsverfahren eingereicht wurde.

Hamburg, den _____

_____
Lisa Franziska Amann